Identification of triterpenoids in *Brachylaena discolor* DC, a plant with antidiabetic activity

Thesis submitted in fulfilment of the requirements for the degree

Master of Science

By

Sithembiso Ntuthuko Mtshali

School of Chemistry and Physics

University of KwaZulu-Natal

Pietermaritzburg

Supervisor: Professor Fanie R. van Heerden

November 2019

ABSTRACT

In recent times, metabolic diseases such as diabetes and hypertension have become a huge burden in populations around the world. Among these diseases, the number of diabetes mellitus cases have been increasing at an alarming rate. Problems such as poor access to medication and side effects of existing drugs are encountered and there is still a need for more therapeutic alternatives. Plants have been used extensively for the treatment of various diseases, among them diabetes. *Brachylaena discolor* DC is a South African medicinal plant that is used by people for the treatment of diabetes and it has been reported previously to have antidiabetic activity with little toxicity. This study aimed to investigate the triterpenoid content of *B. discolor* and further evaluate the plant for *in vitro* antidiabetic activity by inhibition of the enzyme α-glucosidase, a therapeutic target for treatment of diabetes. In literature, it has been reported that some triterpenoids are good inhibitors of α-glucosidase. Chromatographic techniques, including argentation chromatography on silica gel impregnated with silver nitrate, were used in the isolation of compounds. The compounds were identified by 1D and 2D NMR (i.e. ^{1}H, ^{13}C, COSY, DEPT, HSQC and HMBC), IR, GC-MS, and HR-MS.

From the dichloromethane extract of *B. discolor* leaves, eight triterpenoids were isolated, α-amyrin acetate, β-amyrin acetate, ψ-taraxasterol acetate, taraxasterol acetate, lupeol acetate, α-amyrin palmitate, β-amyrin palmitate, and lupeol palmitate. All the compounds are reported for the first time from the plant, except lupeol acetate, which was previously identified in the plant. Hydrolysis of α-amyrin acetate, β-amyrin acetate, ψ-taraxasterol acetate, taraxasterol acetate, and lupeol acetate afforded the alcohol triterpenoids α-amyrin, β-amyrin, ψ-taraxasterol, taraxasterol, and lupeol. The DCM-MeOH (1:1) leaf extract of *B. discolor* was investigated *in vitro* against α-glucosidase and the extract was to inhibit the enzyme significantly with an IC_{50} value of 95.95 μg/mL when compared with the standard inhibitor acarbose with an IC_{50} value of 1149.07 μg/mL. The individual pure compounds were not assayed due to poor solubility in the assay medium. Molecular docking studies revealed that the triterpenoids, α-amyrin, β-amyrin, ψ-taraxasterol, taraxasterol, and lupeol all have binding affinity for the α-glucosidase active site, where α-amyrin and β-amyrin showed more pronounced results with binding energies of -8.90 and -8.00 kcal/mol, respectively. In the study the reported antidiabetic activity of *B. discolor* was corroborated.

PREFACE

The experimental work described in this thesis was carried out in the School of Chemistry and Physics, College of Agriculture, Engineering and Science, University of KwaZulu-Natal, Pietermaritzburg, under the supervision of Professor Fanie R. van Heerden.

I hereby declare that these studies represent original work by the author and have not otherwise been submitted in any form for any degree or diploma to any tertiary institution. Where use has been made of the work of others, it is duly acknowledged in the text.

Signed: [redacted]……

Sithembiso N. Mtshali

Date: 07/02/20……...

Signed: ……[redacted]……

Professor Fanie R. van Heerden (Supervisor)

Date: 07/02/20……...

CONFERENCE CONTRIBUTIONS

The work from this study has been presented at the following conferences:

1. Sithembiso N. Mtshali & Fanie R. Heerden, South African Chemical Institute (SACI)/ChromSA KZN Symposium (March 2019), Durban University of Technology. Oral Presentation. Antidiabetic investigation of triterpenoids from *Brachylaena discolor* DC.

2. Sithembiso N. Mtshali & Fanie R. van Heerden, College of Agriculture, Engineering, and Science, Postgraduate Research & Innovation Symposium (October 2019), University of KwaZulu-Natal (Westville). Oral presentation. Phytochemical investigation of an antidiabetic plant *Brachylaena discolor* DC.

ACKNOWLEDGEMENTS

I would like to convey my sincere appreciation to the following individuals and organisations who contributed directly and indirectly to my MSc journey.

- Professor F.R. van Heerden (my supervisor) for her nurturing guidance and support throughout the entire project.

- My lovely family and all my friends for their sizable love and support.

- Professor H. Baijnath, his help in the identification and collection of the plant material deserves high recognition.

- Professor T. Coetzer and her research group, as they assisted and welcomed me with warm hands in their biochemistry laboratory, where I conducted my biological assay studies.

- Natural products group and Warren lab colleagues, their presence and constructive discussions are always a huge encouragement.

- Dr A. Farokhzad, his computational chemistry expertise was very handy in the conducted molecular docking studies.

- Technical staff, Mrs Caryl Janse van Rensburg, Mr Craig Grimmer, and Dr V. Mzozoyana.

- National Research Foundation (NRF), for financial assistance.

- School of Chemistry and Physics.

TABLE OF CONTENTS

ABSTRACT ii

PREFACE iii

CONFERENCE CONTRIBUTIONS iv

ACKNOWLEDGEMENTS v

TABLE OF CONTENTS vi

LIST OF FIGURES ix

LIST OF TABLES AND SCHEMES xiii

ABBREVIATIONS xiv

CHAPTER 1: INTRODUCTION 1

1.1 BACKGROUND 1

1.2 AIM AND OBJECTIVES OF THE STUDY 3

1.3 STUDY RATIONALE 4

1.4 OUTLINE OF THE DISSERTATION 4

CHAPTER 2: DIABETES MELLITUS - A LITERATURE REVIEW 5

2.1 INTRODUCTION 5

2.2 MAJOR TYPES OF DIABETES MELLITUS AND MEDICATION USED TO TREAT DIABETES MELLITUS 5

2.2.1 Type 1 diabetes mellitus 6

2.2.2 Type 2 diabetes mellitus 6

2.2.3 Medication used to treat diabetes mellitus 6

2.3 ENZYMES (MOLECULAR THERAPY TARGETS) ASSOCIATED WITH DIABETES MELLITUS 9

2.3.1 α-Amylase and α-glucosidase 9

2.3.2 Protein-tyrosine phosphatase 1B (PTP1B) 10

2.4 MEDICINAL PLANTS AND TREATMENT OF DIABETES MELLITUS 10

2.4.1 South African plants used in the management of diabetes mellitus 11
2.4.2 Antidiabetic compounds isolated from plants.....15
2.5 TRITERPENOIDS AND DIABETES MELLITUS.....19
2.5.1 Postprandial hyperglycaemia mitigation by triterpenoids 19
2.5.2 Triterpenoids as protein tyrosine phosphatase 1B (PTP 1B) inhibitors.....23
2.5.3 Other antidiabetic triterpenoids isolated from plants.....26
2.6 CHROMATOGRAPHIC METHODS USED IN THE ANALYSIS OF TRITERPENOIDS.....30
2.6.1 Thin-layer chromatography 30
2.6.2 Gas chromatography 31
2.6.3 High-performance liquid chromatography and other chromatographic methods...33
CHAPTER 3: PHYTOCHEMISTRY AND ANTI-DIABETIC INVESTIGATION OF *BRACHYLAENA DISCOLOR* DC 36
3.1 INTRODUCTION 36
3.2 LITERATURE REVIEW ON *BRACHYLAENA* 36
3.2.1 Chemistry and pharmacology of Asteraceae 36
3.2.2 *Brachylaena* genus.....37
3.2.3 *Brachylaena discolor* taxonomy and phytochemistry 39
3.3 RESULTS AND DISCUSSION.....42
3.3.1 Characterization of α-amyrin acetate (3.20) and β-amyrin acetate (3.21).....43
3.3.2 Characterization of ψ-taraxasterol acetate (3.22) 48
3.3.3 Characterization of taraxasterol acetate (3.23) 54
3.3.4 Characterization of lupeol acetate (3.24).....59
3.3.5 Characterization of α-amyrin palmitate (3.25) and β-amyrin palmitate (3.26) 65
3.3.6 Characterization of lupeol palmitate (3.27) 69
3.3.7 Characterization of α-amyrin (3.28) and β-amyrin (3.29) 75
3.3.8 Characterization of ψ-taraxasterol (3.30).....78
3.3.9 Characterization of taraxasterol (3.31) 81

3.3.10 Characterization of lupeol (3.32) 84
3.3.11 α-Glucosidase Inhibition Assay 87
3.3.12 Molecular Docking Studies 89
CHAPTER 4: EXPERIMENTAL 91
4.1 GENERAL EXPERIMENTAL PROCEDURES 91
4.2 COLLECTION OF PLANT MATERIAL 92
4.3 EXTRACTION OF PLANT MATERIAL 92
4.4 ISOLATION OF TRITERPENOIDS USING ARGENTATION COLUMN CHROMATOGRAPHY 93
4.5 HYDROLYSIS OF THE TRITERPENOID ACETATES 94
4.6 PHYSICAL, CHEMICAL AND SPECTRAL DATA OF ALL COMPOUNDS 94
4.7 α-GLUCOSIDASE INHIBITION ASSAY 98
4.8 COMPUTATIONAL METHODS 98
4.8.1 Initial structure preparation 98
4.8.2 Molecular docking 99
CHAPTER 5: CONCLUSIONS AND FUTURE WORK 100
REFERENCES 102
APPENDIX 112

LIST OF FIGURES

Figure 2.1 Chemical structures of some examples of glycaemic control agents.

Figure 2.2 Gas chromatogram of a methanolic *Terminalia grandiflora* leaf extract (a), and spectral data and structures of the compounds identified by GC-MS.

Figure 2.3 HPLC chromatogram for *Chaenomeles sinensis* extract (B) and that of the standard compounds (A).

Figure 3.1 Geographical distribution of *Brachylaena discolor* var. *discolor*.

Figure 3.2 Behaviour of the unsaturated triterpenoid isomers (fraction Sm-2-18C) when run on different TLC plates, normal silica gel (A) and $AgNO_3$-impregnated silica gel (B).

Figure 3.3 GC-MS chromatogram of the α-amyrin acetate **(3.20)** (peak B) and β-amyrin acetate **(3.21)** (peak A) mixture.

Figure 3.4 EI-MS spectra of β-amyrin acetate **(3.21)** (above) and α-amyrin acetate **(3.20)** (bottom).

Figure 3.5 HR-ESI-(+)-MS spectrum of the mixture of α-amyrin acetate **(3.20)** and β-amyrin acetate **(3.21)**.

Figure 3.6 FT-IR spectrum of the α-amyrin acetate **(3.20)** and β-amyrin acetate **(3.21)** mixture.

Figure 3.7 ^{1}H NMR spectrum of the α-amyrin acetate **(3.20)** and β-amyrin acetate mixture **(3.21)** in $CDCl_3$ (400 MHz).

Figure 3.8 ^{13}C NMR spectrum of the α-amyrin acetate **(3.20)** and β-amyrin acetate **(3.21)** mixture in $CDCl_3$ (100 MHz).

Figure 3.9 HSQC NMR spectrum of the α-amyrin acetate **(3.20)** and β-amyrin acetate **(3.21)** mixture.

Figure 3.10 HMBC NMR spectrum of the α-amyrin acetate **(3.20)** and β-amyrin acetate **(3.21)** mixture.

Figure 3.11 GC-MS chromatogram of ψ-taraxasterol acetate **(3.22)**.

Figure 3.12 EI-MS spectrum of ψ-taraxasterol acetate **(3.22)**.

Figure 3.13 HR-ESI-(+)-MS spectrum of ψ-taraxasterol acetate **(3.22)**.

Figure 3.14 ^{1}H NMR of ψ-taraxasterol acetate **(3.22)** in $CDCl_3$ (400 MHz).

Figure 3.15 ^{13}C and DEPT-135 NMR spectra of ψ-taraxasterol acetate **(3.22)** in $CDCl_3$ (100 MHz).

Figure 3.16 HSQC NMR spectrum of ψ-taraxasterol acetate **(3.22)**.

Figure 3.17 HMBC NMR spectrum of ψ-taraxasterol acetate **(3.22)**.

Figure 3.18 Selected HMBC ^{1}H-^{13}C correlations for the structural elucidation of ψ-taraxasterol acetate **(3.22)**.

Figure 3.18 (Cont.) Selected HMBC ^{1}H-^{13}C correlations for the structural elucidation of ψ-taraxasterol acetate **(3.22)**.

Figure 3.19 GC-MS chromatogram of taraxasterol acetate **(3.23)**.

Figure 3.20 EI-MS spectrum of taraxasterol acetate **(3.23)**.

Figure 3.21 HR-ESI-(+)-MS spectrum of taraxasterol acetate **(3.23)**.

Figure 3.22 ^{1}H NMR of taraxasterol acetate **(3.23)** in $CDCl_3$ (400 MHz).

Figure 3.23 ^{13}C and DEPT-135 NMR spectra of taraxasterol acetate **(3.23)** in $CDCl_3$ (100 MHz).

Figure 3.24 HSQC NMR spectrum of taraxasterol acetate **(3.23)**.

Figure 3.25 HMBC NMR spectrum of taraxasterol acetate **(3.23)**.

Figure 3.26 GC-MS chromatogram of lupeol acetate **(3.24)**.

Figure 3.27 EI-MS spectra of lupeol acetate **(3.24)**, sample (above) and library based (below).

Figure 3.28 HR-ESI-(+)-MS spectrum of lupeol acetate **(3.24)**.

Figure 3.29 FT-IR spectrum of lupeol acetate **(3.24)**.

Figure 3.30 ^{1}H NMR of lupeol acetate **(3.24)** in $CDCl_3$ (400 MHz).

Figure 3.31 ^{13}C and DEPT-135 NMR spectra of lupeol acetate **(3.24)** in $CDCl_3$ (100 MHz).

Figure 3.32 HSQC NMR spectrum of lupeol acetate **(3.24)**.

Figure 3.33 HMBC NMR spectrum of lupeol acetate **(3.24)**.

Figure 3.34 HR-API-(+)-MS spectrum of the α-amyrin palmitate **(3.25)** and β-amyrin palmitate **(3.26)** mixture.

Figure 3.35 FT-IR spectrum of the α-amyrin palmitate **(3.25)** and β-amyrin palmitate **(3.26)** mixture.

Figure 3.36 ^{1}H NMR spectrum of the α-amyrin palmitate **(3.25)** and β-amyrin palmitate **(3.26)** mixture in $CDCl_3$ (400 MHz).

Figure 3.37 ^{13}C NMR spectrum of the α-amyrin palmitate **(3.25)** and β-amyrin palmitate **(3.26)** mixture in $CDCl_3$ (100 MHz).

Figure 3.38 HSQC NMR spectrum of the α-amyrin palmitate **(3.25)** and β-amyrin palmitate **(3.26)** mixture in $CDCl_3$ (100 MHz).

Figure 3.39 HMBC NMR spectrum of the an α-amyrin palmitate **(3.25)** and β-amyrin palmitate **(3.26)** mixture.

Figure 3.40 HR-API-(+)-MS spectrum of lupeol palmitate **(3.27)**.

Figure 3.41 FT-IR spectrum of lupeol palmitate **(3.27)**.

Figure 3.42 ^{1}H NMR of lupeol palmitate **(3.27)** in $CDCl_3$ (400 MHz).

Figure 3.43 ^{13}C and DEPT-135 NMR spectra of lupeol palmitate **(3.27)** in $CDCl_3$ (100 MHz).

Figure 3.44 HSQC NMR spectrum of lupeol palmitate **(3.27)**.

Figure 3.45 HMBC NMR spectrum of lupeol palmitate **(3.27)**.

Figure 3.46 GC-MS chromatogram of the α-amyrin **(3.28)** and β-amyrin **(3.29)** mixture.

Figure 3.47 EI-MS spectra of β-amyrin **(3.29)** (above) and α-amyrin **(3.28)** (bottom).

Figure 3.48 HR-API-(+)-MS spectrum of the α-amyrin **(3.28)** and β-amyrin mixture **(3.29)**.

Figure 3.49 ^{1}H NMR spectrum of the α-amyrin **(3.28)** and β-amyrin **(3.28)** mixture in $CDCl_3$ (400 MHz).

Figure 3.50 GC-MS chromatogram of ψ-taraxasterol **(3.30)**.

Figure 3.51 EI-MS spectrum of ψ-taraxasterol **(3.30)**.

Figure 3.52 HR-API-(+)-MS spectrum of ψ-taraxasterol **(3.30)**.

Figure 3.53 ^{1}H NMR spectrum of ψ-taraxasterol **(3.30)** in $CDCl_3$ (400 MHz).

Figure 3.54 GC-MS chromatogram of taraxasterol **(3.31)**.

Figure 3.55 EI-MS spectrum of taraxasterol **(3.31)**.

Figure 3.56 HR-API-(+)-MS spectrum of taraxasterol **(3.31)**.

Figure 3.57 ^{1}H NMR of taraxasterol **(3.31)** in $CDCl_3$ (400 MHz).

Figure 3.58 GC-MS chromatogram of lupeol **(3.32)**.

Figure 3.59 EI-MS spectrum of lupeol **(3.32)**.

Figure 3.60 HR-API-(+)-MS spectrum of lupeol **(3.32)**.

Figure 3.61 ^{1}H NMR spectrum of lupeol **(3.32)** in $CDCl_3$ (400 MHz).

Figure 3.62 Molecular docking interactions of α-amyrin **(A)**, β-amyrin **(B)**, lupeol **(C)**, ψ-taraxasterol **(D)** and taraxasterol **(E)** with α-glucosidase binding site.

Figure 3.63 Inhibition of α-glucosidase by a DCM-MeOH (1:1) leaf extract.

Figure 4.1 Flow chart of the purification of triterpenoids from *B. discolor* leaves DCM extract.

Figure 4.2 Flow chart of the hydrolysis of the triterpenoid acetate compounds.

LIST OF TABLES AND SCHEMES

Table 2.1 Summary of glycaemic control therapeutic agents.

Table 2.2 Plants used for the management of diabetes mellitus in South Africa.

Table 2.3 Triterpenoid inhibitors of α-amylase and α-glucosidase.

Table 2.4 Triterpenoid inhibitors of PTP1B.

Table 2.5 LC/HPLC chromatography methods used in the analysis of triterpenoids and related compounds.

Table 3.1 ^{1}H (400 MHz) and ^{13}C (100 MHz) NMR data for ψ-taraxasterol acetate **(3.22)** in $CDCl_3$.

Table 3.2 ^{1}H (400 MHz) and ^{13}C (100 MHz) NMR data for taraxasterol acetate **(3.23)** in $CDCl_3$.

Table 3.3 ^{1}H (400 MHz) and ^{13}C (100 MHz) NMR data for lupeol acetate **(3.24)** in $CDCl_3$.

Table 3.4 ^{1}H (400 MHz) and ^{13}C (100 MHz) NMR data for lupeol palmitate **(3.27)** in $CDCl_3$.

Table 3.5 ^{1}H NMR (400 MHz) data for ψ-taraxasterol **(3.30)** in $CDCl_3$.

Table 3.6 ^{1}H NMR (400 MHz) data for taraxasterol **(3.31)** in $CDCl_3$.

Table 3.7 ^{1}H NMR (400 MHz) data for lupeol **(3.32)** in $CDCl_3$.

Table 4.1 Fractions obtained by VLC of a DCM extract of *B. discolor* leaves.

Table 4.2 Summary of the eluents used in the performed purifications.

Scheme 3.1 Formation of a characteristic ursane triterpenoid MS base peak.

Scheme 3.2 Remote hydrogen rearrangement of triterpenoid alcohols in the HR-MS.

ABBREVIATIONS

ALA	Alanine
APCI	Atmospheric pressure chemical ionisation
$AgNO_3$-CC	Silver nitrate impregnated silica column chromatography
°C	Degrees Celsius
^{13}C	Carbon-13
$CDCl_3$	Deuterated chloroform
COSY	Correlation spectroscopy
C2C12	C2C12 Mouse myoblast cell line
cm^{-1}	Wavenumber (per centimetre)
d	Doublet
dd	Doublet of doublets
DCM	Dichloromethane
DEPT	Distortionless enhancement by polarization transfer
1D	One-dimensional
2D	Two-dimensional
EI-MS	Electron ionisation-mass spectrometry
ELSD	Evaporative light scattering detector
FID	Flame ionisation detector
FTIR	Fourier transform infrared spectroscopy
gal	Galactose
GC-MS	Gas chromatography-mass Spectrometry
glc	Glucose
GLP	Glucagon-like peptide
^1H	Proton
Hex	Hexane
HPLC	High performance liquid chromatography
HPTLC	High performance thin-layer chromatography
HMBC	Heteronuclear multiple-bond correlation
HSQC	Heteronuclear single-quantum correlation
h	Hour(s)
HRMS	High-resolution mass spectrometry
Hz	Hertz
IC_{50}	Half maximal inhibitory concentration
IR	Infrared spectroscopy
J	Coupling constant
Kg	Kilogram
LC-MS	Liquid chromatography-mass spectrometry
LYS	Lysine
m	Metre
MeOH	Methanol
mg	Milligram
min	Minute(s)
mL	Millilitre
mL/min	Millilitre per minute
MS	Mass spectrometry
m/z	Mass-to-charge ratio
NMR	Nuclear magnetic resonance

PHE	Phenylalanine
ppm	Parts per million
R_t	Retention time
s	Singlet
t	Triplet
td	Triplet of doublets
TRP	Tryptophan
SFC	Supercritical fluid chromatography
STZ	Streptozotocin
TLC	Thin-layer chromatography
T2DM	Type-2 diabetes mellitus
UV	Ultraviolet
VLC	Vacuum liquid chromatography
WHO	World Health Organisation
μM	Micromolar

CHAPTER 1: INTRODUCTION

1.1 BACKGROUND

The importance and exploitation of natural products continue to be relevant and prevalent in current days as a result of the substantial chemical diversity and accessibility as opposed to synthetic products.[1-2] Natural product chemistry is among the arsenal of approaches employed by drug discovery in the development of pharmaceuticals for the treatment of communicable and non-communicable human diseases.[3]

Reviews by Newman and Cragg have documented information on the sources of different types of drugs approved by regulatory agencies over the years. These include amongst others, antibacterial, antifungal, antiviral, antiparasitic, anti-infective, anticancer, and antidiabetic drugs.[2,4-6] The analysis of these authors showed that 65% of all small-molecule drugs that were approved by United States FDA (Food and Drug Administration) were natural products, natural product derivatives, contain natural product pharmacophores, or were natural product mimics. In particular, natural products and their derivatives continue to play a significant role in the discovery of antibacterial and anticancer drugs.[2]

Some of the recently approved antibacterial drugs include meropenem **(1.1)**, a natural product derivative. This intravenous drug was approved in the United States of America by the FDA in 2017.[7] In the same year, two anticancer drugs, midostaurin **(1.2)** and forodesin hydrochloride **(1.3)**, were also approved.[7] Midostaurin **(1.2)**, an indolocarbazole, is a derivative of the alkaloid staurosporine obtained from the bacterium *Streptomyces staurosporeus*,[8] and was introduced to the market in the United States of America early in 2017.[9-10] Forodesin, discovered in New York at the Albert Einstein College of Medicine, is a purine nucleoside phosphorylase (PNP) inhibitor and a valuable therapeutic for peripheral T-cell lymphoma. It was approved in Japan as an anticancer agent.[7]

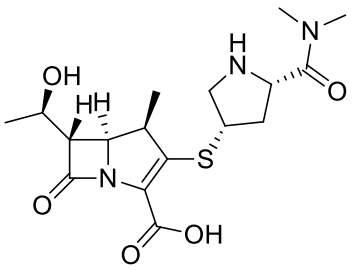

Meropenem **(1.1)**

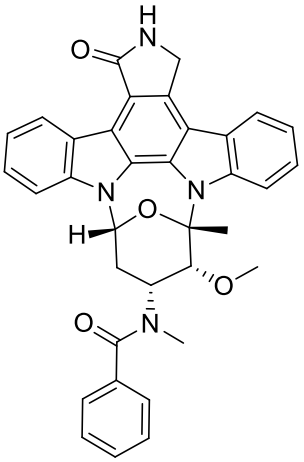

Midostaurin **(1.2)**

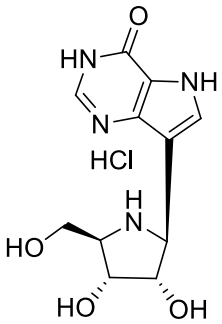

Forodesin hydrochloride **(1.3)**

Between 1981 and 2014, fifty-two antidiabetic drugs have been approved by the FDA of which only four were not natural products or natural product-inspired drugs.[2] The FDA-approved antidiabetic drugs derived from natural products are metformin, voglibose, acarbose, miglitol, extenamide, triproamylin acetate, liraglutide, and lixisenatide (structures of the drugs are given in Chapter 2). In 1995, a drug of plant origin metformin (see Chapter 2.4), was introduced for the treatment of type 2 diabetes mellitus (T2DM).[11] At the moment, metformin is one of the preferred medications for the management of T2DM.[12] In addition to these drugs, the USA FDA in 2017 approved a natural product derivative, semaglutide, as a T2DM drug. Semaglutide is a glycaemic control agent and is useful in adjunct with proper diet and exercise.[7,13] This drug was developed by the Danish pharmaceutical company, Novo Nordisk.[13]

In primary human healthcare, traditional medicine is of importance. Traditional medicines are defined as health traditions of indigenous communities that are of relevance in the treatment of physical or mental health conditions and are generally based on animal or plant sources.[14] The use of traditional medicine over centuries have also drawn the attention of researchers, and several active therapeutics have been isolated from medicinal plants. Classic examples of active principles isolated from plant material include alkaloids from a medicinal plant, *Papaver somniferum* L (also known as opium poppy).[15] Morphine **(1.4)** was isolated from the latex of *P. somniferum* as a pure compound in 1805 by Serturner and is used for pain relief.[15] Other alkaloids from *P. somniferum* include codeine **(1.5)**, an analgesic, and papaverine **(1.6)**. Codeine was isolated by a French chemist, Pierre Jean Robiquet in 1832 and in 1848 Georg Merck discovered papaverine, which is useful against several ailments, including the treatment of erectile dysfunction.[16]

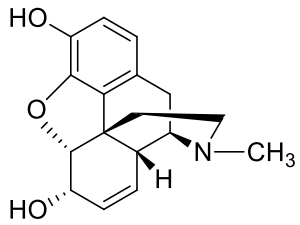

Morphine **(1.4)**

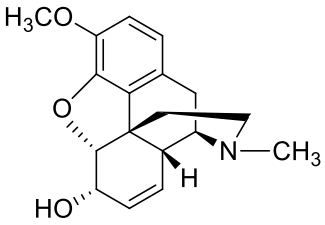

Codeine **(1.5)**

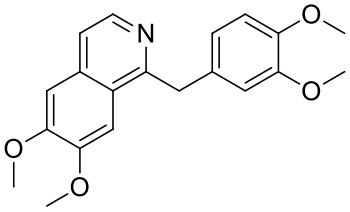

Papaverine **(1.6)**

1.2 AIM AND OBJECTIVES OF THE STUDY

The aim of this study was to investigate the triterpenoids present in a medicinal plant *Brachylaena discolor* DC that is used traditionally to treat diabetes.

The study objectives were to:

- Collect and extract *Brachylaena discolor* plant material
- Isolate triterpenoids

- Elucidate the structures of the isolated compounds
- Hydrolyse or derivatise the isolated compounds
- Perform molecular docking studies on isolates against a diabetes molecular therapy targets (α-glucosidase, α-amylase and protein tyrosine phosphatase-1B)
- Evaluate the inhibitory effect of the extract and compounds on α-glucosidase

1.3 STUDY RATIONALE

In recent times, human diseases like diabetes mellitus are increasingly becoming a huge burden. In developing countries, particularly, diseases like diabetes pose considerable challenges, not only with regards to healthcare but it also impacts on economic issues.[17] The potential of novel diabetes drugs originating from plant sources, and the lack of regulation of herbal therapeutics as a potential alternative in the management of the disease, present an unexplored opportunity for research.[18] Several natural triterpenoids have been reported as inhibitors of α-glucosidase and α-amylase, two established diabetes molecular therapy targets, and protein tyrosine phosphatase 1B (PTP1B), a potential target for new antidiabetic drugs.[19-20] South African plants are a rich source of triterpenoids and some of these triterpenoids have good antidiabetic properties.[21-23] In this study, a plant traditionally used for the management of diabetes (*Brachylaena discolor* DC) is evaluated. Limited documented literature on the plant has revealed that it has promising antidiabetic properties.[24-25]

1.4 OUTLINE OF THE DISSERTATION

The dissertation consists of five chapters. Chapter 1 is a brief general introduction to natural products. Chapter 2 gives a literature review on diabetes mellitus, medicinal plants used for diabetes, and triterpenoids. In chapter 3, the phytochemistry and antidiabetic properties of *Brachylaena discolor* DC are discussed. The literature on the Asteraceae plant family, genus *Brachylaena*, and the known phytochemistry of *B. discolor* is briefly reviewed. After that, the results are outlined and discussed in detail. Chapter 4 comprises the experimental and methodology of the project. In chapter 5, conclusions on the study are drawn.

CHAPTER 2: DIABETES MELLITUS - A LITERATURE REVIEW

2.1 INTRODUCTION

Diabetes mellitus is a group of metabolic disorders that is characterised by an abnormal rise in blood glucose levels (hyperglycaemia).[26-27] Symptoms of hyperglycaemia include most commonly polyuria, polydipsia, weight loss, sometimes with polyphagia, and blurred vision.[26] Hyperglycaemia consequently leads to microvascular damage, which can include retinopathy, nephropathy, and neuropathy.[26] These microvascular damages increase the risk of macrovascular complications, i.e. ischaemic heart disease, stroke, and peripheral vascular disease, hence life expectancy is compromised.[26,28] This chronic disease results in cases when the pancreas does not produce insulin and hence leads to insulin deficiency, which is responsible for the regulation of blood sugar, or when the insulin produced by the pancreas cannot be effectively utilised by the body (insulin resistance).[29]

According to the World Health Organisation (WHO), the prevalence of this non-communicable disease (NCD) has been increasing steadily and significantly over the past few decades.[30] Diabetes is progressing in populations globally, and the International Diabetes Federation (IDF) estimates that about 693 million people (18-99 years age group) will be suffering from diabetes in 2045.[31] The magnitude of this destructive human disease calls for special attention.

2.2 MAJOR TYPES OF DIABETES MELLITUS AND MEDICATION USED TO TREAT DIABETES MELLITUS

Diabetes mellitus as defined earlier, results from hyperglycaemia, which may be caused by different conditions, hence we have several types of diabetes mellitus of which the most common types are type 1 and type 2 diabetes mellitus.[26] There are also some other types of diabetes/hyperglycaemia disorders, e.g. gestational diabetes mellitus (GDM), endocrine disorders, and exocrine pancreas disorders.[27] The two major types of diabetes are briefly discussed below.

2.2.1 Type 1 diabetes mellitus

Type 1 diabetes was previously termed insulin-dependent diabetes mellitus (IDDM) since its management is dependent upon insulin injections/supplements.[32] T1DM results from an insulin secretion deficiency because of the destruction of the beta cells in the Islets of Langerhans in the pancreas. The destruction is typically from immunological factors.[32-33]

2.2.2 Type 2 diabetes mellitus

This condition is the most common type of diabetes (in western countries it accounts for 90-95% of all reported diabetes mellitus cases) and is usually connected with metabolic syndrome.[34] It results from cellular resistance to insulin action. However, in some cases, insulin resistance is accompanied by defective insulin secretion. Type 2 diabetes mellitus can remain symptomless for an extended period before diagnosis. This type of diabetes was formerly known as non-insulin dependent diabetes mellitus (NIDDM).[32,35]

2.2.3 Medication used to treat diabetes mellitus

Approved medications (glycaemic control agents) for T2DM are summarised in **Table 2.1.**, with some examples of the respective classes of medication, route of administration, mechanism of action, risks of hypoglycaemia upon use, and possible side effects. The adverse effects of the current therapies emphasise the need for more therapeutic agents in addition to the existing ones.

Table 2.1. Summary of glycaemic control therapeutic agents.[36-37]

Class of medication (administration)	**Mechanism of action**	**Examples**	**Adverse effects**
Insulin (Parenteral)	Activates insulin receptors and facilitates downstream signalling in multiple sensitive tissues.	**Short-acting** (Humulin R and Novolin R) **Intermediate** Isophane insulin **Long-acting** Insulin glargine Insulin detemir Insulin degludec **Rapid-acting** Insulin lispro Insulin aspart Insulin glulisine In addition to these, there are also **pre-mixed insulin agents**	Lipoatrophy and lipohypertrophy at sites of injection. Allergy to injection. Risk of hypoglycaemia.
Biguanides (Oral)	Insulin sensitizer	Metformin **(2.1)**	May result in vitamin B12 deficiency, which leads to neuropathy and anaemia.
Sulfonylureas (Oral)	Insulin secretion	Glimepiride **(2.2)** Glipizide Glyburide	Risk of hypoglycaemia.
Thiazolidinediones (Oral)	True insulin sensitizer	Rosiglitazone **(2.3)** Pioglitazone	Bladder cancer and risk of bone fractures.
Meglitinides (Oral)	Insulin secretagogue	Repaglinide Nateglinide	Risk of hypoglycaemia
Glucagon-like-peptide-1 (GLP-1) agonists (Parenteral)	Activates GLP-1 receptor. Insulin secretagogue, decreases glucagon, delays gastric emptying.	Liraglutide **(2.4)** Exenatide Dulaglutide	Nausea, vomiting, pancreatitis, and thyroid cancer.

Dipeptidyl peptidase 4 (DPP-IV) inhibitors (Oral)	Inhibition of degradation of GLP (Glucagon-like peptides)	Sitagliptin **(2.5)** Saxagliptin Vidagliptin Linagliptin Alogliptin	Pancreatitis and upper respiratory tract infection.
Sodium-glucose cotransporter (SGLT2) inhibitors (Oral)	Insulin independent mechanism of action, inhibition of SGLT2 in the renal procalcitonin (PCT).	Canagliflozin **(2.6)** Dapagliflozin Empagliflozin	Bone fractures, genital mycosis, and in rare cases also ketoacidosis.

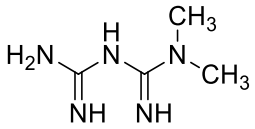

Metformin **(2.1)**

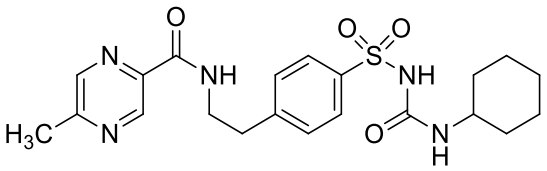

Glipizide **(2.2)**

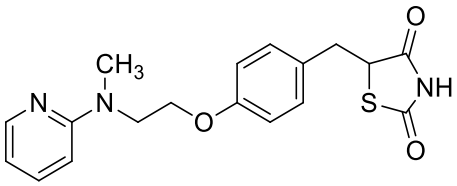

Rosiglitazone **(2.3)**

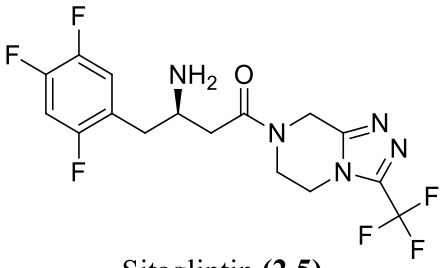

Sitagliptin **(2.5)**

H-His-Ala-Glu-Gly-Thr-Phe-Thr-Ser-Asp-Val-Ser-Ser-Tyr-Leu-Glu-Gly-Gln-Ala-AlaLys(γ-Glu-palmitoyl)-Glu-Phe-Lle-Ala-Trp-Leu-Val-Arg-Gly-Arg-Gly-OH

Liraglutide **(2.4)**

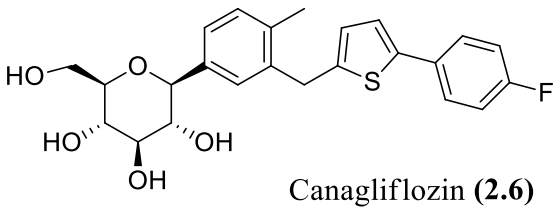

Canagliflozin **(2.6)**

Figure 2.1. Chemical structures of some examples of glycaemic control agents.

2.3 ENZYMES (MOLECULAR THERAPY TARGETS) ASSOCIATED WITH DIABETES MELLITUS

The search for active anti-hyperglycaemic agents has revealed important molecular therapy targets, namely: α-amylase, α-glucosidase, protein tyrosine phosphatase 1B (PTP1B), dipeptidyl peptidase-4 (DPP-4), free fatty acid receptor 1 (FFA1), G protein-coupled receptor (GPCR), peroxisome proliferator-activated receptor (PPARγ), sodium glucose co-transporter (SGLT2), aldose reductase (ALR), glycogen phosphorylase (GP), fructose-1,6-bisphosphatase (FBPase), glucagon receptor (GCGr), and phosphoenolpyruvate carboxykinase (PEPCK).[37] Three of these molecular targets are discussed briefly in the next paragraphs.

2.3.1 α-Amylase and α-glucosidase

Postprandial hyperglycaemia (i.e. after a meal, a rise in plasma sugar levels is observed) suppression is among the useful therapies employed in the management of early diagnosed diabetes. This approach relies on the inhibition of carbohydrate-hydrolysing enzymes, i.e. α-amylase and α-glucosidase.[38] α-Amylase is responsible for the hydrolysis of starch and other forms of carbohydrates by breaking α-1,4-glucan bonds.[38] α-Glucosidase is responsible for the further break down of polysaccharides or oligosaccharides (depending on the enzyme's specificity) into glucose, which is responsible for the rise in blood glucose levels.[38-39] α-Glucosidase inhibitors were introduced to the market in 1998.[40] The drug acarbose **(2.7)**, a trisaccharide, inhibits both the enzymes α-amylase and α-glucosidase.[41]

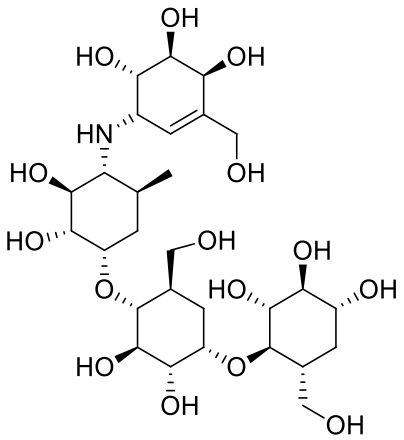

Acarbose **(2.7)**

2.3.2 Protein-tyrosine phosphatase 1B (PTP1B)

PTP1B is an enzyme belonging to the protein tyrosine phosphatase (PTP) family, which comprises at least 100 members.[42] The primary role of PTPs is to remove phosphate from a tyrosine residue in proteins in a form of regulation of physiological processes, hence they are critical for diseases and health.[43-44] Besides PTP1B, there are some validated PTP drug targets, for example, SHP2, which is one of the recently discovered promising therapeutic targets for the treatment of melanoma, a type of human cancer.[45]

According to conducted *in vitro* studies, PTP1B negatively regulates the insulin signalling pathway, hence, its inhibition allows for insulin sensitivity.[46] Therefore these PTP1B inhibitors are a relevant therapy in the management of T2DM and obesity, even though the development of these agents can be challenging,[46] as currently there are no approved PTP-targeted drugs.[44] Despite these challenges, PTP1B has promising structural attributes that offer the possibility of the discovery or development of selective therapeutics.[43] The further exploration of structural biology, medicinal chemistry and inhibitor-assay systems are among the useful approaches in the search for potent PTP1B inhibitors.[43] Triterpenoid compounds have been reported to display significant potency in the inhibition of PTP1B (see section **2.5**) *in vitro* and, *in vivo*. The examples include betulinic acid, and selected lupane-type triterpenoids (i.e. selective allosteric inhibitors of the enzyme).[42]

2.4 MEDICINAL PLANTS AND TREATMENT OF DIABETES MELLITUS

Natural sources such as plants and microbes have provided several drugs for the treatment and management of diseases such as T2DM.[34] For diabetes, noteworthy examples include acarbose **(2.7)**, miglitol **(2.8)**, voglibose **(2.9)**, metformin **(2.1)**.[34]

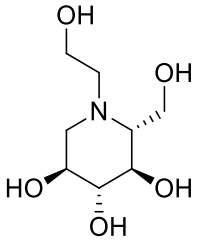

Miglitol **(2.8)**

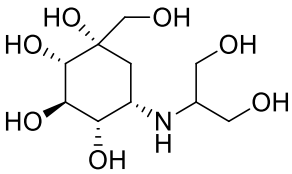

Voglibose **(2.9)**

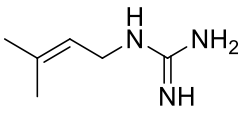

Galegine **(2.10)**

Galega officinalis L. (Fabaceae) was the first medicinal plant for which a potent antidiabetic activity was experimentally observed, and this led to the isolation of galegine **(2.10)**, which is the parent compound of metformin **(2.1)**. This plant has also been investigated and found to have potent anti-obesity activity.[34,47] This history of discoveries signifies the need of exploring natural sources for potential antidiabetic drugs.

2.4.1 South African plants used in the management of diabetes mellitus

Southern Africa is a region rich in biodiversity,[48] hence there is significant use of plants for medicinal purposes.[49-50] However, despite this there is still a shortage of relevant studies conducted on South African flora, partly due to limited documentation of ethnobotanical information.[48] An increasing number of indigenous plants used for diabetes in South Africa have been reported and a summary of these plants are given in **Table 2.2.**

Table 2.2. Plants used for the management of diabetes mellitus in South Africa.

Medicinal plant	**Plant part(s)**	**Reference(s)**
Albuca setosa Jacq. (Hyacinthaceae)	Corms	51
Allium sativum L. (Alliaceae)	Whole plant	51
Aloe ferox Mill. (Asphodelaceae)	Leaves Leaves	51 52
Aloe marlothii A. Berger subsp. *marlothii* (Asphodelaceae)	Leaves and roots	53
Anacampseros ustulata E.Mey ex Fenzl (Anacampserotaceae)	Corms	51
Artemisia afra Jacq. ex Willd. (Asteraceae)	Leaves and roots	49
Brachylaena discolor DC. (Asteraceae)	Leaves, roots and stems Leaves	54 49
Brachylaena elliptica (Thunb.) Less. (Asteraceae)	Leaves	21
Brachylaena ilicifolia (Lam.) Phillips & Schweick. (Asteraceae)	Leaves	55
Bridelia micrantha (Hochst.) Baill. (Euphorbiaceae)	Stem bark	56
Bulbine abyssinica A. Rich. (Xanthorrhoeaceae)	Whole plant	51
Bulbine latifolia (L.f.) Spreng. (Asphodelaceae)	Leaves and roots	57

Bulbine natalensis Mill. (Asphodelaceae)	Roots	[49]
Bulbine frutescens (L.) Willd. (Asphodelaceae)	Roots	[49]
Cadaba aphylla (Thunb.) Wild (Capparaceae)	Leaves and stems	[52]
Callilepis laureola DC. (Asteraceae)	Roots	[53]
Cannabis sativa L. (Cannabaceae)	Leaves	[54]
Carica papaya L. (Caricaceae)	Roots	[53]
Carpobrotus edulis (L.) N.E.Br. (Aizoaceae)	Leaves Leaves, sap and fruits	[53] [52]
Catha edulis (Vahl) Endl. (Celastraceae)	Leaves, roots and stems	[54]
Catharanthus roseus (L.) G. Don. (Apocynaceae)	Leaves and twigs Leaves	[54] [49]
Centella asiatica (L.) Urb. (Apiaceae)	Roots	[53]
Chilianthus olearaceus Burch. (Buddlejaceae)	Leaves and twigs	[49]
Chironia baccifera L. (Gentianaceae)	Whole plant	[54]
Chrysocoma ciliata L. (Asteraceae)	Leaves and roots	[52]
Cinnamomum cassia Blume (Lauraceae)	Bark	[58]
Cissampelos capensis L.f. (Menispermaceae)	Leaves Rhizomes	[54] [59]
Convolvulus capensis Burm. f. (Convolvulaceae)	Bulbs	[52]
Conyza scabrida DC. (Asteraceae)	Leaves	[60]
Crassula muscosa L. (Crassulaceae)	Leaves, stems, flowers, and roots	[52]
Cucurbita pepo L. (Curcuribitaceae)	Leaves and stems	[58]
Cussinia spicata Thunb. (Araliaceae)	Roots	[53]
Cymbopogon citratus (DC.) Stapf. (Poaceae)	Whole plant	[58]
Dianthus thunbergii S.S. Hooper (Caryophyllaceae)	Roots	[51]
Dicerothamnus rhinocerotis (L.f.) Koek. (Asteraceae)	Leaves and stems Leaves	[52] [60]
Elaeodendron transvaalense (Burtt Davy) R.H. Archer (Celastraceae)	Bark	[21]
Englerophytum magalismontanum (Sond.) T.D.Penn. (Sapotaceae)	Bark	[53]
Euclea natalensis A.DC. (Ebenaceae)	Bark and roots	[21]
Euclea undulata Thunb. (Ebenaceae)	Roots	[21]
Euryops abrotanifolius (L.) DC. (Asteraceae)	Leaves and stems	[52]
Ficus carica L. subsp. rupestris (Hausskn.) Browicz (Dncir) (Moraceae)	Roots	[53]
Galium tomentosum Thunb. (Rubiaceae)	Roots	[61]

Gethyllis namaquensis (Schönland) Oberm. (Amaryllidaceae)	Bulbs	[53]
Gnidia deserticola Gilg (Thymelaeaceae)	Leaves, stems and roots	[52]
Harpagophytum procumbens (Burch.) DC. ex. Meisn. (Pedaliaceae)	Corms and roots	[59]
Helichrysum caespititium (DC.) Sond. ex Harv. (Asteraceae)	Whole plant	[53]
Helichrysum gymnocomum DC. (Asteraceae)	Leaves	[51]
Helichrysum nudifolium (L.) Less. (Asteraceae)	Leaves and roots	[49]
Helichrysum odoratissimum L. Sweet (Asteraceae)	Whole plant	[49]
Helichrysum petiolare Hilliard & B.L. Burtt (Asteraceae)	Whole plant	[49]
Hermannia quartiniana A. Rich. (Sterculiaceae)	Roots	[53]
Heteromorphica arborescens Hochst. ex A. Rich. (Apiaceae)	Leaves and roots	[49]
Hoodia currorii (Hook.) Decne. (Asclepiadaceae)	Stems	[59]
Hoodia gordonii (Masson) Sweet ex Decne. (Apocynaceae)	Stems (inner stem)	[52]
Hypoxis argentae Harv. Ex Baker (Hypoxidaceae)	Corms	[51]
Hypoxis colchicifolia Baker (Hypoxidaceae)	Corms	[49]
Hypoxis hemerocallidea Fisch., C.A. Mey. & Avé-Lall (Hypoxidaceae)	Corms Corms	[49] [58]
Hypoxis iridifolia Baker (Hypoxidaceae)	Tuber	[53]
Kedrostis nana Cogn. (Cucurbitaceae)	Underground tuber Root	[21] [50]
Kirkia wilmsii Engl. (Kirkiaceae)	Tuber	[53]
Lannea edulis (Sond.) Engl. (Anacardiaceae)	Bark of the woody underground rootstock	[21]
Lauridia tetragona (L.f.) R.H. Archer (Celastraceae)	Barks	[51]
Leonotis leonurus (L.) R.Br. (Lamiaceae)	Leaves and flowers Leaves roots and flowers	[60] [52]
Lessertia frutescens (L.) Goldblatt & J.C. Manning (Fabaceae)	Leaves	[52]
Lessertia microphylla (Burch. ex DC.) Goldblatt & J.C. Manning (Fabaceae)	Roots	[53]
Lichtensteinia lacera Cham. & Schltdl. (Apiaceae)	Leaves and stems	[52]
Mentha longifolia (L.) L. (Lamiaceae)	Leaves and stems	[52]

Mimusops zeyheri Sond. (Sapotaceae)	Leaves	[53]
Momordica balsamina L. (Cucurbitaceae)	Stems and flowers	[54]
Momordica charantia L. (Cucurbitaceae)	Leaves	[53]
Nuxia floribunda Benth. (Loganiaceae)	Bark and roots	[58]
Momordica foetida Schumach. (Cucurbitaceae)	Whole plant	[54]
Moringa oleifera Lam. (Moringaceae)	Leaves and seeds	[53]
Nymphaea nouchali Burm.f. var. *caerulea* (Savigny) Verdc. (Nymphaeaceae)	Seeds	[21]
Pelargonium antidysentericum (Eckl. & Zeyh.) Kostel. (Geraniaceae)	Roots	[52]
Persea americana Mill. (Lauraceae)	Roots	[53]
Petroselenium crispum Mill. (Apiaceae)	Leaves	[60]
Plumeria obtusa L. (Apocynaceae)	Leaves	[53]
Pteronia divaricata (P. Bergius) Less. (Asteraceae)	Whole plant	[21]
Punica granatum L. (Lythraceae)	Roots	[53]
Opuntia ficus-indica (L.) Mill. (Cactaceae)	Roots	[53]
Ornithogalum longibracteatum Jacq. (Hyacinthaceae)	Bulbs	[62]
Psidium guajava L. (Myrtaceae)	Leaves and roots	[54]
Ricinus communis L. (Euphorbiaceae)	Leaves	[60]
Rosmarinus officinalis L. (Lamiaceae)	Drink like a tea	[61]
Ruta graveolens L. (Rutaceae)	Leaves	[60,62-63]
Schkuhria pinnata (Lam.) Cabrera (Asteraceae)	Whole plant	[21]
Sclerocarya birrea (A.Rich.) Hochst. subsp. c*affra* (Sond.) Kokwaro (Anacardiaceae)	Stems, bark and roots Stem and bark Bark	[54] [64] [65]
Searsia burchellii (Sond. ex Engl.) Moffett. (Anacardiaceae)	Leaves, stems, and roots	[52]
Senna alexandrina Mill. (Caesalpiniaceae)	Leaves	[58]
Solanum aculeastrum Dunal (Solanaceae)	Roots	[51]
Spirostachys africanus Sond. (Euphorbiaceae)	Bark	[21]
Strychnos henningsii Gilg (Loganiaceae)	Bark	[51]
Sutherlandia frutescens (L.) R. Br. (Fabaceae)	Leaves Leaves and stems Leaves	[64] [60] [21]
Tagetes minuta L. (Asteraceae)	Leaves	[52]
Tarchonanthus camphoratus L. (Asteraceae)	Leaves or soft twigs Roots	[62] [53]

Terminalia sericea Burch. ex DC. (Combretaceae)	Stem bark	[57]
Triumfetta sp. (Tilliaceae)	Roots	[53]
Tulbaghia alliacea L.f. (Alliaceae)	Roots	[51]
Tulbaghia violacea Harv. (Alliaceae)	Whole plant Leaves and roots	[62] [52]
Tylecodon paniculatus (L.f.) Toelken (Crassulaceae)	Leaves and stems	[52]
Vinca major L. (Apocynaceae)	Leaves, roots and stems	[54]
Vernonia oligocephala Katt (Asteraceae)	Leaves, twigs and roots Leaves	[49] [60]
Vernonia amygdalina Delile (Asteraceae)	Leaves	[49]
Warburgia salutaris (G.Bertol.) Chiov. (Canellaceae)	Stem bark	[21]
Ziziphus mucronata Willd. (Rhamnaceae)	Leaves	[21]

Among the listed antidiabetic plants there are plants that have not been studied adequately (phytochemical and biological activity studies) to validate the antidiabetic activity claimed.[21]

2.4.2 Antidiabetic compounds isolated from plants

In plants there are chemicals with diverse chemical activities, and these compounds can act through different mechanisms of action, offering therapeutic alternatives for the treatment of diseases, including diabetes.[34] Preliminary research on antidiabetic compounds found in South African medicinal plants with antidiabetic activity have been conducted and is still conducted, to adequately document the active principles in the medicinal plants with an aim of corroborating medicinal claims of the plants and provide possible new antidiabetic agents. Some plants used in South Africa for diabetes are discussed in the following paragraphs.

Catharanthus roseus (L.) G. Don. (Apocynaceae), a plant originally from Madagascar that is widespread in South Africa, is used for the management of diabetes.[49,54] Phytochemical investigations on the plant have revealed the presence of various alkaloids such as catharanthine **(2.11)**, vindoline **(2.12)**, and leurosine **(2.13)** with antidiabetic activity.[21]

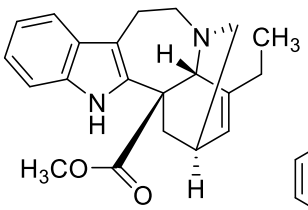

Catharanthine **(2.11)**

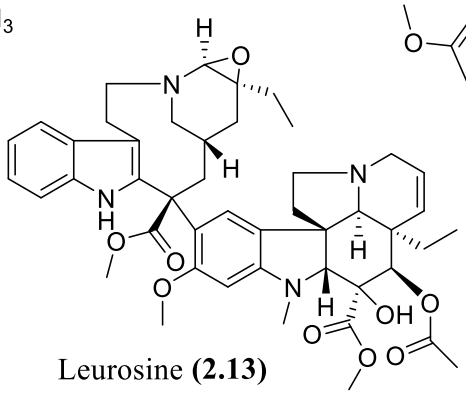

Leurosine **(2.13)**

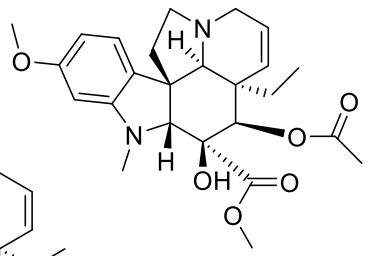

Vindoline **(2.12)**

In *Sutherlandia frutescens* (L.) R. Br. (Fabaceae), the antidiabetic activity is attributed to the presence of a cyclic polyol, D-pinitol **(2.14)**.[57] D-Pinitol is a therapeutic compound used in the management of diabetes mellitus.[66] An *in vivo* study on rats conducted by Gao et al.[66] to elucidate the mechanism of action associated with the antidiabetic effect of the compound, showed that D-pinitol played a positive role in the regulation of insulin-mediated glucose utilisation in the liver through translocation and activation of the PI3K/Akt signalling pathway.

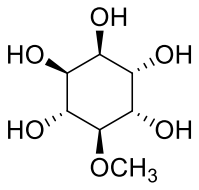

D-Pinitol **(2.14)**

The South African indigenous plant *Leonotis leonurus* (L.) R.Br. (Lamiaceae), also known as wild dagga,[67] is a medicinal herb commonly used as a Zulu, Xhosa, and Sotho traditional medicine in the treatment of several diseases and ailments, including diabetes mellitus.[60] The plant has been found to contain the diterpenoid lactones premarrubiin **(2.15)** and marrubiin **(2.16)**. Marrubiin **(2.16)** is one of the active principles in the plant, since it can enhance insulin secretion, according to an *in vivo* conducted study on rat models.[68] Marrubiin **(2.16)** is a potential therapeutic lead compound, owing to its considerable antidiabetic, anti-atherogenic and anti-inflammatory properties.[52,68]

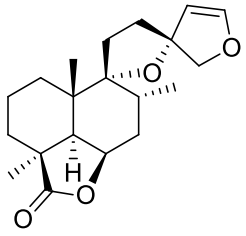

Premarrubiin **(2.15)**

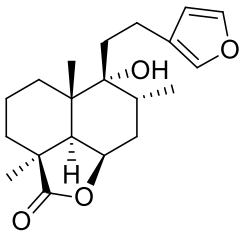

Marrubiin **(2.16)**

Psidium guajava L. (Myrtaceae) commonly known as guava, is among the antidiabetic plants used in South Africa.[54] According to the literature, the guava plant extracts possess hypoglycaemic activity.[54] Previous studies on the plant showed that the hypoglycaemic activity of the extracts comes as a result of the chemical compounds present in the plant, i.e. pentacyclic terpenoids, tannins, flavonoids (i.e. guiajaverin **(2.17)**, quercetin **(2.18)**, and other compounds, e.g. a polyphenol, ellagic acid **(2.19)**).[67,69]

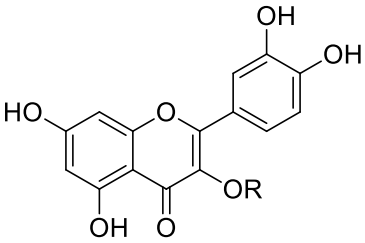

Guiajaverin **(2.17)**: R = L-arabinose
Quercetin **(2.18)**: R = L-rhamnoside

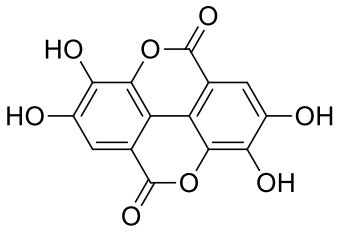

Ellagic acid **(2.19)**

Terminalia sericea Burch. ex DC. (Combretaceae), commonly known as the silver cluster-leaf,[21] has also been investigated for its active antidiabetic principles and several active compounds were obtained, i.e. β-sitosterol **(2.20)**, 3-*O*-acetyl-β-sitosterol **(2.21)**, stigma-4-ene-3-one **(2.22)** and the triterpenoid lupeol **(2.23)**.[23]

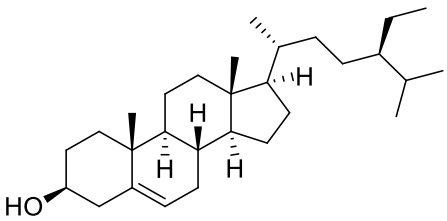

β-Sitosterol **(2.20)**

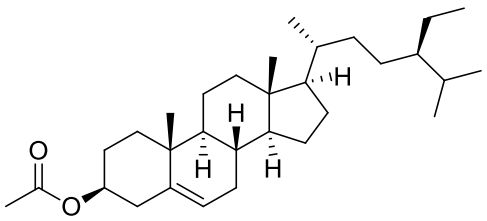

3-*O*-acetyl-β-sitosterol **(2.21)**

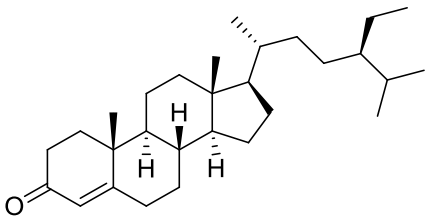

Stigma-4-ene-3-one **(2.22)**

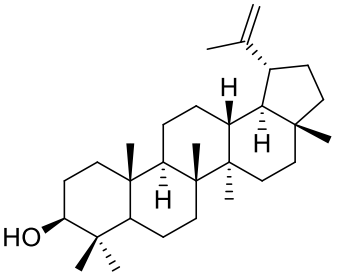

Lupeol **(2.23)**

In South Africa, *Euclea undulata Thunb. (*Ebenaceae) (commonly known as guarri), is used by herbalists and traditional healers from Limpopo (Venda region) to treat diabetes.[21] In the *in vitro* studies by Deutschländer et al.[22] on C2C12 myocytes, it was found that epicatechin **(2.25)** has hypoglycaemic effects. A novel triterpenoid, 3-*O*-(5-hydroxy feruloyl)-α-amyrin **(2.24)**, isolated from the root bark of the plant is an α-glucosidase inhibitor with an IC_{50} value of 7.76 μM, comparable to the positive control acarbose with an IC_{50} value of 7.35 μM.[22]

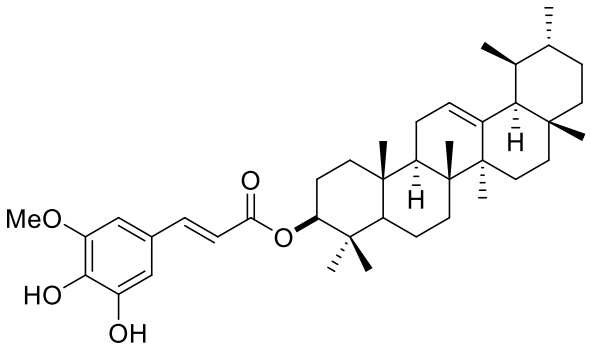

3-*O*-(5-hydroxy feruloyl)-α-amyrin **(2.24)**

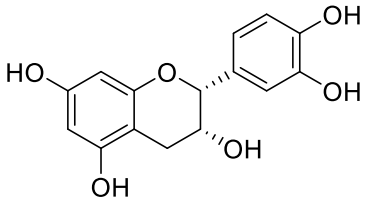

Epicatechin **(2.25)**

Despite the investigations discussed above, there is still a substantial number of unexplored South African medicinal plants in terms of the active compounds, as it can be seen from **Table 2.2**, and this calls for more phytochemical and biological studies on the medicinal plants.

2.5 TRITERPENOIDS AND DIABETES MELLITUS

Secondary metabolites are diverse naturally occurring compounds, and these compounds are classified according to the different biosynthetic origins. Terpenoids are formed by two pathways, the mevalonic acid (MVA) pathway or the methylerythritol phosphate (MEP) pathway, which generally synthesises the terpenoids from C_5 subunits, i.e. isopentenyl pyrophosphate (IPP) or dimethylallyl pyrophosphate (DMAPP).[70] Triterpenoids consist of a characteristic C_{30} backbone, although triterpenoids with less or more than 30 carbon atoms have been reported, since these can arise from either alkylation or degradation of the triterpene parent compound.[71] The first triterpenoid that was isolated is betulin **(2.26)**, which was obtained by Lowitz in 1788 from birch (*Betula sp.*) tree bark and was named in 1831 by Mason.[71]

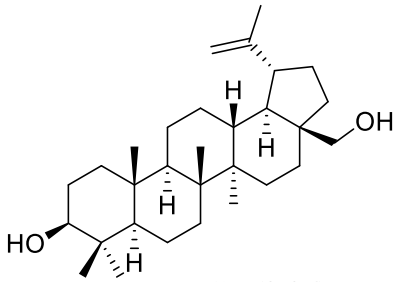

Betulin **(2.26)**

Several triterpenoids with biological activities have been identified from medicinal plants, e.g. the pentacyclic triterpenoids betulinic acid, glycyrrhetinic acid, oleanolic acid, and ursolic acid, and the compounds have been intensively investigated for the promising anti-carcinogenic activities.[72] Owing to the biological activities, terpenoids, in general, have been investigated extensively, and amongst other, have been found to possess antidiabetic activity.[73] Over the years, several *in vitro*, *in vivo*, and *in silico* studies on triterpenoids have been conducted and showed that these compounds are promising multi-target antidiabetic agents.

2.5.1 Postprandial hyperglycaemia mitigation by triterpenoids

In the management of diabetes, one of the important strategies is the management of postprandial rise of blood sugar levels.[74] According to American Diabetes Association (ADA), this is usually achieved through inhibition of carbohydrate metabolism enzymes, the action of rapid insulin secretagogues (i.e. promote insulin secretion), and also rapid-acting

insulin analogues.[74] Investigations of the inhibition of carbohydrate metabolism enzymes by triterpenoids, together with studies evaluating triterpenoids as insulin secretagogues, have been reported.

Table 2.3. Triterpenoid inhibitors of α-amylase and α-glucosidase.

Compound	**Enzyme**	**IC_{50}**	**Plant (family)**	**References**
Oleanolic acid **(2.28)**-ursolic acid **(2.27)** mixture (2:1)	α-amylase	4.41 [a]	*Phyllanthus amarus* Schumach. & Thonn. (Euphorbiaceae)	[19]
Oleanolic acid **(2.28)** Arjunolic acid **(2.29)** Maslinic acid **(2.30)** Asiatic acid **(2.31)** Corosolic acid **(2.32)** 23-Hydroxyursolic acid **(2.33)**	α-glucosidase	6.29 [b] 18.63 5.52 30.03 3.53 8.14	*Lagerstroemia speciose* (L.) Pers. (Lythraceae)	[75]
1,10-*seco*-3β,10α,23-Trihydroxyolean-12-ene-1,28-dioic acid 1,23-lactone **(2.34)** 3β,12α-Dihydroxyoleanan-28,13β-olide **(2.35)** 2,3-*seco*-20(29)-Lupene-2,3-dioic acid **(2.36)**	α-glucosidase	96.2 [a] 29.8 62.1	*Fagus hayatae* Palib ex Hayata (Fagaceae)	[76]
Pistagremic acid **(3.37)**	α-glucosidase	89.12 [a]	*Pistacia integerrima* J.L. Stewart ex Brandis (Anacardiaceae)	[77]
Euscaphic acid **(2.38)** *p*-Coumaroylursolic acid **(2.39)**	α-glucosidase	0.67 [c] 0.62	*Sanguisorba tenuifolia* var. Alba (Rosaceae)	[78]

Ursolic acid **(2.27)** 3β-Hydroxy-30-methoxy-6-oxo-urs-12, 19 (20)-dien-28-oic acid **(2.40)**	α-glucosidase	16 [a] 49	*Uncaria laevigata* Wall. ex G. Don (Rubiaceae)	[79]

[a] IC_{50} values in μM
[b] IC_{50} values in μg/mL
[c] IC_{50} values in mM

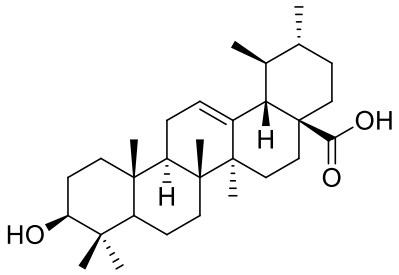

Ursolic acid **(2.27)**

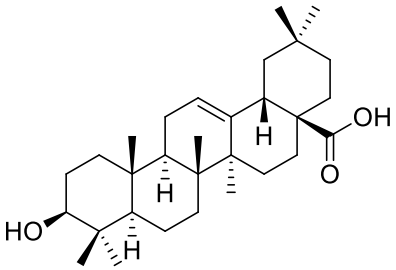

Oleanolic acid **(2.28)**

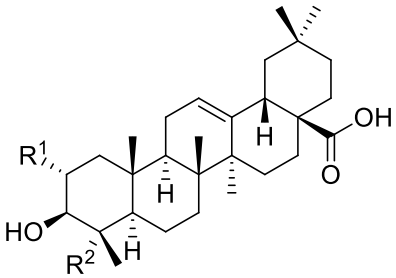

Arjunolic acid **(2.29)**: R^1 = OH, R^2 = CH_2OH
Maslinic acid **(2.30)**: R^1 = OH, R^2 = CH_3

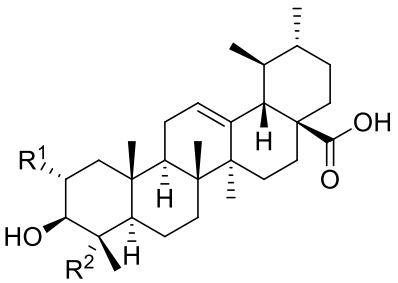

Asiatic acid **(2.31)**: R^1 = OH, R^2 = CH_2OH
Corosolic acid **(2.32)**: R^1 = OH, R^2 = CH_3
23-Hydroxyursolic acid **(2.33)**: R^1 = H, R^2 = CH_2OH

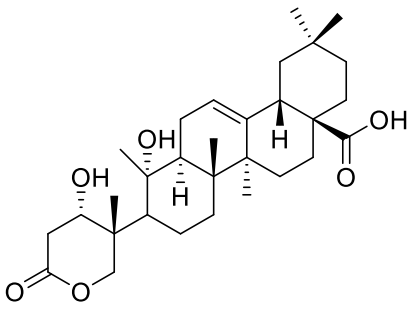

(2.34)

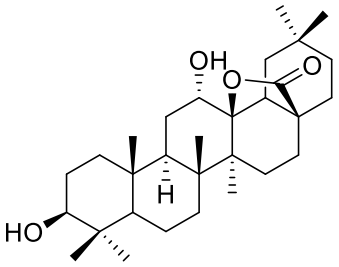

(2.35)

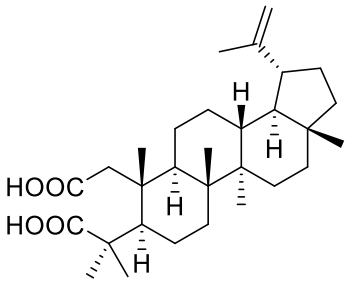

(2.36)

(2.34): 1,10-*seco*-3β,10α,23-Trihydroxyolean-12-ene-1,28-dioic acid 1,23-lactone

(2.35): 3β,12α-Dihydroxyoleanan-28,13β-olide

(2.36): 2,3-*seco*-20(29)-Lupene-2,3-dioic acid

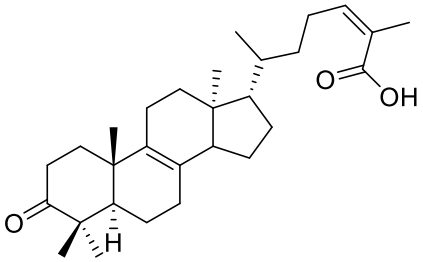

Pistagremic acid **(2.37)**

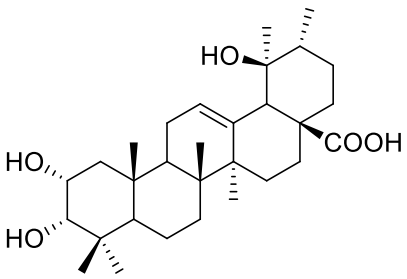

Euscaphic acid **(2.38)**

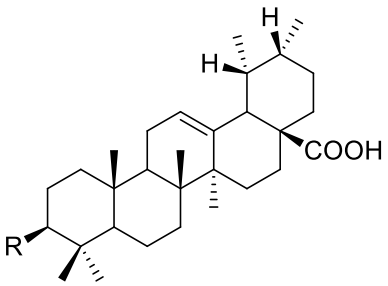

3-*O*-(*p*-Coumaroyl)-ursolic acid **(2.39)**
R = β-*O*-coumaroyloxy

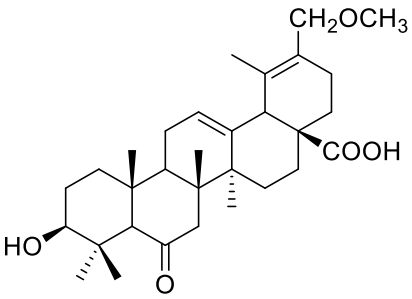

3β-Hydroxy-30-methoxy-6-oxo-urs-12,19(20)-dien-28-oic acid **(2.40)**

In some studies, tetracyclic triterpenoids are promising insulin secretagogues. Two lanostane triterpenoids were isolated from the bulbs of *Prosthechea michuacana* (Lex.) W.E. Higgins

(Orchidaceae) and were identified as 24-hydroxy-24-methyl-5α-lanosta-9(11),25-dien-3α-acetate **(2.41)** and 24-hydroxy-24-methyl-5-lanosta-9(11)-en-3α-acetate **(2.42)** and were found to reduce blood glucose by increasing insulin secretion and protect pancreatic β-cells from degradation in streptozotocin-nicotinamide-induced mildly diabetic mice.[80] Ma et al.[81] isolated a novel cucurbitane-type triterpenoid glycoside, momordicoside U **(2.43)** from *Momordica charantia* L. (whole plant), and the compound improved insulin secretion *in vitro*.

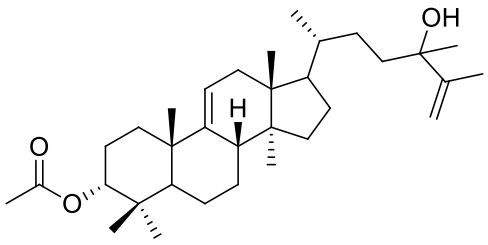

(2.41)

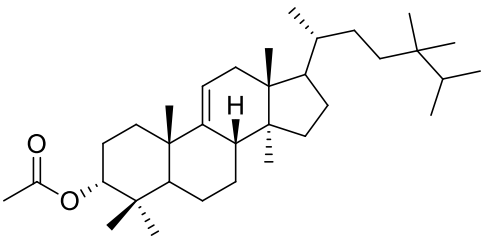

(2.42)

(2.41): 24-hydroxy-24-methyl-5α-lanosta-9(11),25-dien-3α-acetate
(2.42): 24-hydroxy-24-methyl-5-lanosta-9(11)-en-3α-acetate

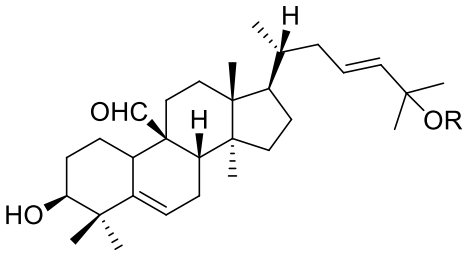

Momordicoside U **(2.43)**: R = Glc

2.5.2 Triterpenoids as protein tyrosine phosphatase 1B (PTP 1B) inhibitors

As discussed previously in diabetes molecular therapeutic targets (section **2.3.2**), PTP1B is a promising target for the management of type 2 diabetes mellitus and related metabolic disorders, like obesity. As a result, several triterpenoids have been evaluated for their PTP1B inhibitory activity. From the studies conducted, a variety of potent compounds were isolated from medicinal plants (see **Table 2.4.**).

Table 2.4. Triterpenoid inhibitors of PTP1B.

Compound	**IC_{50} (μM)**	**Plant (family)**	**References**
16α-Acetoxy-22α-angeloyloxy-3β,15α,28-trihydroxyolean-12-ene	4.87	*Camellia crapnelliana* Tutcher (Theaceae)	[82]
15α-Acetoxy-22α-angeloyloxy-3β,16α,28-trihydroxyolean-12-ene	7.40		
22-*O*-Angeloyl-A1-barrigenol	2.56		
Camelliagenin A	8.93		
3β,11α,13β-Trihydroxyolean-12-one	1.34		
Lupeol **(2.23)**	3.68		
Maslinic acid **(2.31)**	3.21	*Miconia albicans* (Sw.) Steud. (Melastomataceae)	[83]
3-*epi*-Sumaresinolic acid	2.87		
Sumaresinolic acid	1.84		
3-*O-cis-p*-Coumaroylmaslinic acid	0.46		
3-*O-trans-p*-Coumaroylmaslinic acid	1.08		
3-*O-trans-p*-Coumaroyl-2α-hydroxydulcioic acid	1.6		
Oleanolic acid **(2.28)**	2.88		
Ursolic acid **(2.27)**	2.18		
β-Acetoxyolean-12-en-28-acid	7.8	*Styrax japonicus* Siebold & Zucc. (Styracaceae)	[84]
3β-Acetoxyolean-12-en-28-aldehyde	9.3		
Lupenone Lupeol **(2.23)**	13.7 5.6	*Sorbus commixta* Hedl. (Rosaceae)	[85]
Ursolic acid **(2.27)** Oleanolic acid **(2.28)**	4.1 14.4	*Sambucus adnate* Wall. ex DC. (Adoxaceae)	[86]

Rotungenic acid Pomolic acid **(2.45)** 24-Hydroxyursolic acid Ursolic acid **(2.27)** 19,24-Dihydroxyurs-12-en-3-on-28-oic acid Oleanolic acid **(2.28)** Spathodic acid	10.9 3.9 13.8 3.1 8.1 7.6 18.8	*Diospyros kaki* L.f. (Ebenaceae)	[87]
Lupenone Lupeol **(2.23)**	15 38.89	*Pueraria lobate* (Fabaceae)	[20]
Ursolic acid **(2.27)** Oleanolic acid **(2.28)** Moronic acid Morolic acid	2.3 13.2 9.5 9.1	*Phoradendron reichenbachianum* (Seem.) Oliv. (Santalaceae)	[88]
Hopane-6α,22-diol	3.7	*Lecidella carpathica* (Lecanoraceae)	[89]
3β,23-Dihydroxyursa-12,20(30)-dien-28-oic acid Ursolic acid **(2.27)** Corosolic acid **(2.32)** Rotundic acid 2α,3α,23-Trihydroxyursa-12,20(30)-dien-28-oic acid 23-Hydroxyursolic acid **(2.33)** Actinidic acid	6.3 3.1 7.0 20.1 17.4 7.4 18.0	*Rhododendron brachycarpum* G. Don (Ericaceae)	[90]
3-Oxoolean-12-en-27-oic acid 3β-Hydroxyolean-12-en-27-oic acid 3β-Hydroxyurs-12-en-27-oic acid	6.8 5.2 4.9	*Astilbe koreana* (Kom.) Nakai (Saxifragaceae)	[91]
Ursolic acid **(2.27)** Corosolic cid **(2.32)**	3.8 7.2	*Symplocos paniculate* (Thunb.) Miq. (Symplocaceae)	[92]

2α,3β-Dihydroxy-24-nor-urs-4(23),11-dien-28,13β-olide 2α,3β-Dihydroxy-24-nor-urs-4(23),12-dien-28-oic acid	29.1 5.3	*Weigela subsessilis* (Nakai) L.H. Bailey (Caprifoliaceae)	[93]
Gypensapogenin E Gypensapogenin G 3β-Hydroxyetio-17β-dammaranic Acid Gypensapogenin A Gypensapogenin B	23 24.5 13.1 19.7 24.5	*Gynostemma pentaphyllum* (Thunb.) Makino (Cucurbitaceae)	[94]

2.5.3 Other antidiabetic triterpenoids isolated from plants

Ursane-type triterpenoids, i.e. corosolic acid **(2.32)**, ilekudinol B **(2.44)**, ursolic acid **(2.27)**, and pomolic acid **(2.45)**, obtained from the leaves of *Weigela subsessilis* (Nakai) L.H. Bailey (Caprifoliaceae) were evaluated for their antidiabetic potency (i.e. glucose uptake activity) against basal and insulin-stimulated myotubes.[95] The findings labelled these triterpenoids as insulin mimetics and insulin sensitizers. In early studies, Perez et al.[96] reported that ursolic acid and oleanolic acid isolated from *Bouvardia terniflora* (Rubiaceae) lower blood glucose in *in vivo* assays on normal and alloxan-induced diabetic mice.

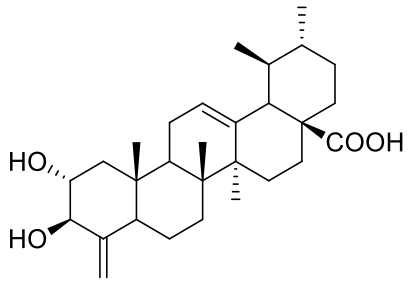

Ilekudinol B **(2.44)**

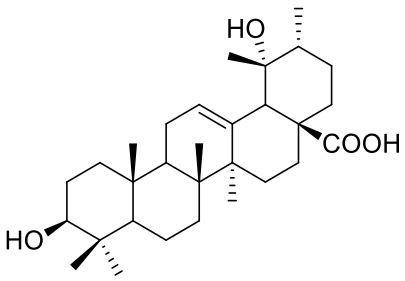

Pomolic acid **(2.45)**

Ardiles et al.,[97] in a study of friedelane-type triterpenoids isolated from the root bark of *Celastrus vulcanicola* (Celastraceae), evaluated the *in vitro* antidiabetic activity in insulin resistant Huh7 human hepatic cells, and found that 7β-hydroxy-3-oxo-D:A-friedooleanan-

28-oic acid **(2.46)** and 7β,29-dihydroxy-3-oxo-D:A-friedooleanane **(2.47)**, two novel compounds, exhibited strong insulin-mediated signalling (i.e. are insulin sensitizers).

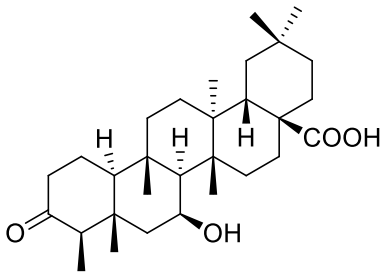

7β-Hydroxy-3-oxo-D:A-friedooleanan-28-oic acid **(2.46)**

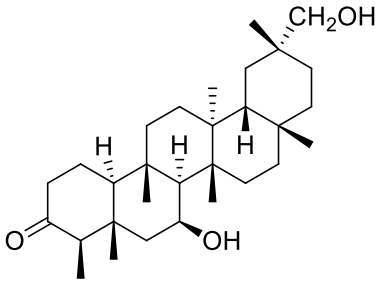

7β,29-Dihydroxy-3-oxo-D:A-friedooleanane **(2.47)**

Increased levels of the enzyme 11β-hydroxysteroid dehydrogenase type 1 (11β-HSD1) in the body may result in insulin resistance. However, the mechanism how this occurs is still not clearly understood.[98] Inhibition of the enzyme has proven to lower insulin resistance *in vivo*, which means its inhibition can be beneficial in the management of diabetes mellitus and its co-morbiditues.[98] Guo et al.[99] isolated six euphane-type triterpenoids from the roots of *Euphorbia kansui* S.L. Liou ex S.B. Ho (Euphorbiaceae) with significant inhibitory effect in human 11β-hydroxysteroid dehydrogenase type 1 (11β-HSD1). The compounds were eupane-3β,20-dihydroxy-24-ene **(2.48)**, kansuinone **(2.49)**, euphol **(2.50)**, kansenone **(2.51)**, (24*R*)-eupha-8,25-diene-3β-,24-diol **(2.52)** and (20*R*,23*E*)-eupha-8,23-diene-3β,25-diol **(2.53)**, having IC_{50} values of 34.86 nM, 1.115 μM, 16.08 nM, 2.815 nM, 26.47 nM, 15.99 nM, and 41.86 nM, respectively.

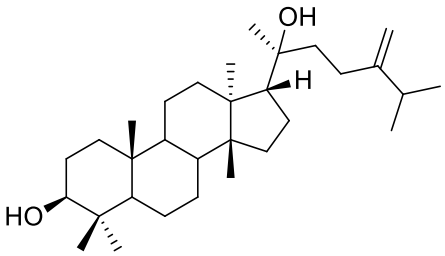

Eupane-3β,20-dihydroxy-24-ene **(2.48)**

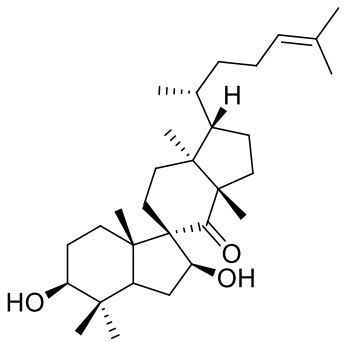

Kansuinone **(2.49)**

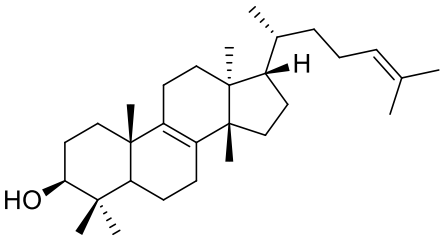

Euphol **(2.50)**

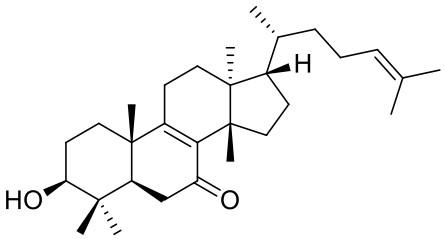

Kansenone **(2.51)**

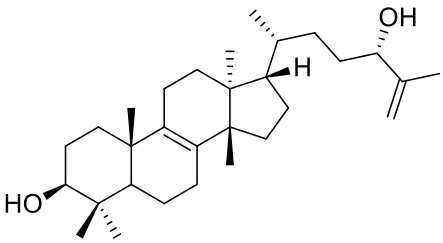

(24*R*)-Eupha-8,25-diene-3β-,24-diol **(2.52)**

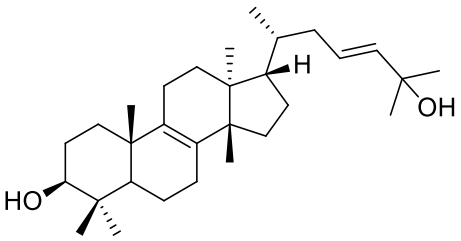

(20*R*,23*E*)-Eupha-8,23-diene-3β,25-diol **(2.53)**

In previous investigations, it was observed that the medicinal plant *Momordica charantia* L. (Cucurbitaceae) is rich in cucurbitane-type triterpenoids. Jiang et al.[100] obtained nine cucurbitane-type triterpenoids and among them (19*R*,23*E*)-5β, 19-epoxy-19-methoxycucurbita-6,23,25-trien-3β-ol **(2.54)** was evaluated for its antidiabetic potency *in vivo* against C57BL/6J diabetic alloxan-induced mice. The compound reduced blood glucose (31–48.6%) and blood lipids, i.e. triglycerides and cholesterol (13.5–42.8%).

In a recent study conducted by Han et al.[101] on the same plant, four cucurbitane-type triterpenoids were isolated, compounds **2.55**, **2.56**, **2.57**, and **2.58**.[102] The compounds improved glucose uptake in C2C12 myotubes, and also enhanced glycogen storage and lowered blood glucose levels *in vivo* in streptozotocin (STZ)-induced diabetic mice, with compound **2.56** having the most pronounced effect. Taraxerol **(2.59)**, a pentacyclic oleanane type triterpenoid isolated from the leaves of *Abroma augusta* (L.) L.f. (Malvaceae), also

proved to be potent against *in vivo* STZ-induced diabetic mice, where the compound stimulated glucose metabolism in skeletal muscles and regulated blood glycaemia in type 2 diabetic mice.[103]

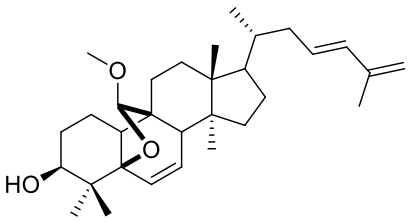

(19*R*,23*E*)-5β,19-epoxy-19-methoxycucurbita 6,23,25-trien-3β-ol **(2.54)**

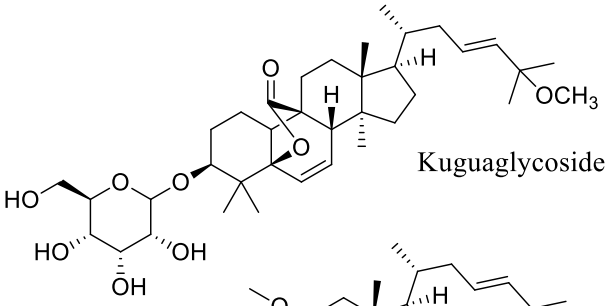

Kuguaglycoside I **(2.55)**

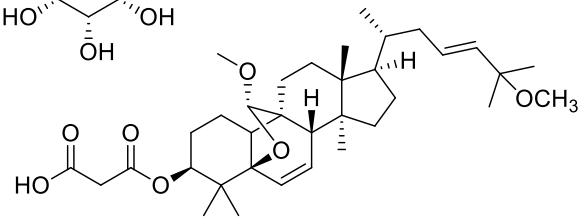

3-[(5β,19-Epoxy-19,25-dimethoxycucurbita-6,23-dien-3-yl)oxy]-3-oxopropanoic acid **(2.56)**

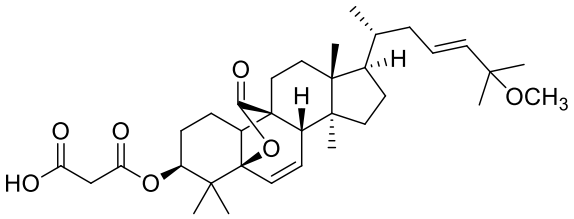

3-[(25-*O*-Methylkaravilagenin D-3-yl)oxy]-2-oxoacetic acid **(2.57)**

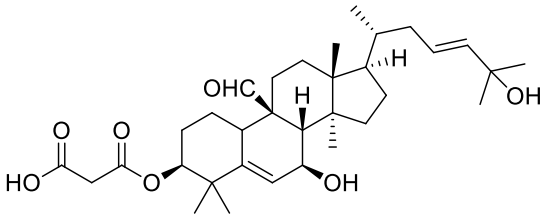

3-[(5-Formyl-7β,25-dihydroxymethoxycucurbita-5,23-dien-3-yl)-oxy]-3-oxopropanoic acid **(2.58)**

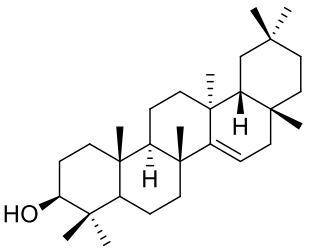

Taraxerol **(2.59)**

2.6 CHROMATOGRAPHIC METHODS USED IN THE ANALYSIS OF TRITERPENOIDS

In phytochemical analyses, chromatographic methods have proven to be extremely useful owing to their advantages, which include specificity, application in qualitative and quantitative analysis.[104] Generally the most commonly used methods are one- and two-dimensional paper chromatography, thin-layer chromatography (TLC), high-performance liquid chromatography (HPLC), gas chromatography (GC), and counter-current chromatography (CCC).[104] Among several other medicinal secondary metabolites, triterpenoids have noteworthy pharmacological properties, and as a result, their sources are of great interest in the research fields.[104]

Triterpenoid identification in phytochemistry is crucial to monitor their occurrence and their quantities in different medicinal herbs.[104] This is where the chromatography techniques and instruments come into play. However, the choice of chromatographic method may vary from studies since there are different types of triterpenoids. The variation in these compounds arises as a result of different functional groups, ranging from alcohols, aldehydes, carboxylic acids, esters, ethers, and there are also triterpenoid glycosides. In the glycosides, there is also a significant structural variation since the sugar moieties can exist in different multiplicities. Some triterpenoids exist as isomers or derivatives in the same plant, and this comes as a result of natural biosynthetic pathways.[105] In this section some of the methods used in the analysis of triterpenoids are highlighted, including TLC, GC, HPLC and related methods.

2.6.1 Thin-layer chromatography

Thin-layer chromatography is one of the most straightforward techniques, and its use in sample profiling offers all components of the mixture in question in one chromatogram.[106] This principle has been used in the evaluation of triterpenoids, with the reported TLC methods being silica thin-layer chromatography, reversed-phase (C_{18}) thin-layer chromatography and high-performance thin-layer chromatography (HPTLC). TLC is a handy tool for the preliminary profiling of the extract when analysing for the number of components present in mixtures of triterpenoids,[107] and this method can be followed by other qualitative methods or with appropriate standards, the compounds can be sometimes

identified using TLC alone. Some TLC methods like TLC-densitometry allows for the identification of triterpenoids and the technique renderers quantitative information of the respective triterpenoids present in the sample. James and Dubery[108] found the method to be useful, accessible, and cost effective in the identification of the major triterpenoids present in *Centella asiatica* (L.) Urb. (Apiaceae), namely asiatic acid, madecassic acid, asiaticoside and madecassoside.

In recent years a considerably efficient TLC method, HPTLC has gained popularity in the analysis of triterpenoids.[109] Naumoska and Vovk[110] reported a TLC-MS^2 method for identification of triterpenoids, which combines the benefits of the rapid TLC and MS, to identify compounds with a custom-built mass spectral library. In the study, for HPTLC, two phases were applied, a normal silica phase and a C_{18} reversed phase, to allow for the separation of the triterpenoids.

HPTLC, coupled with densitometry or a digital profile, has been used for the analysis of triterpenoids since it allows for qualitative and quantitative analysis of the compounds. The method is precise, fast, repeatable, specific, and cost effective.[111-112] In a study aiming to distinguish between two closely related *Isodon* plant species, *Isodon lophanthoides* and *Isodon lophanthoides* var. *gerardianus*, triterpenoid profiling of the respective species using HPTLC coupled with a digital profile provided a solution.[112] Kaur et al.[111] used HPTLC-densitometry and compound standards to analyse the triterpenoid content of five *Swertia* plant species, *S. paniculate*, *S. cordata, S. angustifolia*, *S. chirata* and *S. chirata*. The presence and relative concentrations of four pentacyclic triterpenoids, ursolic acid, oleanolic acid, betulinic acid, and lupeol was observed.

2.6.2 Gas chromatography

This method is useful in the analysis of thermally stable, volatile compounds.[113] In the analysis of triterpenoids, gas chromatography methods are among the commonly used techniques,[109] including GC-FID, GC-MS, and other hyphenated methods. In the analysis of triterpenoids from almond hulls, GC-FID was among the useful instruments where three triterpenoid esters were identified as methyl oleanolate, methyl betulinate and methyl ursolate.[114]

In the terpenoid analysis or profiling of Sicilian *Pistacia vera* L. oleoresin phytocomplex, GC-MS and GC-FID were used for qualitative and quantitative purposes respectively.[115] Burdziej et al.[116] analysed sterol and triterpenoid compositions from eight grapevine species of genus *Vitis* using GC-MS coupled with an FID detector. The GC-MS was useful in the qualitative analysis of the compounds making use of mass spectra libraries, and the FID revealed the respective quantities of the compounds.

GC-MS has also been applied on its own in the analyses of triterpenoids in several studies, owing to the availability of mass spectral databases. This allows for the identification of the compounds to some extent.[116] Courtney et al.[117] working with a methanolic *Terminalia grandiflora* leaf extract, used GC-MS to identify three lanostane and two pentacyclic triterpenoids. This was achieved by comparing the gas chromatogram and mass spectral data with GC-MS mass and spectral database **(Fig. 2.2)**. This method has been considered to be very useful for the analysis of triterpenoids in plant extracts.[118-119]

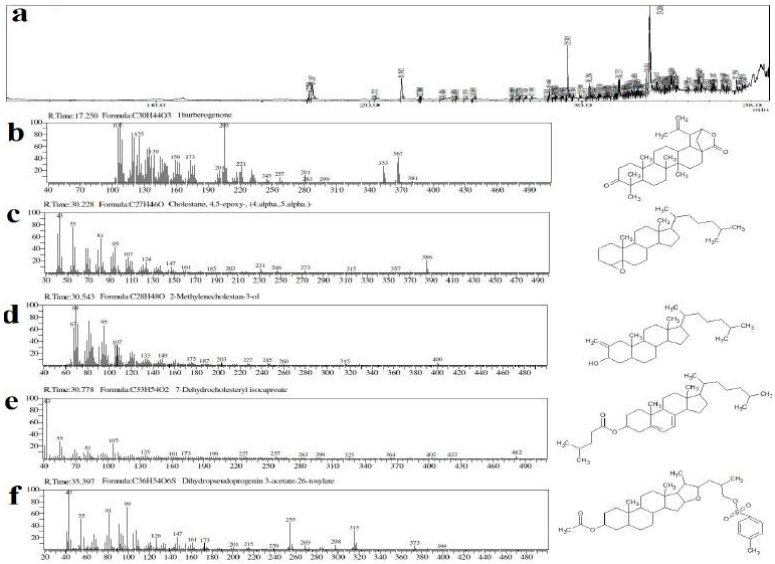

Figure 2.2. Gas chromatogram of a methanolic *Terminalia grandiflora* leaf extract (a), and spectral data and structures of the compounds identified by GC-MS.[117]

2.6.3 High-performance liquid chromatography and other chromatographic methods

HPLC, like most chromatography techniques, has separation properties and is specifically useful in the analysis of samples that are soluble in liquid(s),[106] including thermally unstable and the non-volatile compounds.[113] HPLC can be used for both the identification and quantification of compounds in mixtures.[106] The HPLC methods have been reported to be useful in the analysis of triterpenoids and related compounds, like saponins and sterols. Table 2.5 below summarises some of the studies reported.

Table 2.5. LC/HPLC chromatography methods used in the analysis of triterpenoids and related compounds.

Chromatographic method	**Plant name**	**Type of Compounds/Compounds**	**References**
LC-MS^n	S*ymplocos chinensis* (Lour.) Druce	Triterpenoid saponins	[120]
HPLC-ELSD	*Centella asiatica* (L.) Urb.	Triterpenoid glycosides (asiaticoside, madecassoside and asiaticoside-B)	[121]
HPLC-MS	*Prunus dulcis* (Mill.) D.A. Webb	Triterpenoid esters (methyl oleanolate, methyl betulinate and methyl ursolate)	[114]
HPLC-ELSD	*Chaenomeles* species (*C. cathayensis*, *C. lagenaria*, *C. thibetica*, *C. sinensis*, *C. japonica*)	Betulin, erythodiol, acetyl ursolic acid, ursolic acid, oleanolic acid, pomolic acid and betulinic acid	[122]
HPLC-MS^n	*Codonopsis lanceolate* (Siebold. & Zucc.) Benth. & Hook.f. ex Trautv.	3,28-bidesmosidic triterpenoid saponins (lancemaside A, foetidissimoside A, aster saponin Hb, lancemaside E, lancemaside B, lancemaside F, lancemaside G, lancemaside C, and lancemaside D)	[123]

HPLC-ELSD and HPLC-MS	*Achyranthes bidentata* Blume	Triterpenoid saponins (Ginsenoside Ro, chikusetsusaponin Iva, zingibroside R_1, chikusetsusaponin Iva ethyl ester, 28-desglucosyl-chikusetsusaponin Iva, PJS-1, 28-desglucosyl-chikusetsusaponin Iva butyl ester) and oleanolic acid	[124]
HPLC-UV and HPLC-APCI-MS^n	Extracts of oak, rosemary sage tomatoes, and cabbage	Triterpenoids (α-amyrin, β-amyrin, δ-amyrin, lupeol, lupeol acetate, lupenone, ursolic acid, oleanolic acid, cycloartenol and cycloartenol acetate) and sterols (sigmasterol and β-sitosterol)	[125]
HPLC-HRMS	*Quercus petraea* (Matt.) Liebl.	3-*O*-Galloylarjungenin, 24-*O*-galloylsericic acid, 3-*O*-galloylsericic acid, quercotriterpenoside VII, quercotriterpenoside VIII, quercotriterpenoside IX, quercotriterpenoside X, quercotriterpenoside XI, arjunglucoside I and 23-*O*-galloylarjungenin (11)	[105]

Yang et al.[122] reported a new HPLC-MS method developed for the analysis of triterpenoids from *Chaenomeles* species, and the method proved to be useful in the simultaneous determination of major pentacyclic triterpenoids (see **Table 2.5**) from these plant species. The identification of the compounds was achieved by comparing the extract chromatograms with the chromatogram of standards **(Fig.2.3)**.

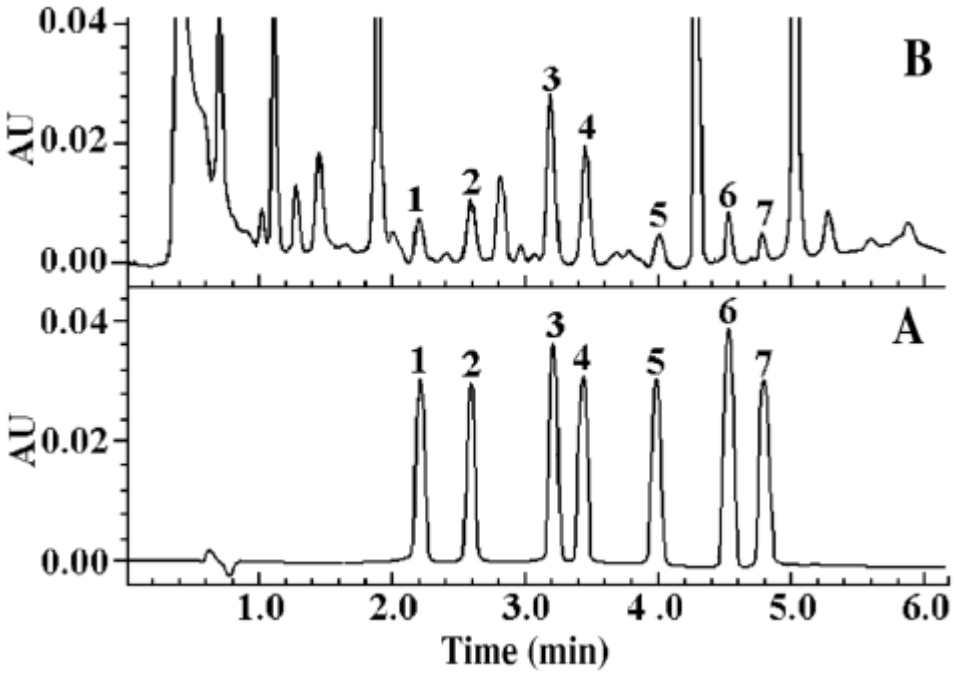

Figure 2.3. HPLC chromatogram for *Chaenomeles sinensis* extract (B) and that of the standard compounds (A).[122]

Among the useful chromatographic methods in the analysis of triterpenoids, there is also supercritical fluid chromatography (SFC). This method is somewhat similar to gas and liquid chromatography, and what is unique about it is that for a mobile phase, it uses a fluid with intermediate properties between those of gases and liquids.[126] Jarvis et al.[107] used SFC together with TLC and HPLC to determine triterpenoids in seeds of *Azadirachta indica* A. Juss. (Meliaceae) and eleven tetranortriterpenoids were identified as nimbin, desacetyl-nimbin, salannin, desacetyl-salannin, 3-tigloyl-azadirachtol, isosalanninolide, salanninolide, azadirachtin, azadirachtinin, azadirachtin I and azadirachtin D.

CHAPTER 3: PHYTOCHEMISTRY AND ANTI-DIABETIC INVESTIGATION OF *BRACHYLAENA DISCOLOR* DC

3.1 INTRODUCTION

South Africa is among the countries on the African continent that are affected by diabetes.[31] In South Africa in 2017, 1865021 diabetes cases were reported for the 18-99 year age group.[31] The diabetes epidemic demands serious attention, amongst others in the search for more therapeutic options that are accessible to populations in different regions of the world. In Africa, herbal remedies are the preferred mode of medication owing to their minimal adverse effects, accessibility, low toxicity, and affordability.[127-128] In sight of the intensive use of the herbal remedies by many people, there is a pressing need to validate the properties of the medicinal plants to ensure and improve the quality of the medication and maintain good standards.[127] South Africa, in particular, has been reported to be rich in medicinal plants used for diabetes, and this encourages research focused on the investigation of the antidiabetic principles in plants, and further understand the mechanisms of action when compared with conventional medication.[128-129] In this study, one of the South African antidiabetic medicinal plants, *Brachylaena discolor* DC, was investigated.

3.2 LITERATURE REVIEW ON *BRACHYLAENA*

3.2.1 Chemistry and pharmacology of Asteraceae

The plant family Asteraceae belongs to the flowering plants and have about 1700 genera recognised globally, and 24000-30000 recorded species.[130] Species of this plant family have been used widely as sources of medication, human edibles, rubber, pesticides, and owing to the flowering properties, as ornamental plants.[131] Asteraceae plants produce numerous phytochemicals. In earlier studies, Zdero and Bohlmann,[132] reported that out of the investigated 5000 species about 7000 compounds were isolated, including, monoterpenoids, diterpenoids, sesquiterpenoids, sesquiterpenoid lactones, triterpenoids, flavonoids, polyacetylenes, coumarins, acetophenones, phenylpropanes, benzofurans and alkaloids.[130,132] Plants and some isolates from the family have been linked with several biological activities, e.g. antioxidant, antimicrobial, antidiabetic, antispasmodic, anti-

inflammatory, and hepatoprotective activities.[133] These highlight the significance of Asteraceae species as medicinal herbs and as noteworthy sources of potential therapeutic principles.

3.2.2 *Brachylaena* genus

This genus belongs to the Asteraceae family. *Brachylaena* is known to be distributed in Madagascar, Comoro Islands, and in southern and eastern African countries, including Uganda, Kenya, Tanzania, Mozambique, Zimbabwe, Angola, Swaziland, Botswana, and South Africa.[134] Beentje,[134] in the early 2000s, reported that the genus has eleven species distributed in the locations mentioned above, but some of the species also have varieties, e.g. *Brachylaena discolor* DC and *Brachylaena ramiflora* (DC.) Humbert. The species in this genus are *B. stellulifera* Humbert, *B. perrieri* Humbert, *B. microphylla* Humbert, *B. ilicifolia* (Lam.) E. Phillips & Schweick, *B. huillensis* O. Hoffm., *B. merana* (Baker) Humbert, *B. elliptica* (Thunb.) DC., *B. glabra* (L.f.) Druce, *B. neriifolia* (L.) R. Br, *B. discolor* DC (with var. *discolor*, var. *transvaalensis* and var. *rotundata*), and *B. ramiflora* (DC.) Humbert (with var. *ramiflora*, var. *bernieri*, and var. *comorensis*).[134-135] In a later classification, all the three *B. discolor* subspecies are recognised as main species, viz. *B. discolor* DC., *B.transvaalensis* E. Phillips & Schweick, and *B. rotundata* S. Moore.[136]

Early phytochemical investigations on *Brachylaena* species has revealed the presence of a significant number of sesquiterpenoid compounds and their various derivatives.[137-142] Among the isolated phytochemicals are also pentacyclic triterpenoids, including lupeol **(2.25)**, lupeol acetate **(3.1)**, and neolupenyl acetate **(3.2)**.[142] Zdero et al.,[142] in a phytochemical analysis of two *Brachylaena* species, *B. perrieri*, and *B. huillensis*, isolated lupeol **(2.25)** and its acetate in both species. Lupeol acetate **(3.1)** and the Δ^{12} isomer, neolupenyl acetate, has also been previously isolated from *B. discolor*,[141,143] *B. transvaalensis* Hutch. ex Phill. et Schweick, and *B. rotundata*.[137]

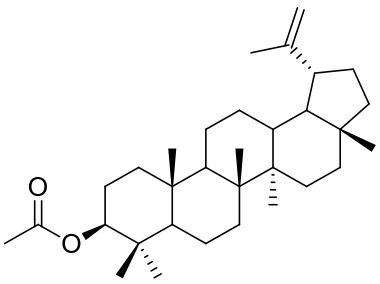

Lupeol acetate **(3.1)**

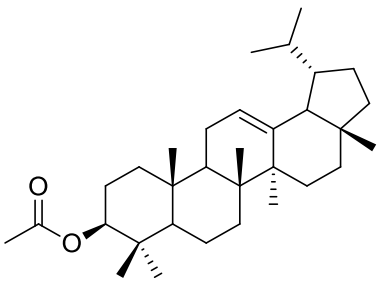

Neolupenyl acetate **(3.2)**

From a bioassay-guided isolation of compounds from *B. ramiflora*,, Chaturvedula et al.[144] reported seven triterpenoids, including two novel palmitates, kairatenyl palmitate **(3.3)** and hopenyl palmitate **(3.4)**, alongside the known triterpenoids, α-amyrin palmitate **(3.5)**, β-amyrin palmitate **(3.6)**, β-amyrin acetate **(3.7)**, lupeol acetate **(3.1)**, and lupeol **(2.25)**. The compounds were tested against A2780 human ovarian cancer cell lines but did not show significant activity.[144] In the investigation of *B. ramiflora* as a source of bioactive phytochemicals, the profile of its compounds has been evaluated in a study working with the leaf and bark medicinal preparations (infusions and decoctions).[145] *B. ramiflora* was found to contain flavonoids, tannins, monoterpenes, organic acids, and vitamins.[145] (The individual compounds were not identified).

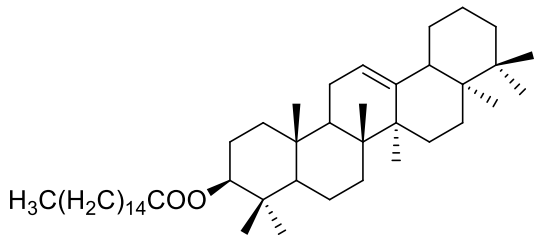

Kairatenyl palmitate **(3.3)**

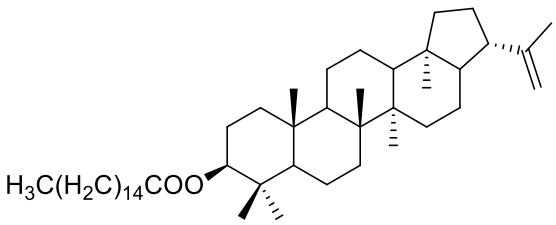

Hopenyl palmitate **(3.4)**

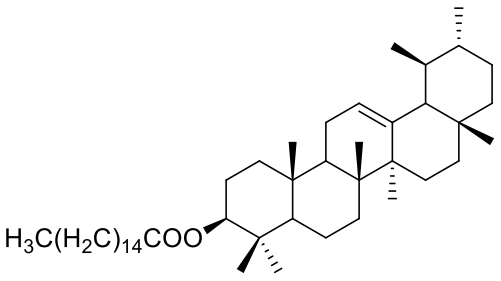

α-Amyrin palmitate **(3.5)**

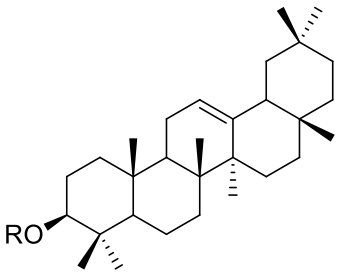

β-Amyrin palmitate **(3.6)**: R = $CH_3(CH_2)_{14}COO$

β-Amyrin acetate **(3.7)**: R = CH_3COO

3.2.3 *Brachylaena discolor* taxonomy and phytochemistry

B. discolor is commonly known in different languages as coast silver oak (English), kusvaalbos (Afrikaans), muakawura, mupasa (Shona) and iphahla/umpahla (isiZulu).[21] Depending on the environmental factors, the evergreen plant can grow to be a bushy shrub or small tree of about 10 m high.[21] Other characteristic features include dark-green (above) leathery leaves with silvery hairs below, and a leaf margin that can be entire or irregularly toothed.[21] The bark is brownish and rough, and the plant produces creamy whitish flowers which seed in a nutlet.[146] *B. discolor* is distributed in the coastal regions of South Africa and Mozambique **(Fig. 3.1)** and naturally prefers dunes and coastal places as habitat.[134,147]

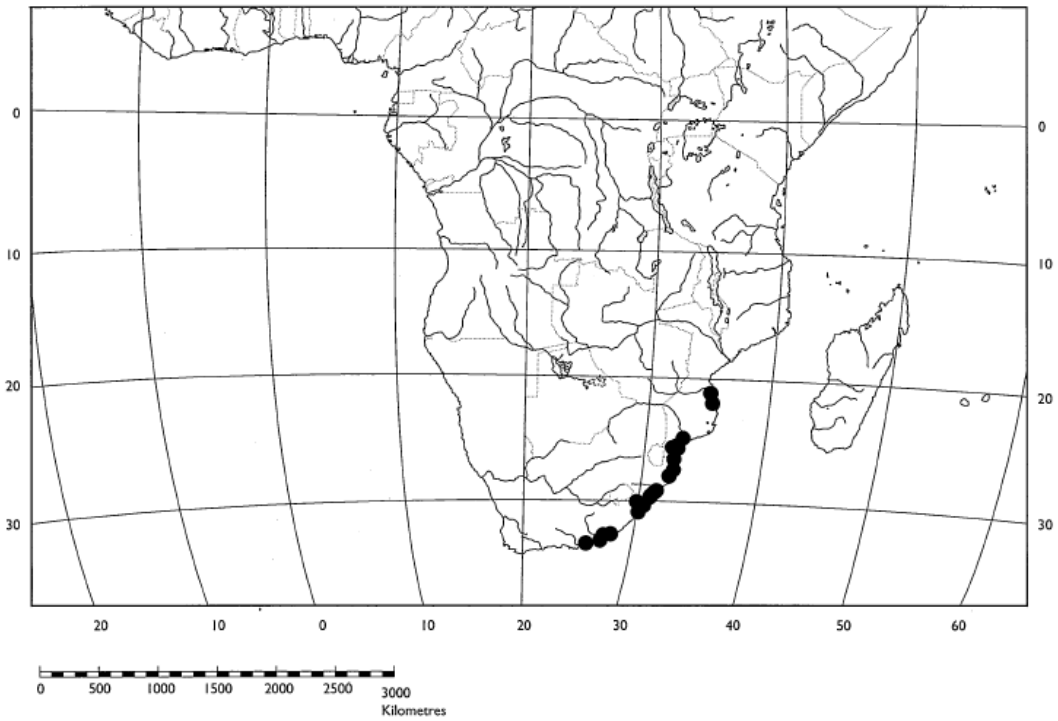

Figure 3.1. Geographical distribution of *Brachylaena discolor* (adopted from Beentje[134]).

Brachylaena species have been used in different places as medicinal herbs. *B. discolor* is used in South Africa in the management of diabetes, together with two other *Brachylaena* species, *B. ilicifolia*, and *B. elliptica* Thunb.[21,54-55] The latter was found to have hypoglycaemic activity by restoring and maintaining the normal functioning state of the β-cells and the pancreas.[148] *B. discolor* is also used in northern Maputuland (KwaZulu-Natal) for the treatment of dermatological conditions.[149]

Limited phytochemical and bioactivity studies have been performed on *B. discolor*. The hypoglycaemic effect of the extract of the plant has been evaluated. Mellem et al.[25] found that the leaf methanol extract is significantly potent in the inhibition of α-glucosidase and proved to be less toxic against cell lines. The methanol extract of the plant has also been investigated *in vivo* in streptozotocin (STZ)-induced diabetic rats, and it was observed to exert hypoglycaemic effects.[24] In a study by van der Venter et al.,[54] a *B. discolor* dichloromethane-methanol (1:1) extract was found to be potent when evaluated in glucose utilization assays using Chang liver, 3T3-L1 adipose, and C2C12 muscle cells.

Early studies on *B. discolor* revealed the presence of a sesquiterpenoid lactone, onopordopicrin **(3.8)**, which was also isolated from *B. rotundata*.[141] The sesquiterpenoid lactone was obtained from *B. discolor* along with two pentacyclic triterpenoids, lupeol acetate **(3.1)** and neolupenyl acetate **(3.2)**.[141] Compound **3.1** was also isolated from the plant in a study by Adam,[143] together with, β-sitosteryl linelonate, α-tocopherol and genkwanin 5-*O*-β-D-glucopyranoside.

Six months after commencing with the current study, Monjane et al.[150] published a paper reporting the isolation of twelve compounds from the aerial parts of *B. discolor*, including onopordopicrin **(3.8)**, its epoxide derivative (alonitelonide-8-*O*-2´,3´-isobutyrate **(3.9)**), hydroxytyrosol **(3.10)**, dihydroxysinapic acid **(3.11)**, 6´´-*O*-acetyl homoplantaginin **(3.12)**, onoporidin **(3.13)**, 3´-hydroxygenkwanin **(3.14)**, luteolin **(3.15)**, quercetin 3-*O*-glucoside-7,3´,4´-trimethyl ether **(3.16)**, quercetin 3-*O*-β-*D*-galactopyranoside **(3.17)**, eupafolin **(3.18)** and quercetin-7-galactopyranoside **(3.19)**. Onopordopicrin **(3.8)** has leishmanicidal activity when evaluated against *Leishmania amazonensis* and *Leishmania braziliensis* (IC_{50} values of 39.6 and 27.9 μM, respectively) compared to a standard compound (miltefosine) with IC_{50} values of 12.5 and 12.0 μM, respectively.

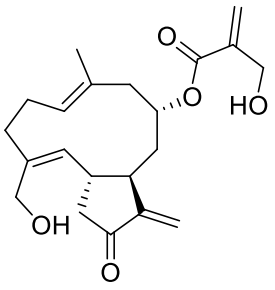

Onopordopicrin **(3.8)**

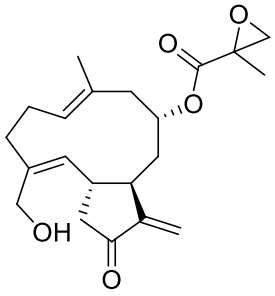

Alonitelonide-8-*O*-2',3'-isobutyrate **(3.9)**

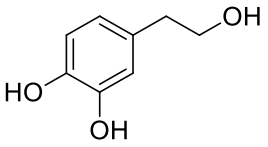

Hydroxytyrosol **(3.10)**

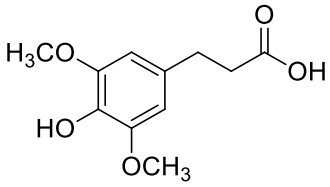

Dihydroxysinapic acid **(3.11)**

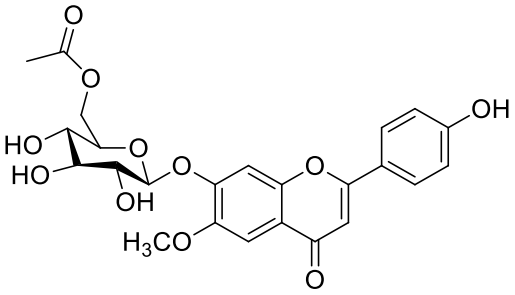

6''-*O*-Acetyl homoplantaginin **(3.12)**

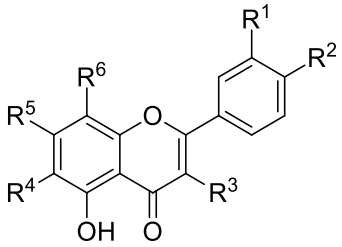

		R^1	R^2	R^3	R^4	R^5	R^6
Onoporidin **(3.13)**	:	OH	OH	H	H	OH	OCH_3
3´-Hydroxygenkwanin **(3.14)**	:	OH	OH	H	H	OCH_3	H
Luteolin **(3.15)**	:	OH	OH	H	H	OH	H
3-*O*-β-Glucoside-7,3´,4´- tri-*O*-methyl ether quercetin **(3.16)**	:	OCH_3	OCH_3	H	H	OH	OCH_3
Quercetin 3-*O*-β-*D*-galactopyranoside **(3.17)**	:	OCH_3	OCH_3	O-*glc*	H	OH	H
Eupafolin **(3.18)**	:	OH	OH	O-*gal*	H	OH	H
Quercetin 7-galactopyranoside **(3.19)**	:	H	OH	OH	H	O-*gal*	H

The reported presence of the unusual neolupenyl acetate **(3.2)** stimulated our interest in the phytochemistry of *B. discolor*. As discussed earlier, many triterpenoids show good inhibitory activity against enzymes that are molecular targets for diabetes treatment. Neolupenyl acetate **(3.2)** has never been evaluated for antidiabetic activity. The initial aim of this investigation was to isolate neolupenyl acetate **(3.2)**, amongst other triterpenoids, and to assess the compounds for antidiabetic activity.

3.3 RESULTS AND DISCUSSION

In the analysis of the triterpenoid contents of the leaf of *B. discolor*, the leaf material was extracted with dichloromethane (DCM) by maceration. The crude extract was further fractionated using vacuum-liquid chromatography (VLC) and various hexane-DCM solvent systems and methanol to afford six subfractions. The subfractions were analysed by GC-MS to identify the triterpenoids. Fractions containing triterpenoids and triterpenoid isomers (i.e. Sm-2-18B, Sm-2-18C, Sm-2-18D and Sm-2-18E) were then taken for purification using argentation column chromatography, and eight pentacyclic triterpenoids were obtained.

The purification of isomeric triterpenoids on silica gel can be a challenging task since these compounds have closely related chemical features.[125] This was observed with a mixture of triterpenoid acetates which appeared as a single spot on a silica-coated TLC plate. However, after the impregnation of the silica with $AgNO_3$, the compounds were effectively separated (see **Fig. 3.2**). The Ag^+ ions adsorbed onto the silica, form weak interactions with unsaturated centers in molecules.[151] This principle of separation is strictly dependent on the number, position, and types of unsaturated centers present in the molecules in question.[151] α-Amyrin acetate and β-amyrin acetate were not separable because the π-bond is situated in the same position of the carbon skeleton of the two compounds. All compounds were identified by 1D and 2D NMR (i.e. ^1H, ^{13}C, COSY, DEPT, HSQC and HMBC), IR, GC-MS, and HR-MS. The characterization of the compounds is described below.

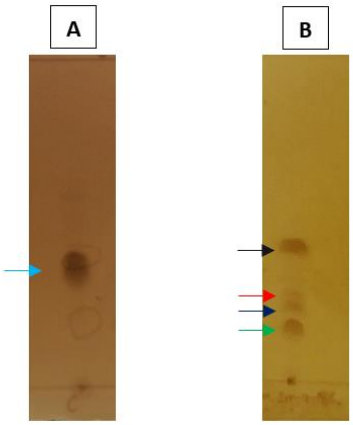

Figure 3.2. Behaviour of the unsaturated triterpenoid isomers (fraction Sm-2-18C) when run on different TLC plates, normal silica gel (A) and $AgNO_3$-impregnated silica gel (B).

3.3.1 Characterization of α-amyrin acetate (3.20) and β-amyrin acetate (3.21)

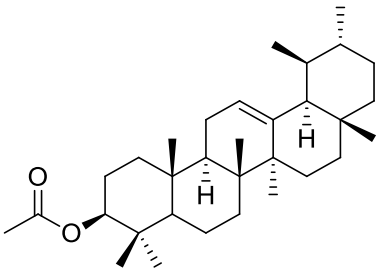

α-Amyrin acetate **(3.20)**

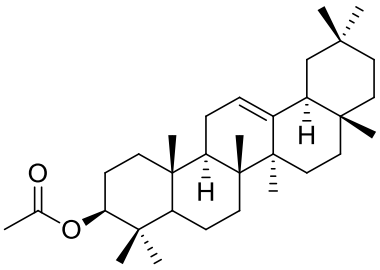

β-Amyrin acetate **(3.21)**

After the purification of fraction Sm-2-18C with argentation column chromatography, five pentacyclic triterpenoid acetates were obtained. Firstly, a mixture of α-amyrin acetate **(3.20)** and β-amyrin acetate **(3.21)** was afforded as a white amorphous solid. The mixture was evaluated for purity by GC-MS, and the chromatogram confirmed the presence of two components **(Fig. 3.3)**. The EI-MS spectra of the components (A and B) were also obtained and were used in the identification of the compounds.

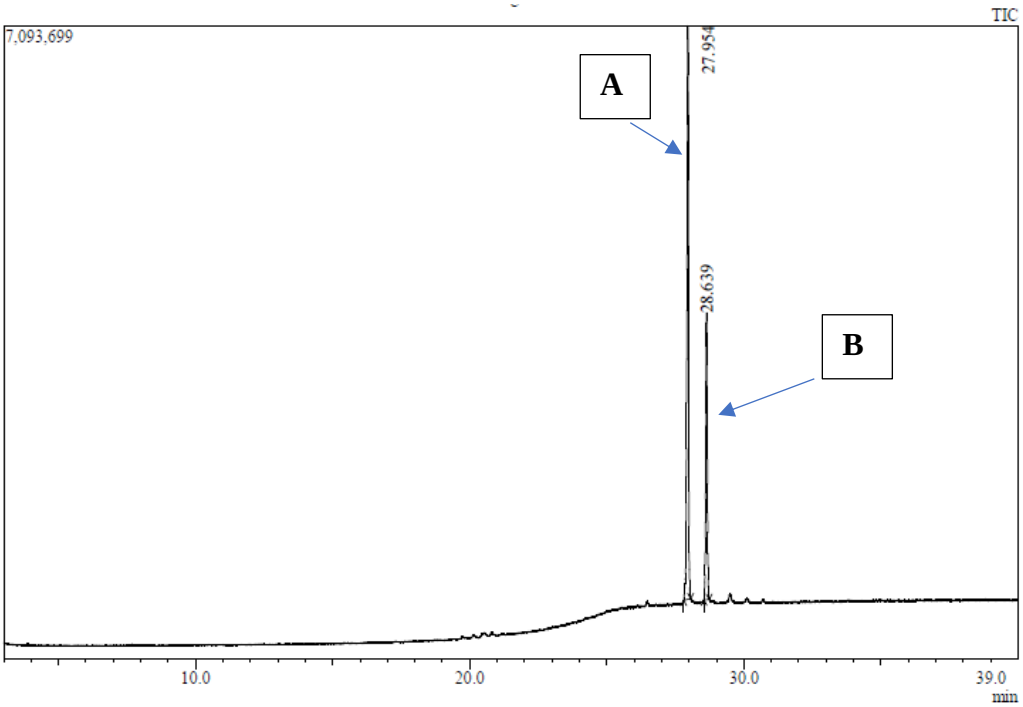

Figure 3.3. GC-MS chromatogram of the α-amyrin acetate **(3.20)** (peak B) and β-amyrin acetate **(3.21)** (peak A) mixture.

The two peaks, A and B were identified as β-amyrin acetate (R_t 27.954 min) and α-amyrin acetate (R_t 28.639 min), respectively, from their EI-MS spectra. The peak areas were used in establishing the ratio of **3.20** : **3.21**, and was determined to be about 3:7. α-Amyrin acetate **(3.20)** has an M^+ ion of *m/z* 468, which corresponds to that of β-amyrin acetate **(3.20)**, a base peak of *m/z* 218, and other characteristic fragments (i.e. *m/z* 453, 408, 249, 203, and 189). The fragments and their relative intensities are comparable with those given in the literature.[152] β-Amyrin acetate **(3.21)** also had a molecular ion of *m/z* 468, and also shared the same base peak of *m/z* 218 and similar characteristic fragments with the isomer, compound **3.20**. However, the relative intensities of the fragments of the two isomers are a major feature used in distinguishing between the two compounds.[152] For β-amyrin acetate, the *m/z* 203 has twice the intensity of *m/z* 189, whereas in α-amyrin acetate, the two fragments have about the same intensities.[153] Neohopane, neolupane, neogammacerane, oleanane, or ursane group triterpenoid hydrocarbons with a C_{12}-C_{13} double bond are known to share a base peak of *m/z* 218, which arises upon C_9-C_{11} bond cleavage and C_8-C_{14} bond cleavage.[154] Fragmentation of a ursane-type carbon skeleton is used as an example in **Scheme 3.1.**

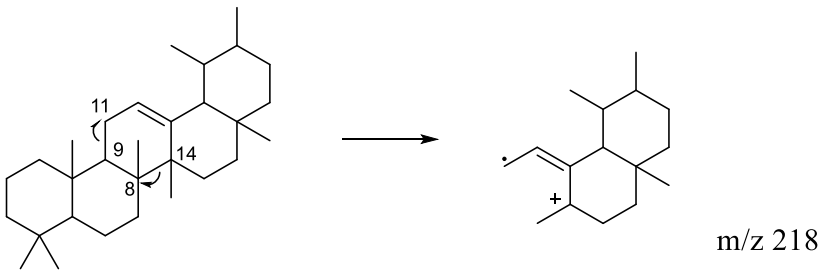

Scheme 3.1. Formation of a characteristic ursane triterpenoid MS base peak.

The mass spectra obtained for α-amyrin acetate and β-amyrin acetate, which separates on GC (**Fig. 3.4**), is given below.

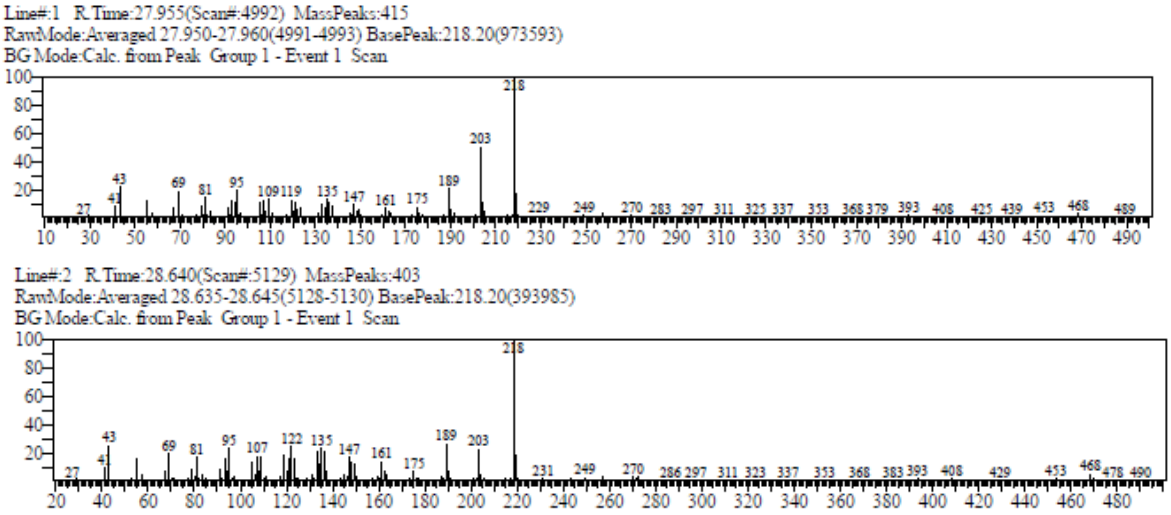

Figure 3.4. EI-MS spectra of β-amyrin acetate **(3.21)** (above) and α-amyrin acetate **(3.20)** (bottom).

The HR-ESI-(+)-MS spectrum **(Fig. 3.5)** of the mixture of the two amyrin isomers was obtained and gave an M+1 ion peak of *m/z* 469.4061, corresponding to a molecular formula of $C_{32}H_{52}O_2$ (calculated for $C_{32}H_{53}O_2$, 469.4046). The IR spectrum revealed the presence of bands at 2916.643 cm^{-1} (medium, C-H), 1731.198 cm^{-1} (sharp, C=O), and 1246.646 cm^{-1} (sharp, C-O).[155]

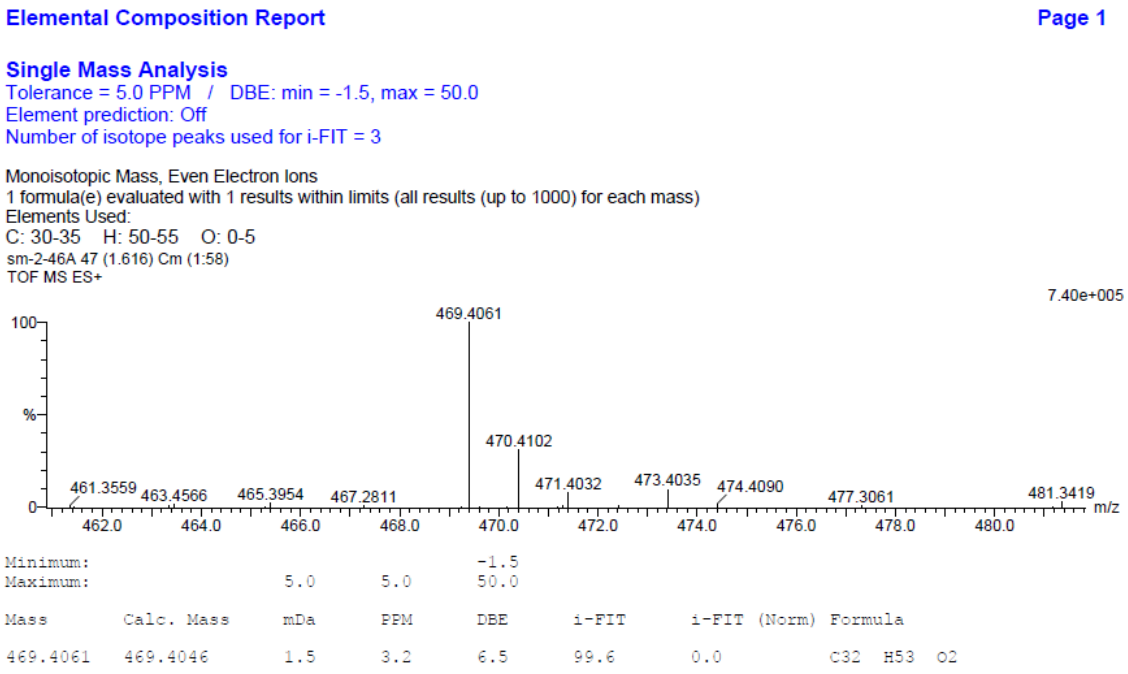

Figure 3.5. HR-ESI-(+)-MS spectrum of the mixture of α-amyrin acetate **(3.20)** and β-amyrin acetate **(3.21)**.

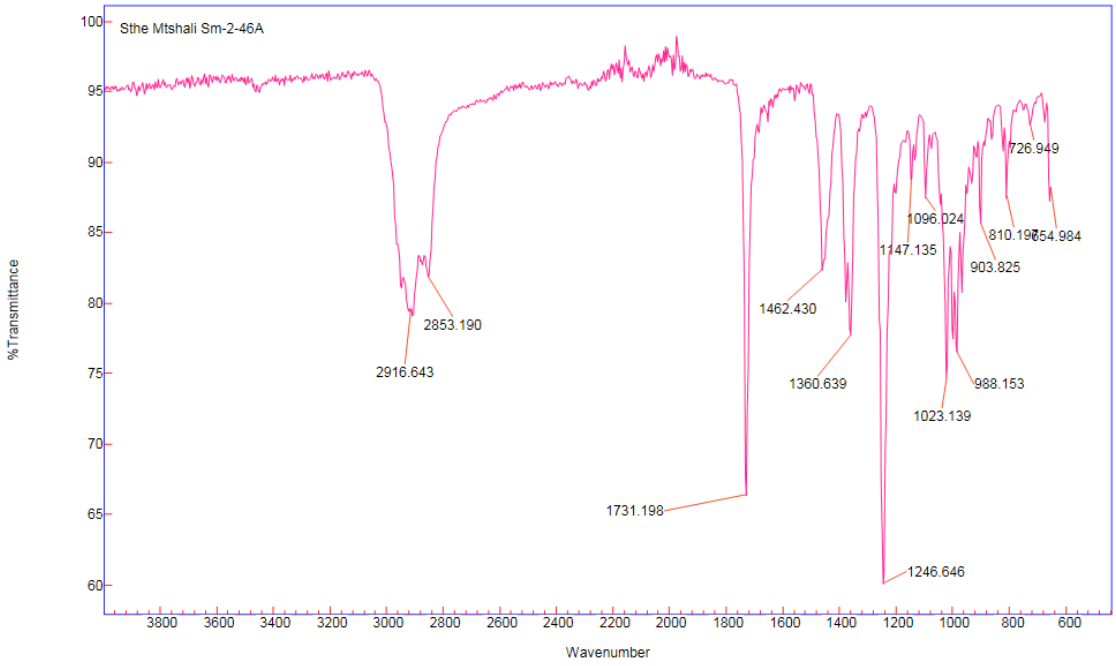

Figure 3.6. FT-IR spectrum of the α-amyrin acetate **(3.20)** and β-amyrin acetate **(3.21)** mixture.

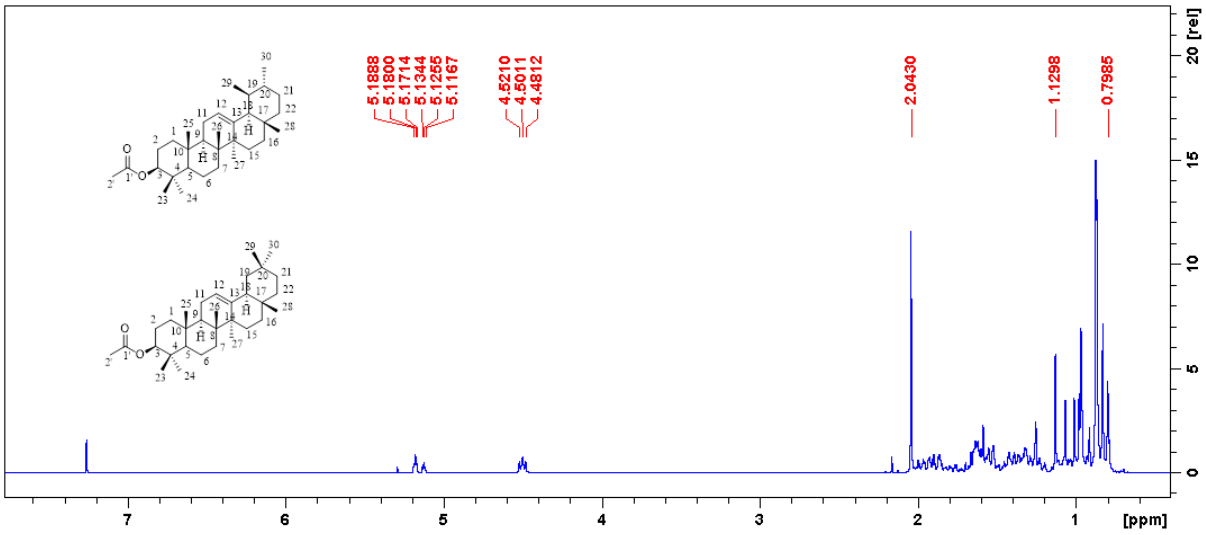

Figure 3.7. ^{1}H NMR spectrum of the α-amyrin acetate **(3.20)** and β-amyrin acetate **(3.21)** mixture in $CDCl_3$ (400 MHz).

In the ^{1}H NMR spectrum **(Fig. 3.7)** of a mixture of compounds **3.20** and **3.21**, the following resonances were observed: δ_H 5.18 (t, *J* = 3.5 Hz, H-12, β-amyrin acetate), δ_H 5.13 (t, *J* = 3.5 Hz, H-12, α-amyrin acetate), δ_H 4.50 (m, H-3, α-amyrin acetate, β-amyrin acetate), δ_H 2.04 (s, OAc, α-amyrin acetate, β-amyrin acetate) and in the upfield region numerous methylene and methyl signals were observed, the latter ranges from δ_H 0.79– δ_H 1.13.

The ^{1}H NMR data were comparable to the data reported by Okoye et al.[156] In the ^{13}C NMR spectrum **(Fig. 3.8)**, since the two compounds are structurally closely related, some of their carbon signals were overlapping. However, despite the overlaps the following noteworthy signals were observed: olefinic carbons, δ_C 121.6 (C-12, β-amyrin acetate), δ_C 145.2 (C-13, β-amyrin acetate), δ_C 124.3 (C-12, α-amyrin acetate), and δ_C 139.6 (C-13, α-amyrin acetate). The carbonyl carbon was observed at δ_C 171.0. DEPT-135 also confirmed this carbonyl carbon since it showed no proton attachment. All the GC-MS and NMR data were supported by literature.[157]

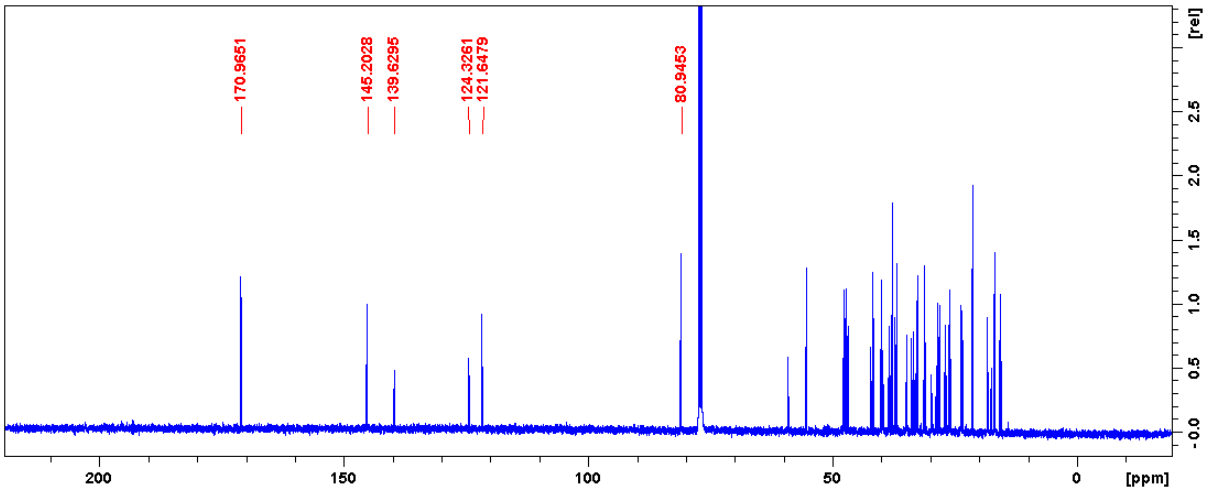

Figure 3.8. ^{13}C NMR spectrum of the α-amyrin acetate **(3.20)** and β-amyrin acetate **(3.21)** mixture in $CDCl_3$ (100 MHz).

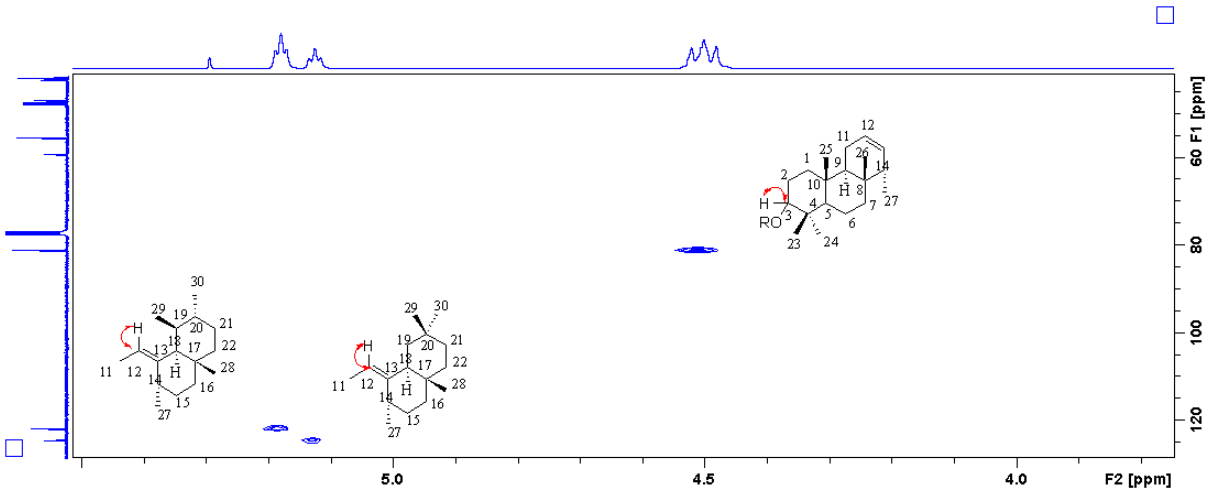

Figure 3.9. HSQC NMR spectrum of the α-amyrin acetate **(3.20)** and β-amyrin acetate **(3.21)** mixture.

The HSQC and HMBC experiments revealed some of the key ^{1}H-^{13}C connections in the compounds. The two triplets were found to be directly attached to C-12 of the oleanane and the ursane carbon skeletons in β-amyrin acetate and α-amyrin acetate, respectively (see **Fig. 3.9**). Also, the overlapping pair of doublets of doublets at δ_H 4.50 was found to be attached to two oxygen-bearing carbons, both resonating at δ_C 81.0. From the HMBC (**Fig. 3.10**) the position of the acetate group was supported by the correlation of carbonyl carbon at δ_C 171.0 with H-3 resonating at δ_H 4.50 and acetate methyl protons observed at δ_H 2.04.

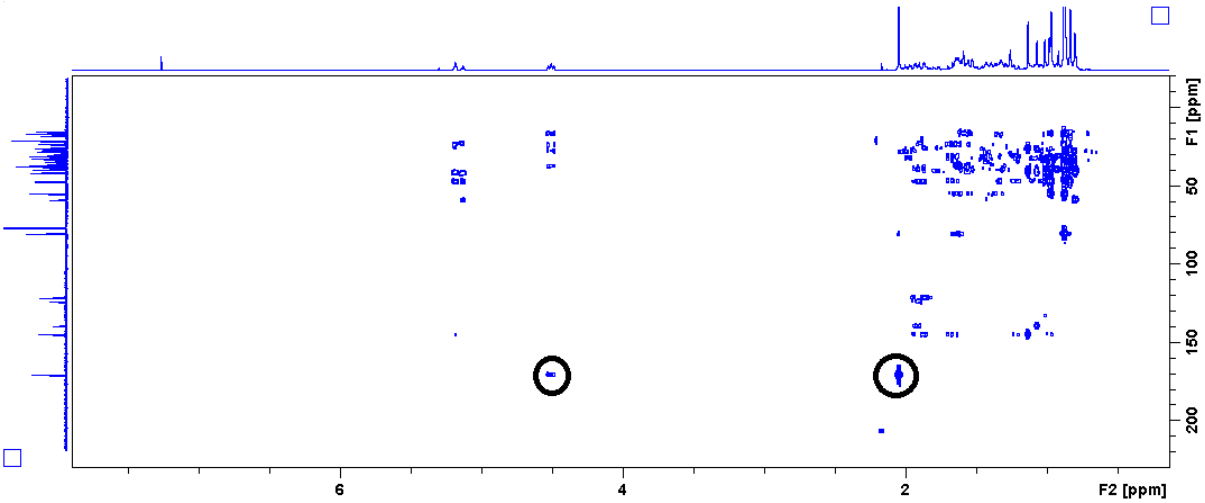

Figure 3.10. HMBC NMR spectrum of the α-amyrin acetate **(3.20)** and β-amyrin acetate **(3.21)** mixture.

In the elucidation of all the compounds, amongst other NMR experiments, COSY NMR was used for the confirmation of the ^{1}H-^{1}H overlaps. All the COSY NMR spectra are attached in the APPENDIX section.

3.3.2 Characterization of ψ-taraxasterol acetate (3.22)

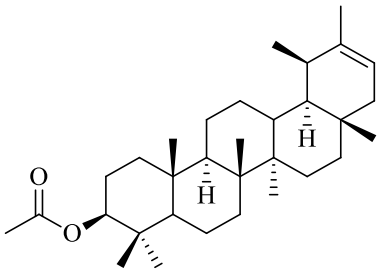

ψ-Taraxasterol acetate **(3.22)**

Purification of the triterpenoid mixture (Sm-2-18C) afforded compound **3.22** as a colourless amorphous solid. In the GC-MS, the compound had a retention time of 30.039 min **(Fig. 3.11)**, and in the EI-MS spectrum **(Fig. 3.12)**, a molecular ion of *m/z* 468 was observed, which is characteristic of pentacyclic acetate-containing triterpenoids. Among the mass fragments, a base peak of *m/z* 189 was observed. The fragment ion *m/z* 43 revealed the presence of an acetate in the compound. The EI-mass spectrum obtained with the GC-MS did not match to any compounds in the NIST11 mass library.

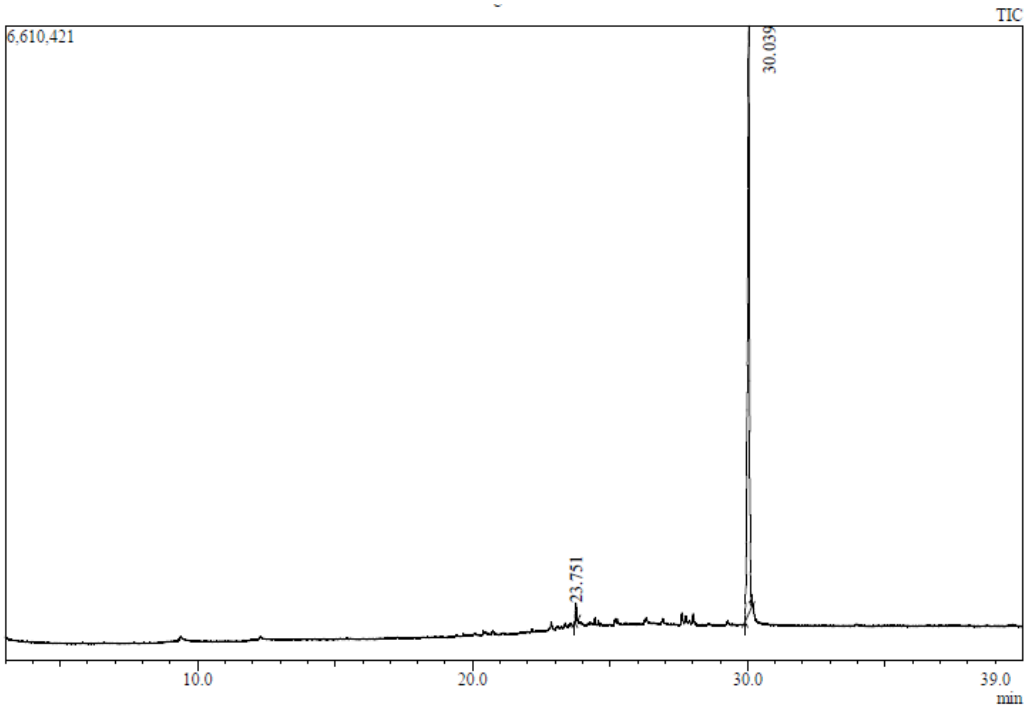

Figure 3.11. GC-MS chromatogram of ψ-taraxasterol acetate **(3.22)**.

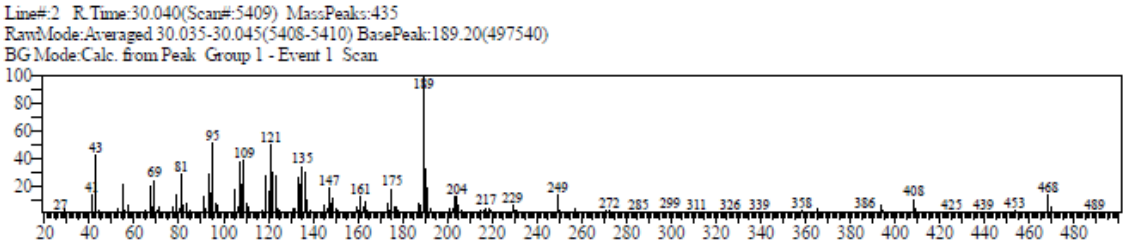

Figure 3.12. EI-MS spectrum of ψ-taraxasterol acetate **(3.22)**.

In the high resolution ESI-(+)-TOF spectrum **(Fig. 3.13)**, a M+1 ion peak of *m/z* 469.4057 was observed, corresponding to the molecular formula of compound **3.22**, $C_{32}H_{52}O_2$ (calculated for $C_{32}H_{53}O_2$, 469.4046). The molecular formula has seven degrees of unsaturation, which are accounted for by the five rings in the ψ-taraxasterol acetate pentacyclic triterpenoid, one C-C double bond and one carbonyl double bond (C=O).

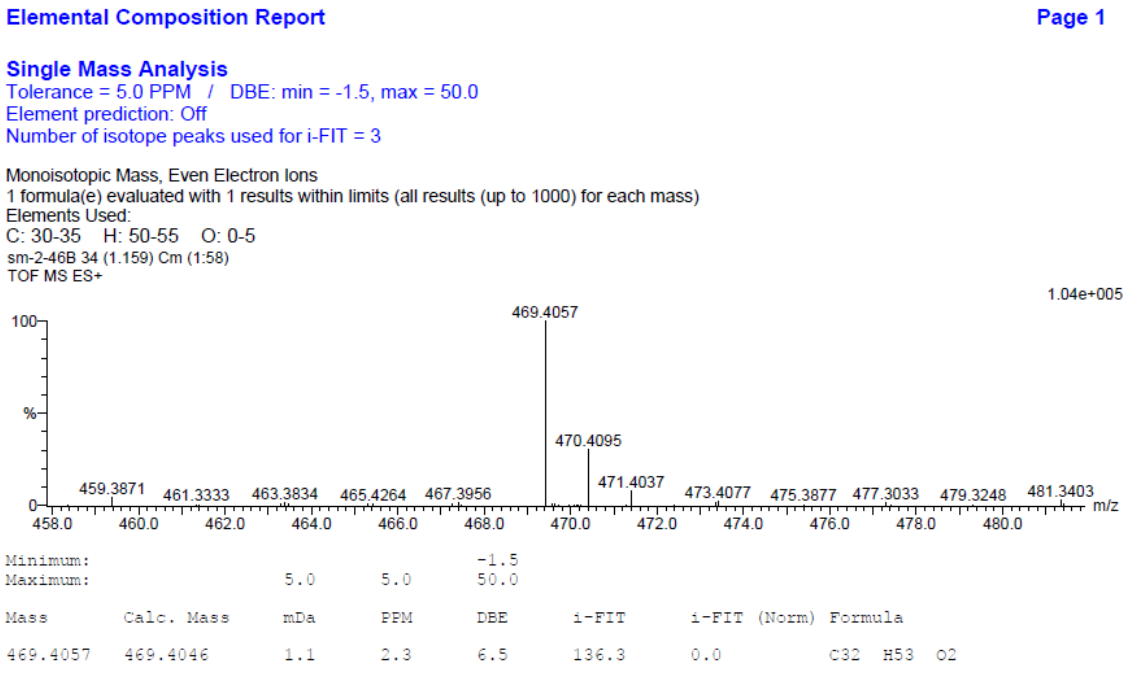

Figure 3.13. HR-ESI-(+)-MS spectrum of ψ-taraxasterol acetate **(3.22)**.

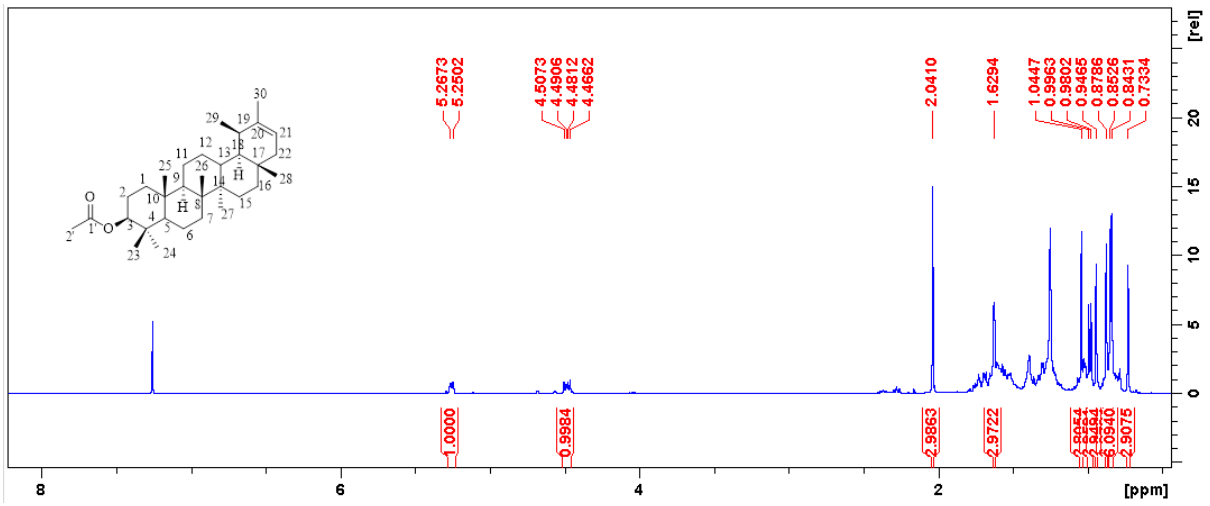

Figure 3.14. ^{1}H NMR spectrum of ψ-taraxasterol acetate **(3.22)** in $CDCl_3$ (400 MHz).

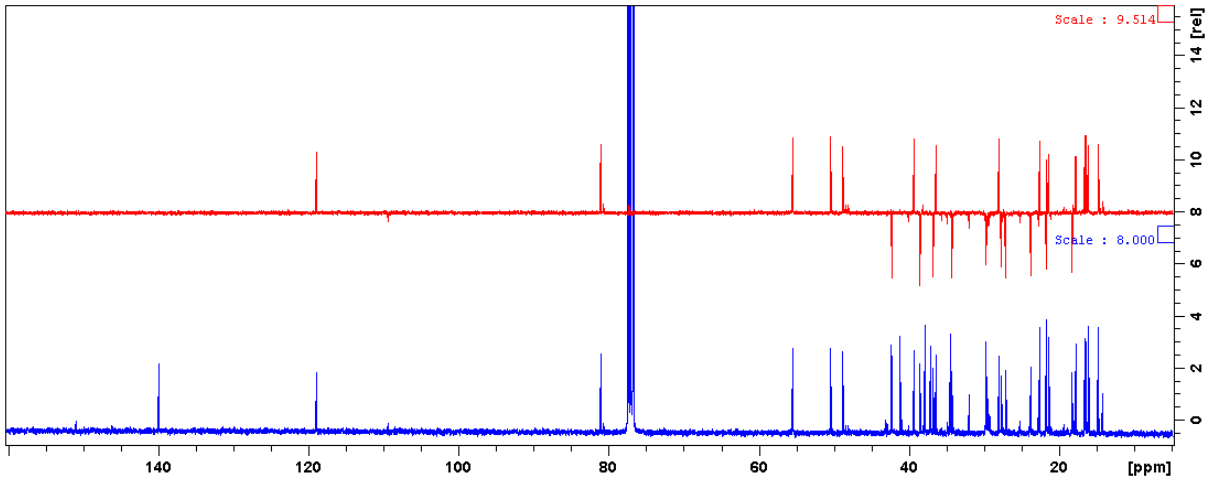

Figure 3.15. ^{13}C and DEPT-135 NMR spectra of ψ-taraxasterol acetate **(3.22)** in $CDCl_3$ (100 MHz).

^{1}H NMR spectrum of compound **3.22 (Fig. 3.14)** clearly showed the presence of eight methyl groups, one olefinic proton and an acetate moiety in the compound. The proton resonating at δ_H 4.49 as a doublet of doublets is a single proton, which according to the HSQC spectrum **(Fig. 3.16)**, is attached to C-3, an oxygen-containing carbon resonating at δ_C 80.9. The downfield doublet proton at δ_H 5.26 was found to be an olefinic proton bonded to C-21 (δ_C 118.9) as shown in the HSQC spectrum. The methyl groups in the compound were singlets, except for one methyl resonating at δ_H 0.99 as a doublet, meaning that it is attached to a methine carbon. The compound has an acetate group as evidenced by the 3H singlet at δ_H 2.04. The ^{13}C spectrum of compound **3.22 (Fig. 3.15)** revealed the presence of 32 carbon atoms, and the DEPT-135 experiment **(Fig. 3.15)** showed that the compound has seven methine carbons, nine methylene carbons and nine methyl carbons.

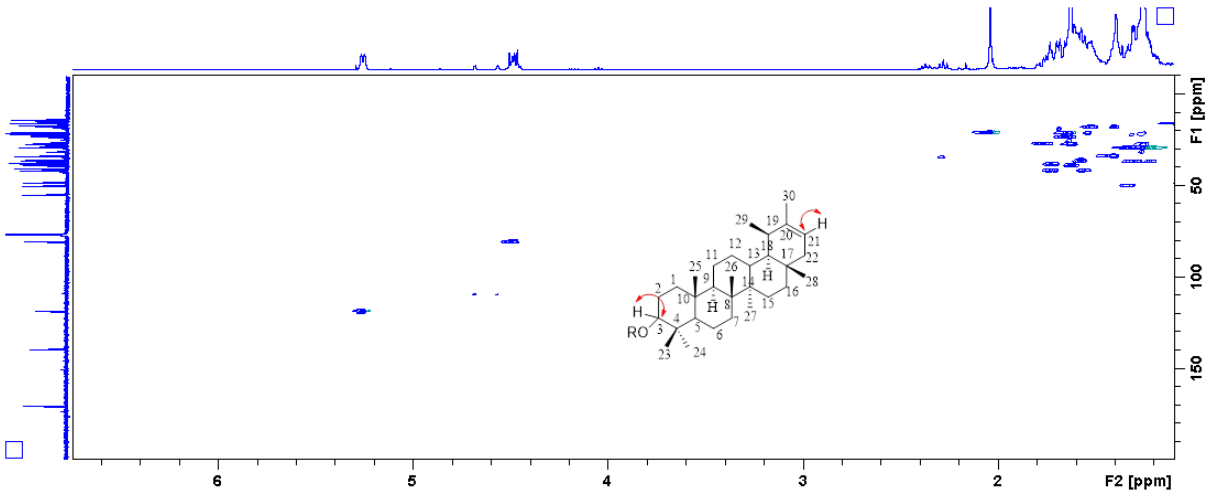

Figure 3.16. HSQC NMR spectrum of ψ-taraxasterol acetate **(3.22)**.

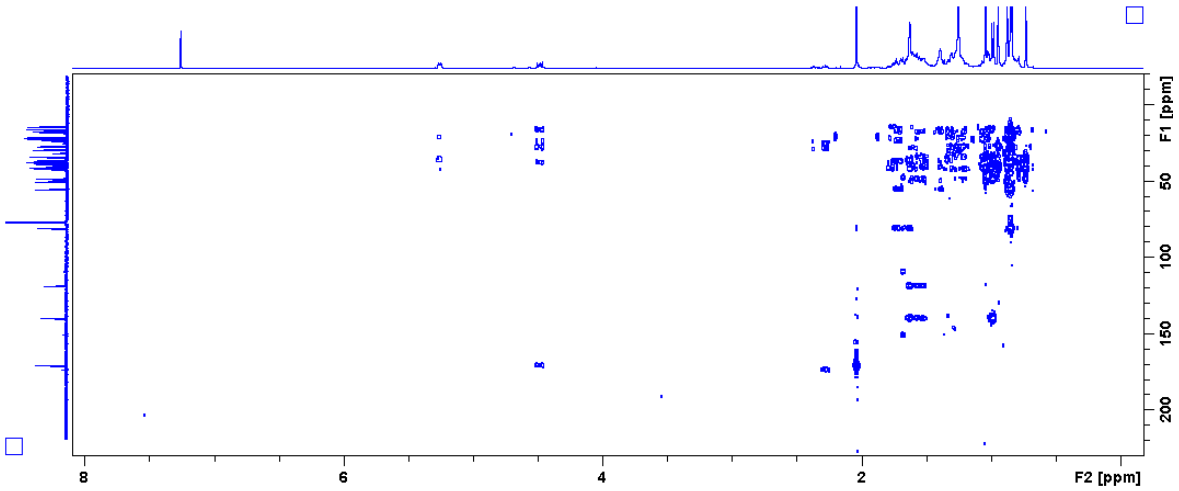

Figure 3.17. HMBC NMR spectrum of ψ-taraxasterol acetate **(3.22)**.

The HMBC was useful in the establishment of the long-range ^{1}H-^{13}C correlations (see **Table 3.1**). The methyl proton correlations were key in the determination of the structure, as clearly shown in **Fig. 3.18** (parts 1 and 2). In the HMBC spectrum (**Fig. 3.17**), the correlations of methyl protons resonating at δ_H 0.85 and δ_H 0.84 with the respective carbon resonances revealed that the two methyl groups are in positions 23 and 24 of the pentacyclic carbon skeleton. Further support for this assignment was the correlations of both these methyl proton signals with carbons resonating at δ_C 80.9, δ_C 37.8, and δ_H 55.4, which are C-3, C-4, and C-5, respectively (these correlations are shown in **Scheme 3.18A**).The position of the double bond in the compound was established using the HMBC correlations of CH_3 protons resonating at δ_H 0.99 (d), δ_H 1.63 (s), and δ_H 0.73 (s), and a single proton resonating at δ_H 5.26 (dd) (as shown in **Fig. 3.18B**). The doublet methyl was assigned to C-29, as it is bound to a methine carbon. The most downfield methyl singlet, δ_H 1.63 (s), was assigned to H-30, a methyl attached to an unsaturated carbon. The carbons with high chemical shifts, δ_C 139.8 and δ_C 118.9, were assigned to olefinic carbons, C-20 and C-21, respectively. The experimentally obtained GC-MS and NMR data used for elucidation of the compound was comparable to data reported in the literature.[157]

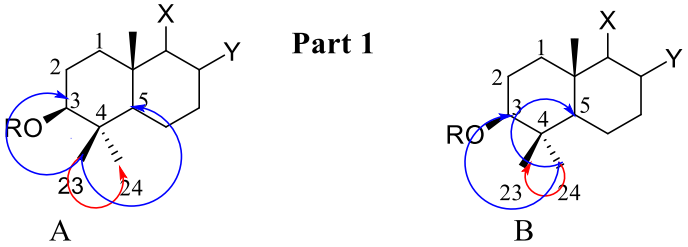

Figure 3.18 Selected HMBC ^{1}H-^{13}C correlations for the structural elucidation of ψ-taraxasterol acetate **(3.22)**.

Part 2

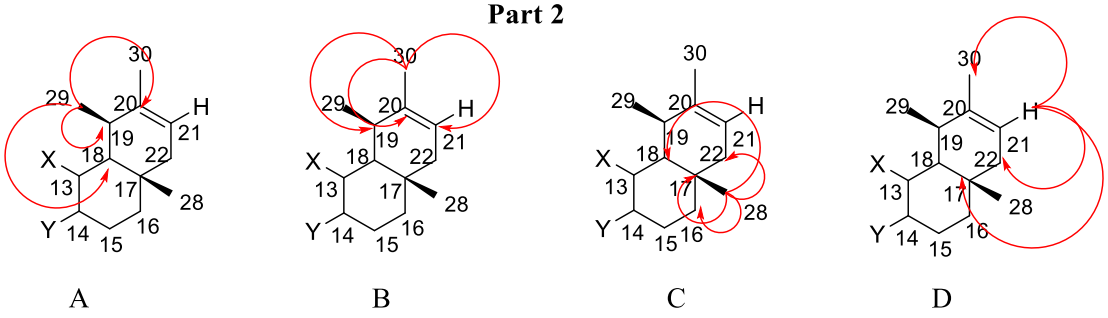

A B C D

Figure 3.18 (Cont.) Selected HMBC ^{1}H-^{13}C correlations for the structural elucidation of ψ-taraxasterol acetate **(3.22)**.

Table 3.1. ^{1}H (400 MHz) and ^{13}C (100 MHz) NMR data for ψ-taraxasterol acetate (**3.22)** in $CDCl_3$.

Position	δ_H (ppm), *J* (Hz)	δ_C (ppm)	HMBC
1		38.5	
2		23.7	
3	4.49 (1H, dd, 6.7, 10.5)	80.9	2, 4, 23, 24, 1´
4	-	37.8	
5		55.4	
6		18.2	
7		34.2	
8	-	41.1	
9		50.4	
10	-	37.0	
11		21.6	
12		27.6	
13		39.2	
14	-	42.3	
15		27.0	
16		36.7	
17	-	34.4	
18		48.7	
19		36.3	
20	-	139.8	
21	5.26 (1H, d, 6.8)	118.9	17, 22, 30
22		42.2	
23	0.85 (3H, s)	27.9	3, 4, 5, 24
24	0.84 (3H, s)	16.5	3, 4, 5, 23
25	0.87 (3H, s)	16.0	4, 5, 9, 10
26	1.04 (3H, s)	16.3	7, 8, 9
27	0.95 (3H, s)	14.7	8, 12, 13, 14, 15
28	0.73 (3H, s)	17.7	16, 17, 18, 22
29	0.99 (3H, d, 6.4)	22.5	18, 19, 20
30	1.63 (3H, s)	21.6	19, 20, 21
1´	-	170.9	
2´	2.04 (s)	21.3	1´

3.3.3 Characterization of taraxasterol acetate (3.23)

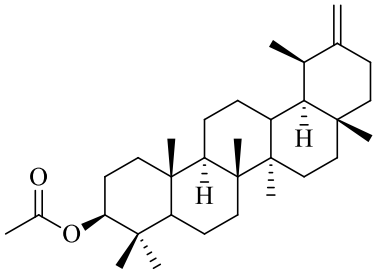

Taraxasterol acetate **(3.23)**

Compound **3.23** was obtained as colourless crystals. The compound was identified using the same methods as the previous compounds. In the GC-MS chromatogram **(Fig. 3.19)**, the compound had a retention time of 30.208 min, and from the EI-MS spectrum **(Fig. 3.20)** an M^+ ion of *m/z* 468 was observed. Similar to **3.22**, the compound had a base peak of *m/z* 189 and had an acetate (*m/z* 43) as well, revealing the isomeric relationship between the two compounds. The GC-MS NIST11 library did not identify the exact compound, but nevertheless the EI-MS information was useful in the compound identification.

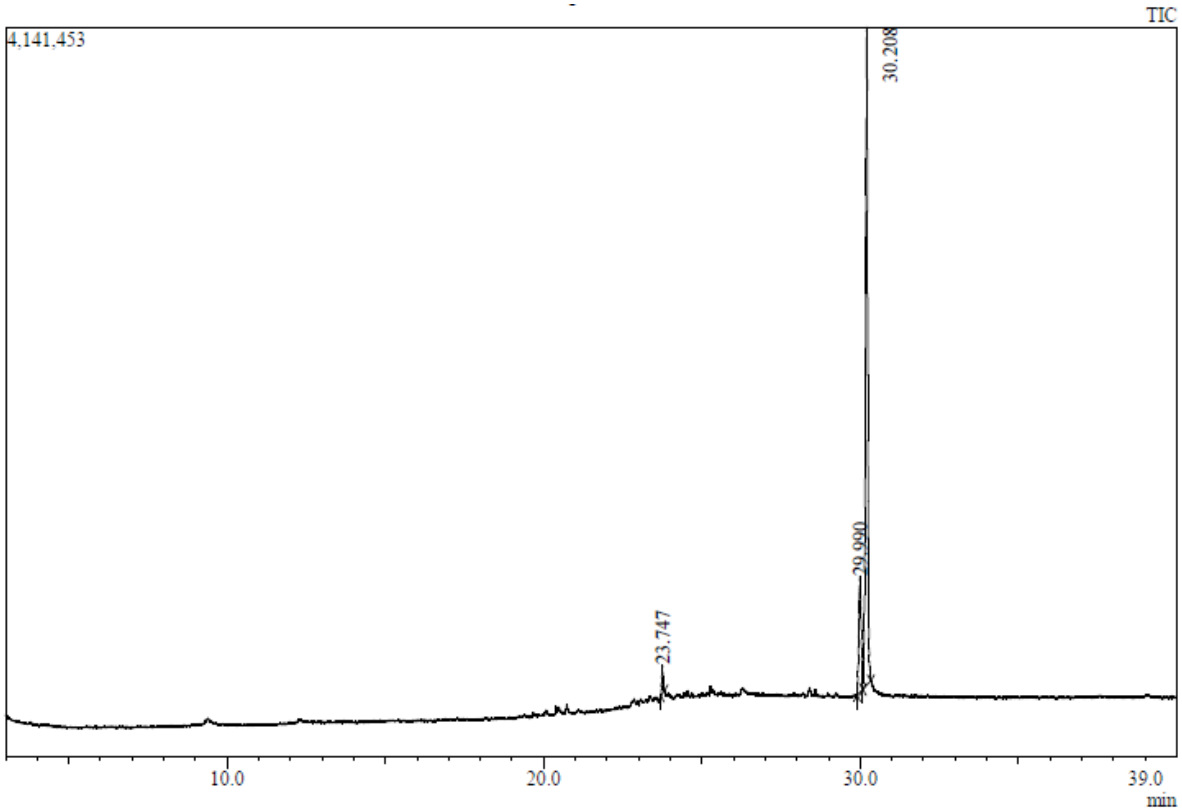

Figure 3.19. GC-MS chromatogram of taraxasterol acetate **(3.23)**.

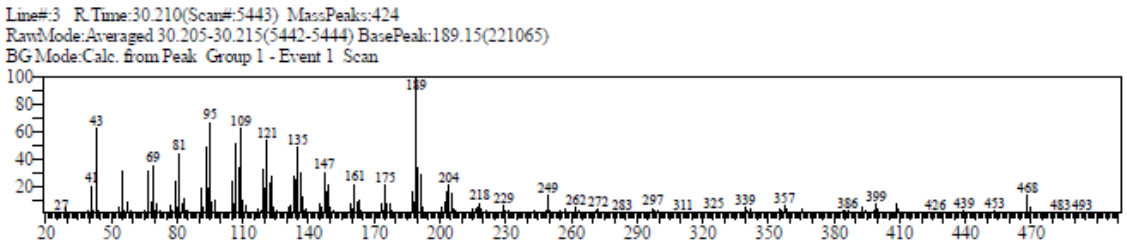

Figure 3.20. EI-MS spectrum of taraxasterol acetate **(3.23)**.

The high-resolution ESI-(+)-TOF results of compound **3.23 (Fig. 3.21)** corroborated the molecular mass suggested by the GC-MS, since it gave an M+1 ion peak at *m/z* 469.4056, which corresponds with the molecular formula of the pentacyclic triterpenoid taraxasterol acetate with molecular formula $C_{32}H_{52}O_2$ (calculated for $C_{32}H_{53}O_2$, 469.4046).

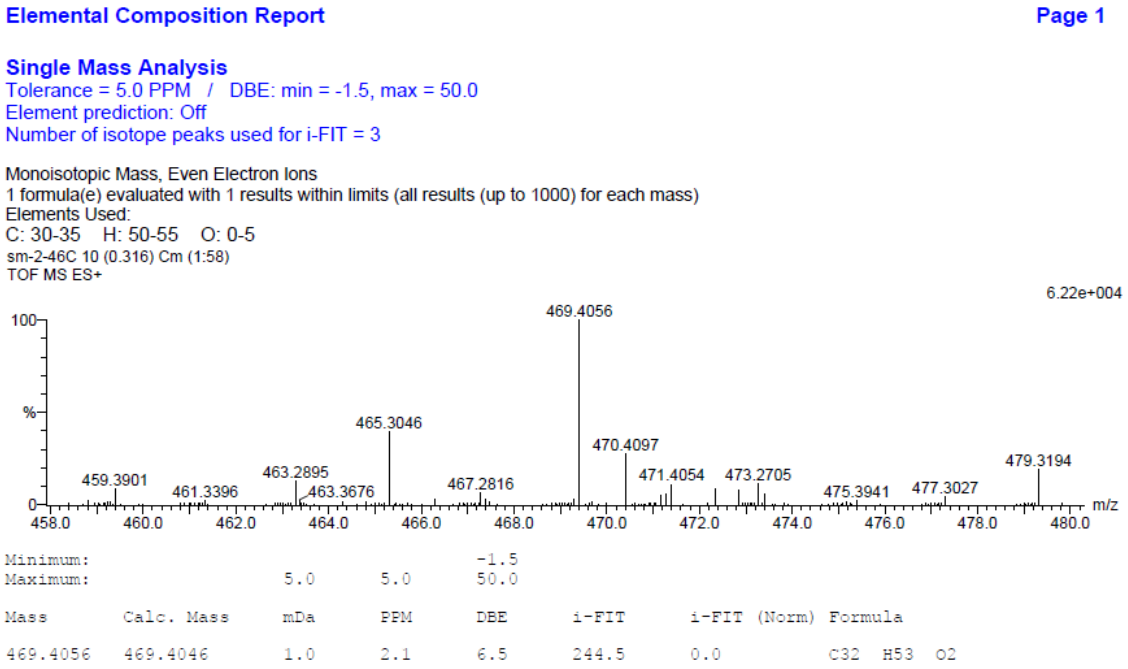

Figure 3.21. HR-ESI-(+)-MS spectrum of taraxasterol acetate **(3.23)**.

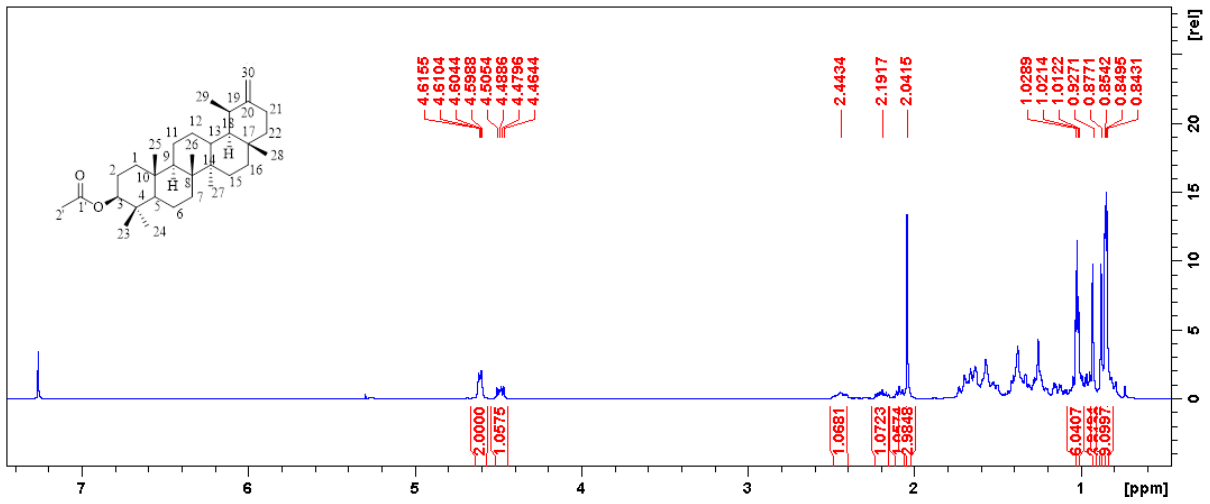

Figure 3.22. ^{1}H NMR of taraxasterol acetate **(3.23)** in $CDCl_3$ (400 MHz).

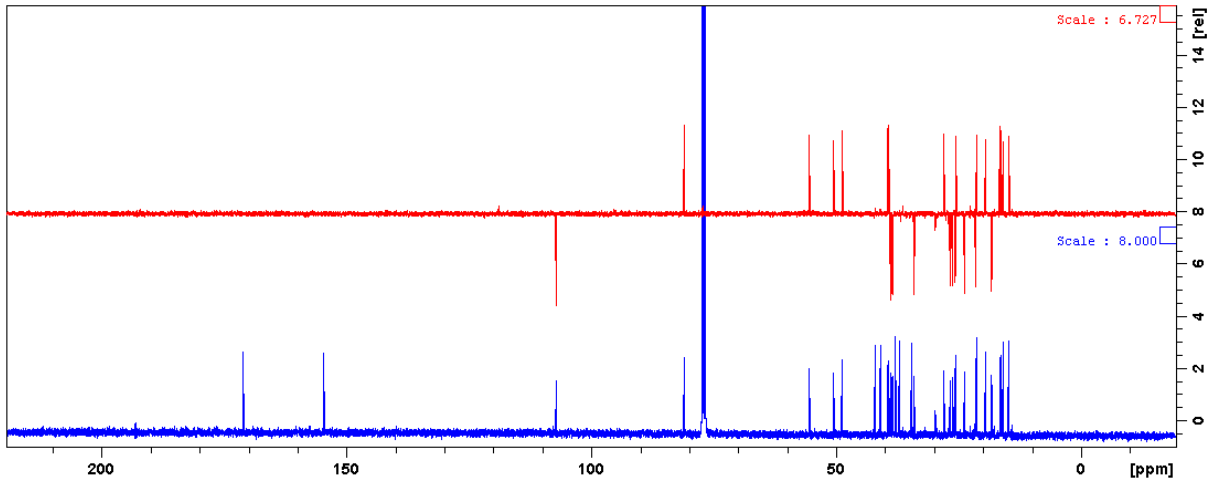

Figure 3.23. ^{13}C and DEPT-135 NMR spectra of taraxasterol acetate **(3.23)** in $CDCl_3$ (100 MHz).

In the ^{1}H NMR spectrum of compound **3.23 (Fig. 3.22)**, it was observed that the compound has seven methyl groups, one *exo*-methylene group, characterised by the downfield signal of δ_H 4.61 that integrates for two protons, and an acetate moiety. All these features, together with ^{1}H-^{13}C correlations observed in the HSQC **(Fig. 3.24)** and HMBC **(Fig. 3.25)** spectra supported a ursane skeleton for the compound.

The ^{13}C NMR spectrum **(Fig. 3.23)** showed that compound **3.22** has 32 carbon atoms, including five quaternary carbons, six methine carbons, ten methylene carbons, eight methyl carbons, two sp^2 carbons, and one carbonyl carbon, as observed in the DEPT-135 spectrum overlapped with the ^{13}C spectrum in **Fig. 3.23**. The carbon nucleus resonating at δ_C 170.9 confirms the presence of an acetate moiety in the compound, as the chemical shift is in the region of an ester carbonyl. GC-MS and NMR data were supported by the data reported in the literature.[157]

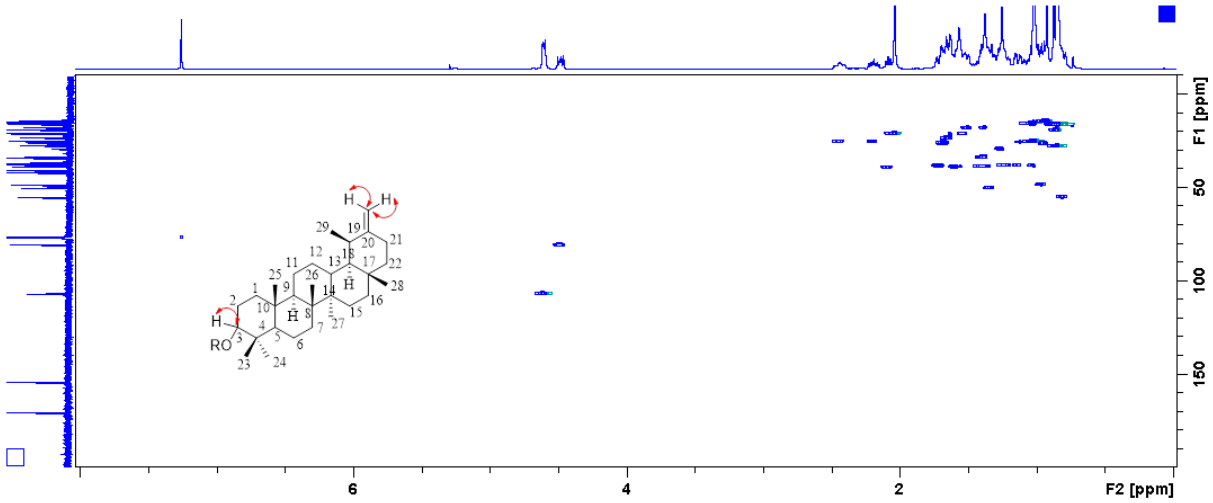

Figure 3.24. HSQC NMR spectrum of taraxasterol acetate **(3.23)**.

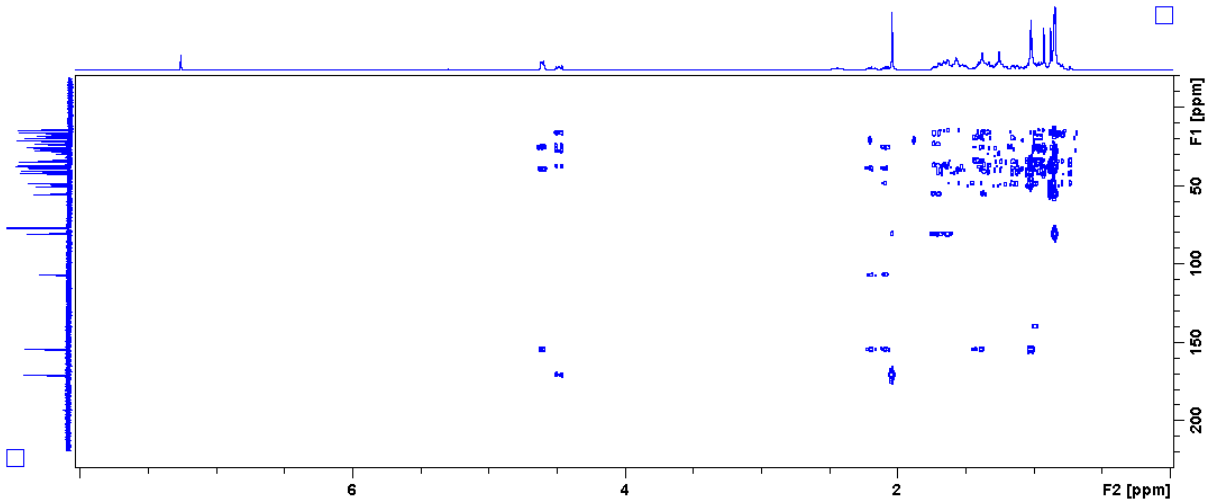

Figure 3.25. HMBC NMR spectrum of taraxasterol acetate **(3.23)**.

Table 3.2. ^{1}H (400 MHz) and ^{13}C (100 MHz) NMR data for taraxasterol acetate (**3.23)** in $CDCl_3$.

Position	δ_H (ppm), *J* (Hz)	δ_C (ppm)	HMBC
1		38.5	
2		23.7	
3	4.48 (1H, dd, 6.6, 10.3)	80.9	2, 4, 23, 24, 1´
4	-	37.8	
5		55.5	
6		18.2	
7		34.0	
8	-	40.9	
9		50.4	
10	-	37.1	
11		21.5	
12		25.6	
13		38.9	
14	-	42.1	
15		26.7	
16		39.2	
17	-	34.5	
18		48.7	
19	2.10 (1H, m)	38.3	20, 21, 22, 30
20	-	154.6	
21	2.20 (1H, m), 2.44 (1H, m)	25.5	20, 22, 30
22		39.4	
23	0.85 (3H, s)	27.9	3, 4, 5, 24
24	0.84 (3H, s)	16.5	3, 4, 5, 23
25	0.88 (3H, s)	15.9	1, 5, 9, 10
26	1.02 (3H, s)	16.3	7, 8, 9, 14
27	0.93 (3H, s)	14.7	5, 8, 13, 14
28	0.85 (3H, s)	26.2	16, 17, 18, 22
29	1.02 (3H, d, 6.7)	19.5	18, 19, 20
30	4.61 (2H, m)	107.1	
1´	-	170.9	
2´	2.04 (3H, s)	21.3	1´

3.3.4 Characterization of lupeol acetate (3.24)

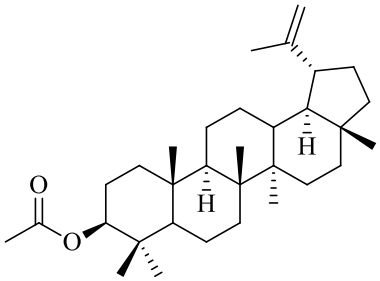

Lupeol acetate **(3.24)**

Compound **3.24** was isolated as an off-white amorphous solid. The compound was identified to be lupeol acetate, based on spectroscopic and the spectrometric experiments. GC-MS was crucial in the identification of the compound, since the MS NIST11 library of compounds identified the compound to be lupeol acetate with a similarity index of 92. The NIST11 library identifies compounds based on their MS fragments in comparison with those of the pre-existing compounds in the library. Compound **3.24** had an M^+ of *m/z* 468, which makes it an isomer of the other pentacyclic triterpenoids discussed earlier. The isomerism of these compounds answers the question as to why it was so difficult to separate the compounds by normal silica gel chromatography.

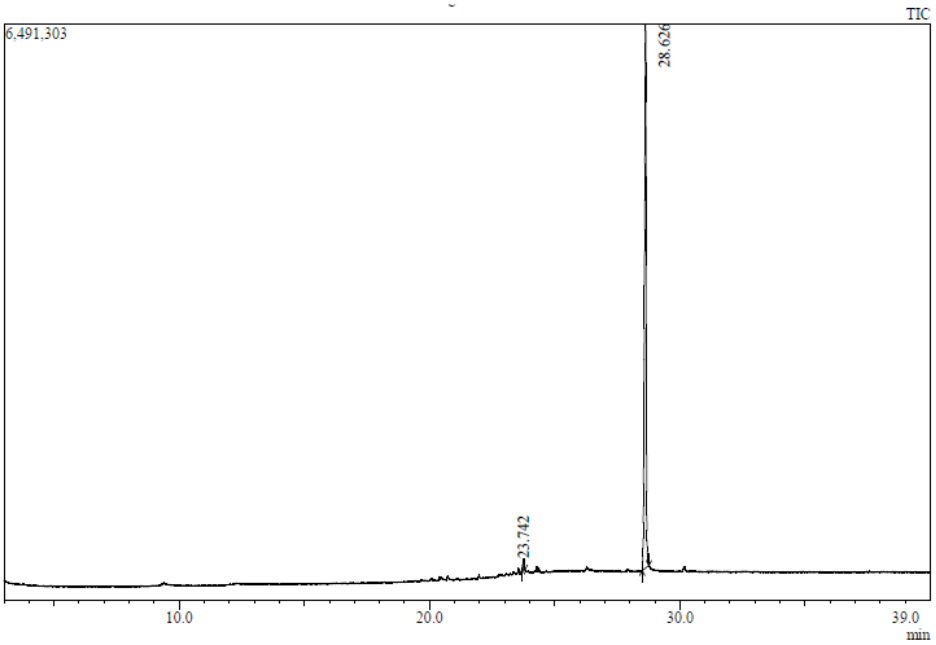

Figure 3.26. GC-MS chromatogram of lupeol acetate **(3.24)**.

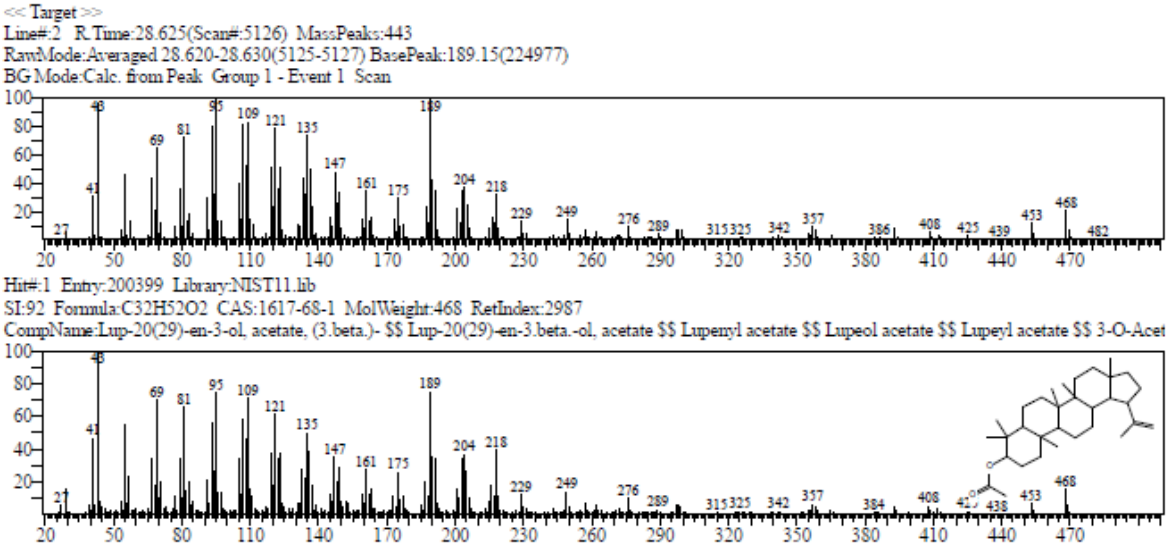

Figure 3.27. EI-MS spectra of lupeol acetate **(3.24)**, sample (above) and library based (below).

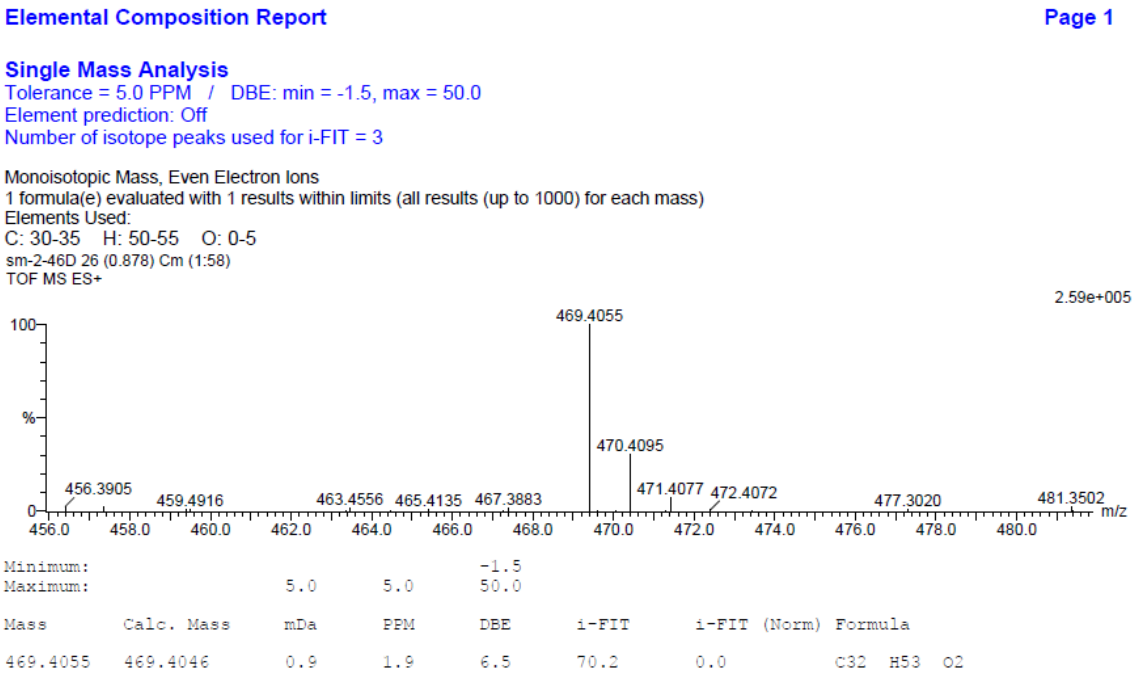

Figure 3.28. HR-ESI-(+)-MS spectrum of lupeol acetate **(3.24)**.

The HR-ESI-(+)-MS spectrum of compound **3.24 (Fig. 3.28)** was obtained and gave an M+1 ion peak at *m/z* 469.4055, corresponding to the molecular formula of lupeol acetate, $C_{32}H_{52}O_2$ (calculated for $C_{32}H_{53}O_2$, 469.4046). The IR spectrum **(Fig. 3.31)** revealed the

presence of bands at 2940.086 cm^{-1} (medium, C-H), 1732.050 cm^{-1} (sharp, C=O), and 1244.101 cm^{-1} (sharp, C-O).[155]

Figure 3.29. FT-IR spectrum of lupeol acetate **(3.24)**.

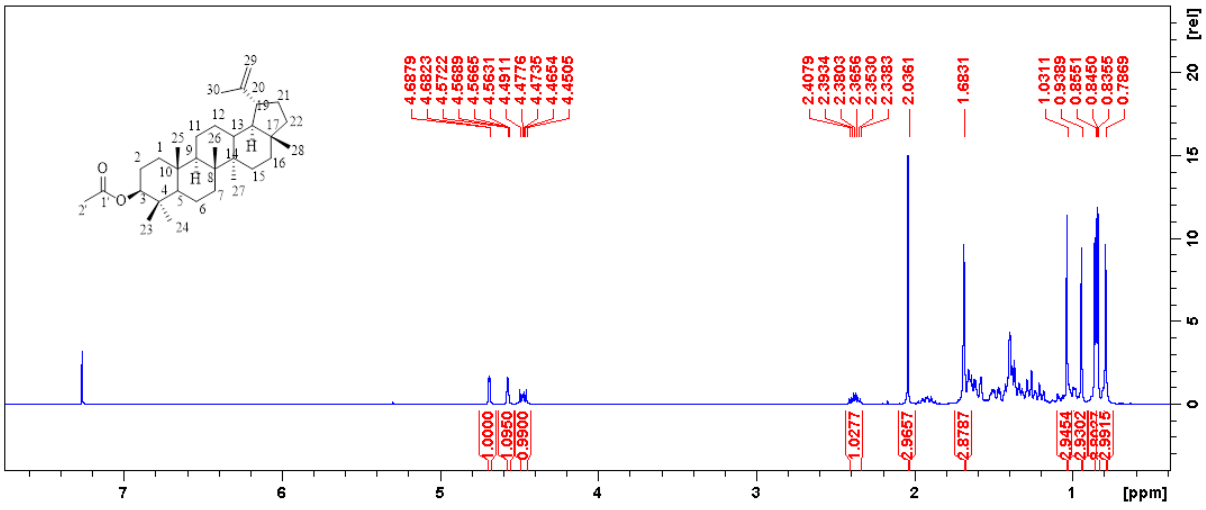

Figure 3.30. ^{1}H NMR spectrum of lupeol acetate **(3.24)** in $CDCl_3$ (400 MHz).

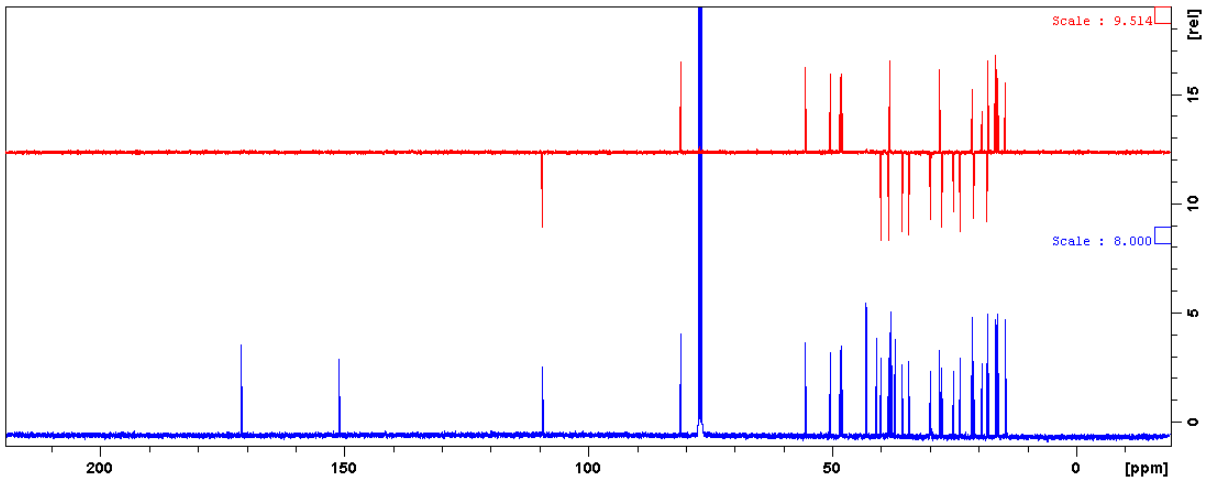

Figure 3.31. ^{13}C and DEPT-135 NMR spectra of lupeol acetate **(3.24)** in $CDCl_3$ (100 MHz).

Analysis of the ^{1}H NMR spectrum **(Fig. 3.30)** revealed the presence of two olefinic proton resonances at δ_H 4.57 and δ_H 4.69 that are attached to an *exo*-methylene carbon (δ_C 109.3), according to analysis of the HSQC spectrum **(Fig 3.32)**. The doublet of doublets at δ_H 4.47 is characteristic of a 3β-substituted triterpenoid and was assigned to the proton on an oxygen-bearing carbon (C-3, δ_C 80.9), owing to its downfield chemical shift. This was further corroborated by HSQC and HMBC **(Fig. 3.33)** proton-carbon correlations.

The other noteworthy signals were a multiplet at δ_H 2.37 and a singlet at δ_H 2.04, which integrates for three protons signifying an acetate methyl. The former resonance was found to be a methine proton attached to C-19 (δ_C 48.0) according to the DEPT-135, ^{13}C NMR and HSQC spectra. The ^{13}C spectrum **(Fig. 3.31)** revealed a total of 32 carbons, including six methine carbons, ten methylene carbons, eight methyl carbons, five quaternary carbons, two unsaturated (sp^2) carbons, and one carbonyl carbon resonating at δ_C 170.9. The GC-MS, and NMR data were comparable to the reported data for lupeol acetate in literature.[157]

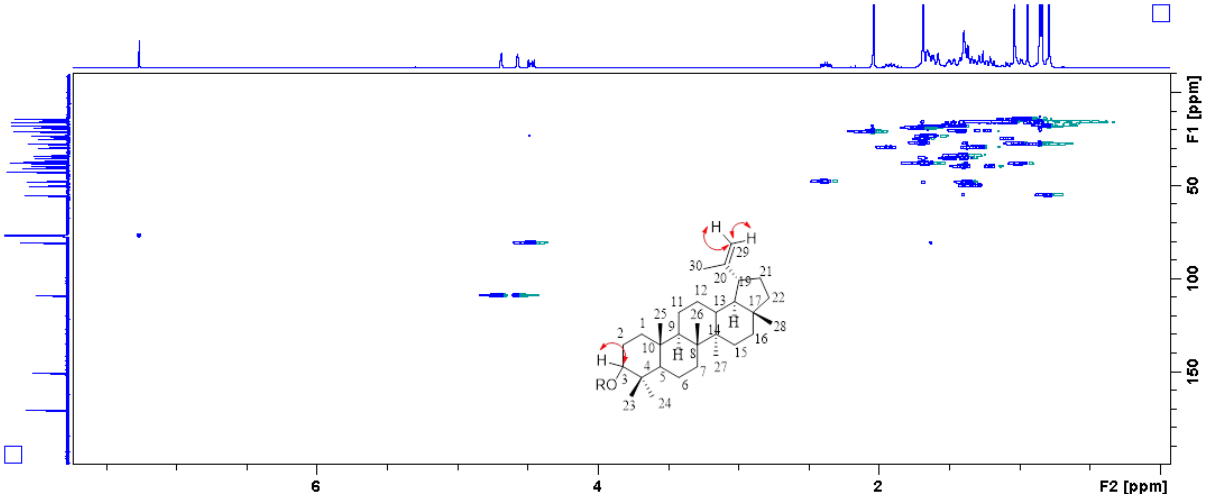

Figure 3.32. HSQC NMR spectrum of lupeol acetate **(3.24)**.

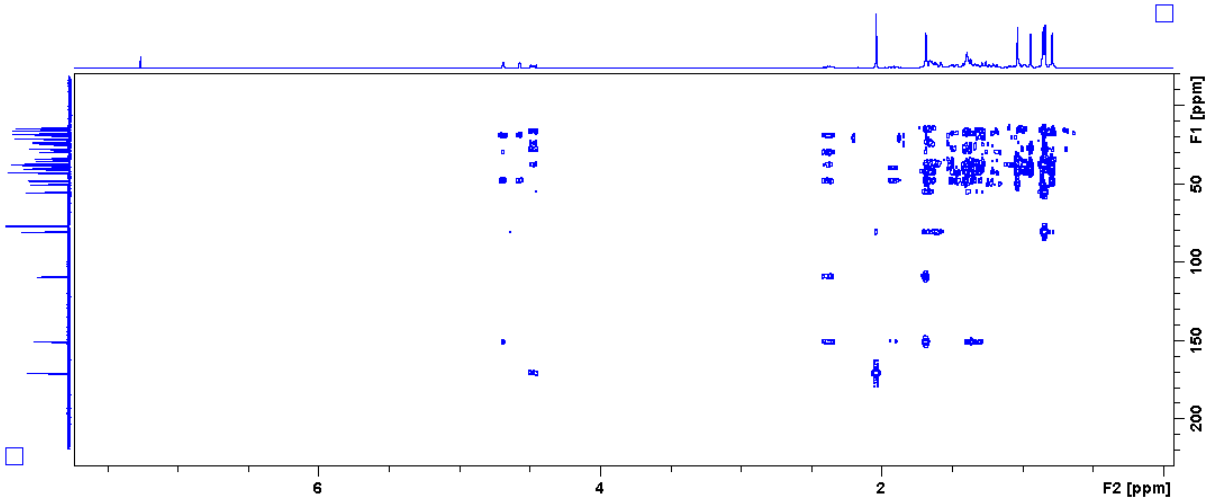

Figure 3.33. HMBC NMR spectrum of lupeol acetate **(3.24)**.

Table 3.3. ^{1}H (400 MHz) and ^{13}C (100 MHz) NMR data for lupeol acetate **(3.24)** in $CDCl_3$.

Position	δ_H (ppm), *J* (Hz)	δ_C (ppm)	HMBC
1		38.4	
2		23.7	
3	4.47 (1H, dd, 5.6, 10.8)	80.9	2, 4, 5, 23, 24, 1´
4	-	37.8	
5		55.4	
6		18.2	
7		34.2	
8	-	40.9	
9		50.4	
10	-	37.1	
11		20.9	
12		25.1	
13		38.1	
14	-	42.8	
15		27.4	
16		35.6	
17	-	42.9	
18		48.3	
19	2.37 (1H, td, 11.0, 5.8)	48.0	18, 20, 21, 22, 29, 30
20	-	150.9	
21		29.8	
22		40.0	
23	0.85 (3H, s)	27.9	3, 4, 5, 24
24	0.84 (3H, s)	16.5	3, 4, 5, 23
25	0.86 (3H, s)	16.2	1, 5, 9, 10
26	1.02 (3H, s)	15.9	7, 8, 9, 14
27	0.94 (3H, s)	14.5	8, 13, 14, 15
28	0.79 (3H, s)	18.0	16, 17, 18, 22
29	4.57 (1H, m), 4.69 (1H, d, 2.2)	109.3	19, 20, 21, 30
30	1.68 (3H, s)	19.3	19, 20, 29
1´	-	170.9	
2´	2.04 (3H, s)	21.3	1´

3.3.5 Characterization of α-amyrin palmitate (3.25) and β-amyrin palmitate (3.26)

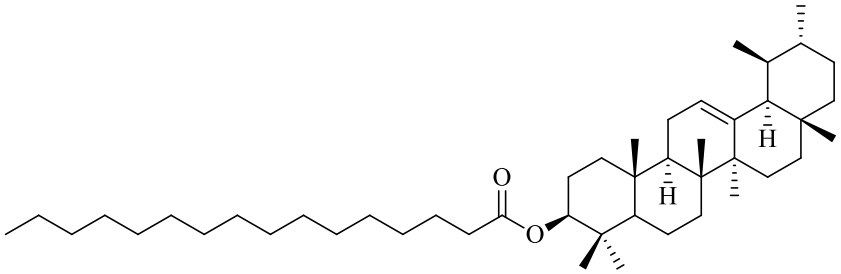

α-Amyrin palmitate **(3.25)**

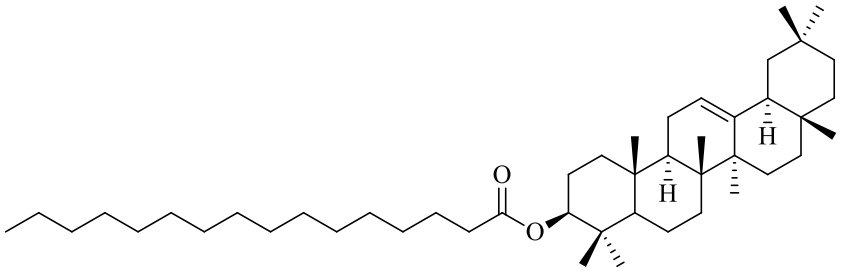

β-Amyrin palmitate **(3.26)**

Purification of a non-polar fraction (Sm-2-18B) afforded a mixture of compounds **3.25** and **3.26** as a colourless viscous substance. In the HR-API-(+)-MS spectrum **(Fig. 3.34)**, the compounds were found to have a molecular formula of $C_{46}H_{80}O_2$, owing to the observed M-1 ion peak of *m/z* 663.6064 (calculated for $C_{46}H_{79}O_2$ 663.6080). API (atmospheric pressure ionization) was used in certain HR-MS experiments rather than ESI (electrospray ionization). Non-polar compounds are notoriously difficult to ionize, and API, which is a softer ionization technique, gives better results in the analysis of non-polar compounds, whereas the ESI is more suitable for polar compounds.[158] Observed characteristic bands in the IR spectrum **(Fig. 3.35)** were the sharp C-H bands at 2916.109 cm^{-1} and 2850.413 cm^{-1}, and a sharp carbonyl resonance at 1728.208 cm^{-1}.

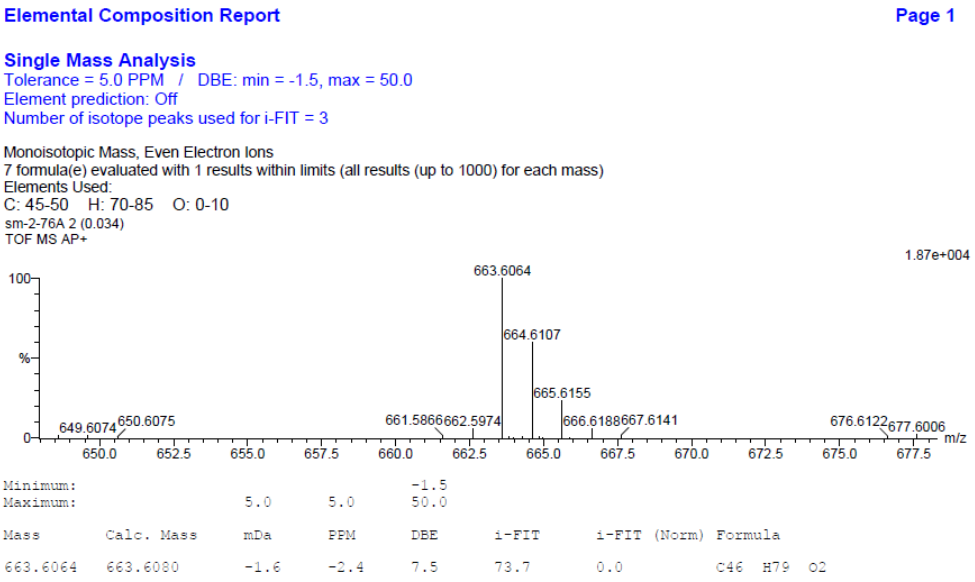

Figure 3.34. HR-API-(+)-MS spectrum of α-amyrin palmitate **(3.25)** and β-amyrin palmitate **(3.26)** mixture.

Figure 3.35. FT-IR spectrum of α-amyrin palmitate **(3.25)** and β-amyrin palmitate **(3.26)** mixture.

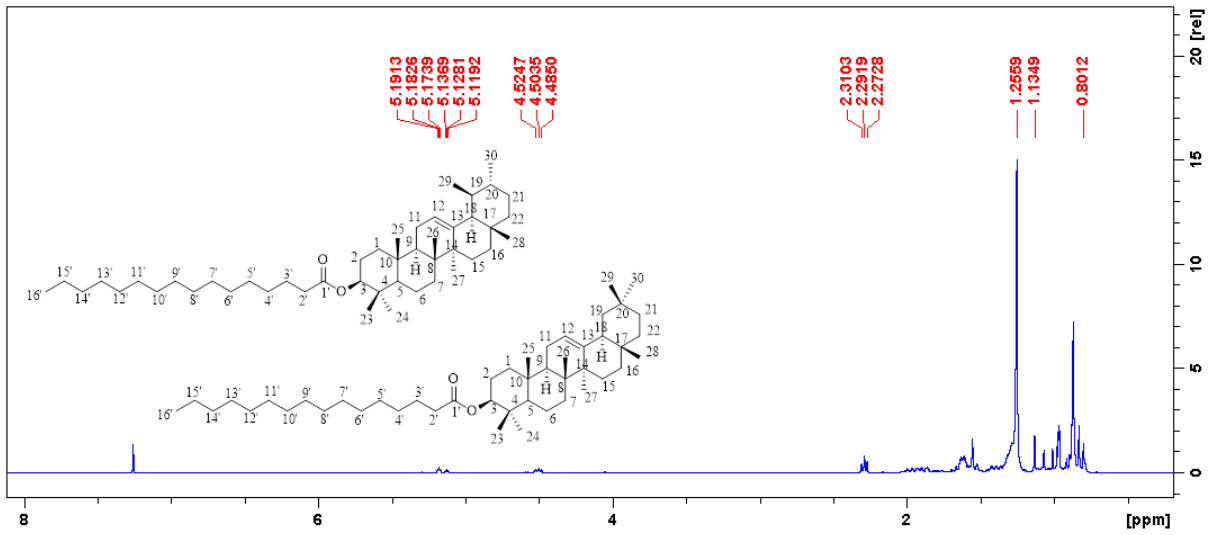

Figure 3.36. ^{1}H NMR spectrum of α-amyrin palmitate **(3.25)** and β-amyrin palmitate **(3.26)** mixture in $CDCl_3$ (400 MHz).

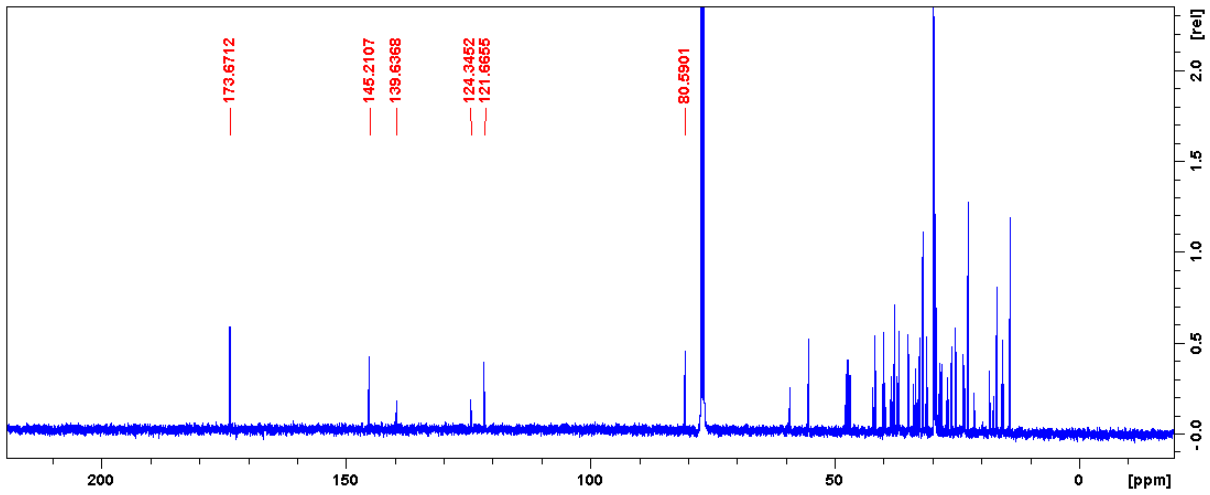

Figure 3.37. ^{13}C NMR spectrum of α-amyrin palmitate and β-amyrin palmitate mixture in $CDCl_3$ (100 MHz).

The two compounds **3.25** and **3.26** were obtained as a mixture and as a result, overlapping of signals can be seen in the NMR results. However, it was possible to determine the identities of the compounds. The ^{1}H NMR spectrum of the mixture **(Fig. 3.36)** showed two triplets at δ_H 5.18 (J = 3.5 Hz) and δ_H 5.13 (J =3.5 Hz) that are characteristic of pentacyclic triterpenoids with a double bond situated at positions C_5-C_6 or in position C_{12}-C_{13}. The compounds were

also found to contain 3β-acyloxy substituents as shown by the observed overlapping signals at δ_H 4.50. The triplet at δ_H 2.29 (J = 7.5 Hz) and a broad singlet at δ_H 1.26 both suggested that the compounds are containing a long-chain substituent as opposed to an acetate group, as it was missing the acetate singlet that was present in the earlier discussed compounds. The methyl group present in the compounds have three-proton resonances ranging from δ_H 0.80-δ_H 1.13.

The ^{13}C spectrum of the mixture of compounds **(Fig. 3.37)** revealed the presence of a carbonyl carbon that was observed at δ_C 173.7. This resonance was not present in the DEPT-135 spectrum, which confirmed that the carbon is not protonated. The ^{13}C NMR spectrum also corroborated the presence of the olefinic carbons in the compound with signals in the downfield region, i.e. δ_C 145.2, δ_C 139.6, δ_C 124.3 and δ_C 121.7. These NMR results were somewhat comparable to those of α-amyrin acetate and β-amyrin acetate, and data reported in literature.[144] Although **3.25** and **3.26** have been isolated previously, the NMR data of these two compounds have not been reported. The molecular formula was obtained by HRMS and the NMR results suggested that the compounds in the mixture were α-amyrin palmitate **(3.25)** and β-amyrin palmitate **(3.26)**. These two compounds have been isolated previously from *B. ramiflora*.[144] However, this is the first report of **3.25** and **3.26** in *B. discolor*. It was reported that β-amyrin palmitate showed antidiabetic activities in *in vivo* experiments in a mouse model.[159]

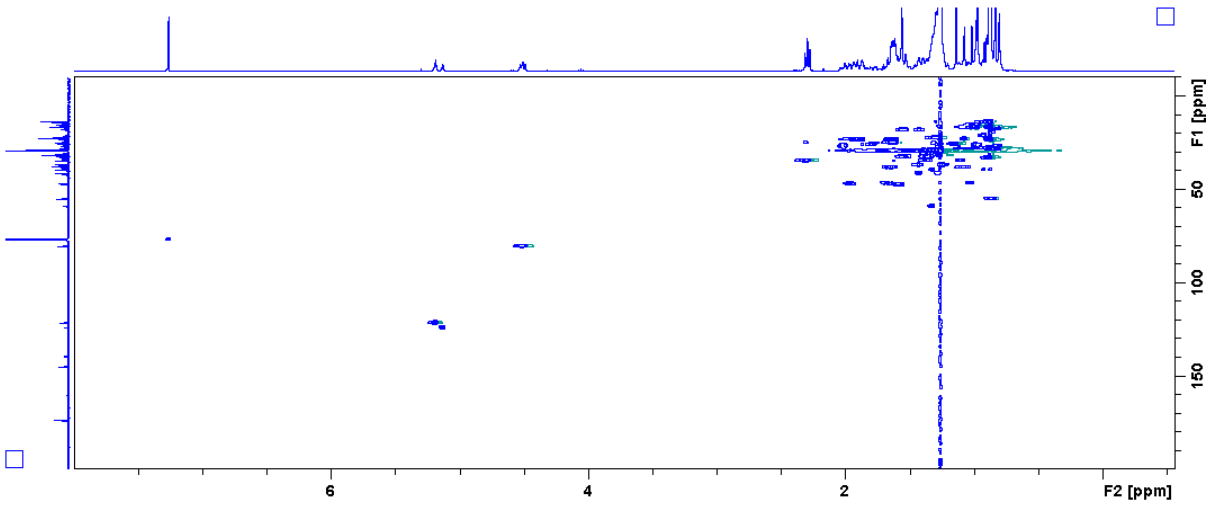

Figure 3.38. HSQC NMR spectrum of α-amyrin palmitate **(3.25)** and β-amyrin palmitate **(3.26)** mixture in $CDCl_3$ (100 MHz).

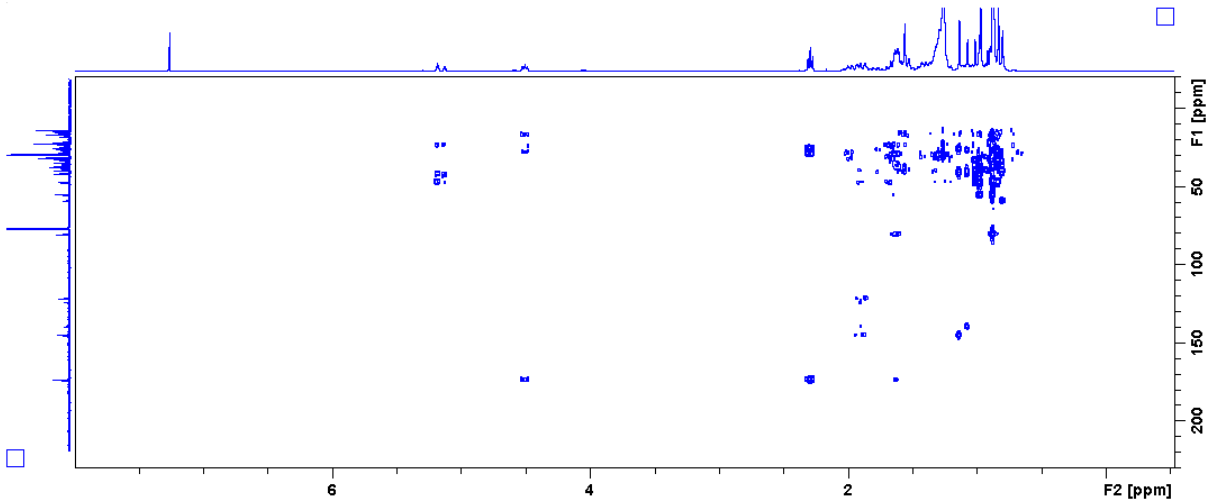

Figure 3.39. HMBC NMR spectrum of an α-amyrin palmitate **(3.25)** and β-amyrin palmitate **(3.26)** mixture.

3.3.6 Characterization of lupeol palmitate (3.27)

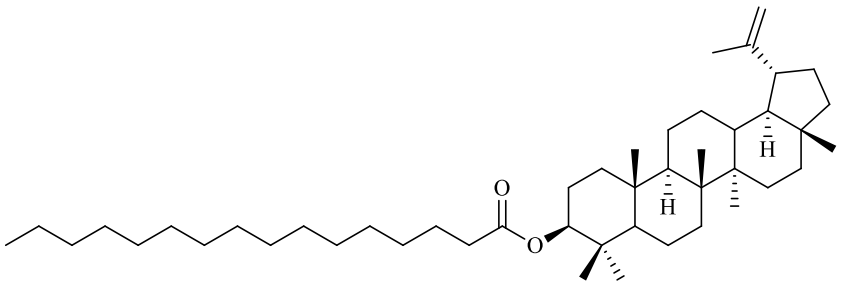

Lupeol palmitate **(3.27)**

Compound **3.27** was afforded from fraction Sm-2-18B as a white amorphous solid and was shown to have a molecular formula of $C_{46}H_{80}O_2$ by HRMS **(Fig. 3.40)**, with an M-1 ion peak of *m/z* 663.6076 (calculated for 663.6080). The IR spectrum **(Fig. 3.41)** of the compound revealed the sharp C-H stretch bands at 2914.376 cm^{-1} and 2849.471 cm^{-1} and most importantly the carbonyl band was observed at 1726.171 cm^{-1}.

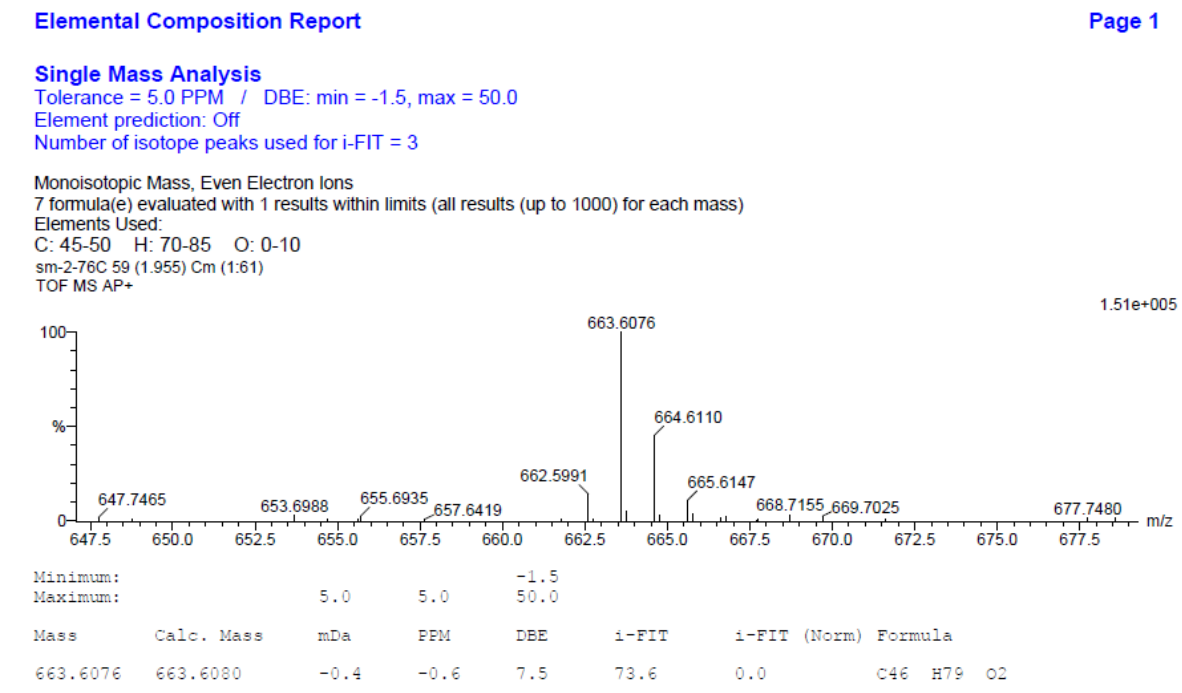

Figure 3.40. HR-API-(+)-MS spectrum of lupeol palmitate **(3.27)**.

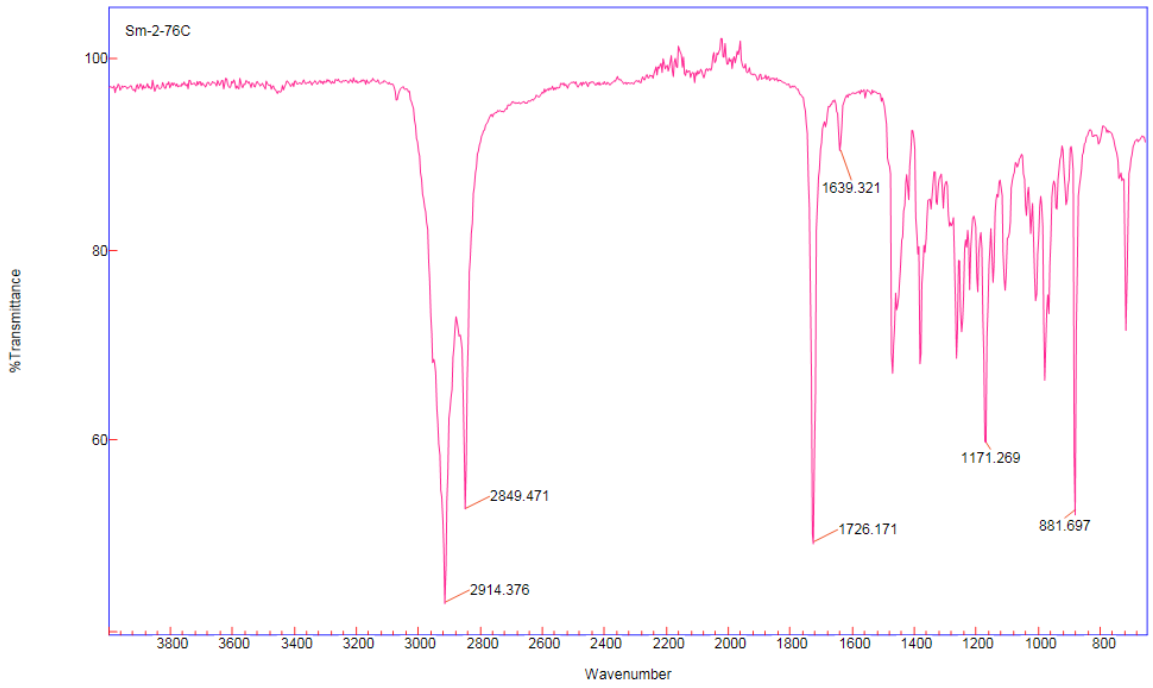

Figure 3.41. FT-IR spectrum of lupeol palmitate **(3.27)**.

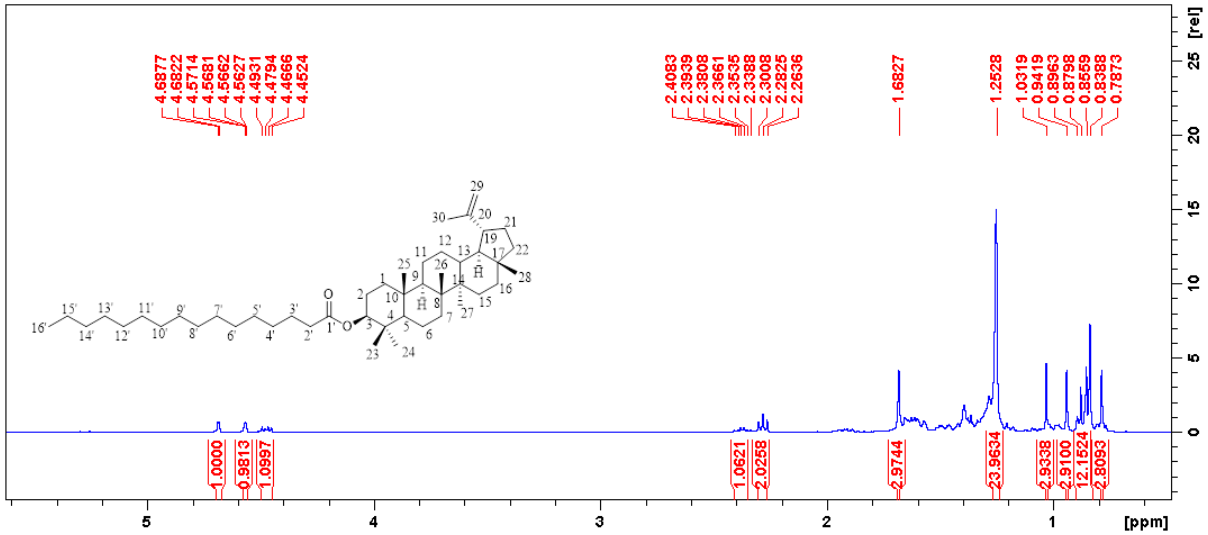

Figure 3.42. ^{1}H NMR of lupeol palmitate **(3.27)** in $CDCl_3$ (400 MHz).

The ^{1}H NMR spectrum of the compound **(Fig. 3.42)** revealed a 3β-substituted lupane-type carbon skeleton, based on the two olefinic proton resonances at δ_H 4.57 and δ_H 4.68, the 3β proton doublet of doublets resonating at δ_H 4.47 (1H, dd, J = 5.6, 10.7 Hz), and the multiplet at δ_H 2.37. Eight methyl groups were observed, together with a triplet at δ_H 2.28 (2H, t, J = 7.4 Hz) and a broad singlet integrating for 24 protons at δ_H 1.25. These signals suggested the presence of a long-chain moiety in this lupane-type carbon skeleton. However, the task was to determine its identity.

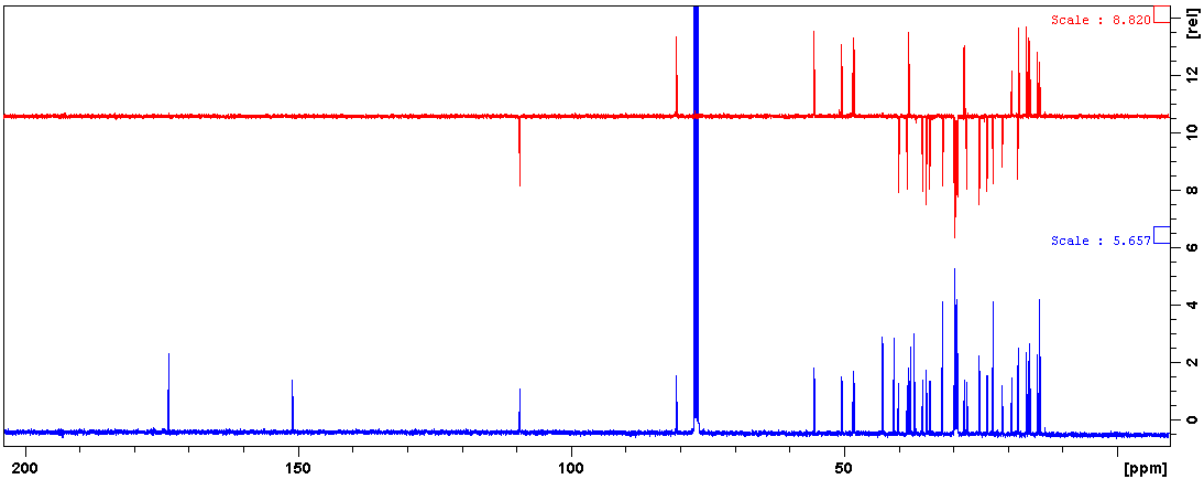

Figure 3.43. ^{13}C and DEPT-135 NMR spectra of lupeol palmitate **(3.27)** in $CDCl_3$ (100 MHz).

The ^{13}C NMR alone was not sufficient to determine the number of carbons present in the molecule since the methylene carbons in the long fatty chain were overlapping. The number of carbons were revealed by the HRMS, which gave the mass and the molecular formula of the compound as $C_{46}H_{80}O_2$.

The molecular mass of compound **3.27** suggested the substituent to be a palmitate moiety (with the molecular mass 255). The ^{13}C NMR spectrum **(Fig. 3.43)** confirmed the presence of a carbonyl carbon at δ_C 173.7 and olefinic carbons at δ_C 150.9 and δ_C 109.3, the latter correlated with the two olefinic protons in the HSQC spectrum **(Fig. 3.44)**, and as a result, it was labelled as an *exo*-methylene, as can also been seen from the DEPT-135 spectrum **(Fig. 3.43)**. The carbon resonating at δ_C 80.6 was found to be directly attached to a proton with resonance at δ_H 4.47. This further revealed the position of the palmitate substituent. The COSY revealed the position of H-3´ at δ_H 1.62, where it overlapped with the H-2´ triplet in the spectrum. The HSQC was useful in establishing the single-bond proton and carbon correlations. The HMBC correlations **(Fig. 3.45)** were key in assigning the carbons in the ^{13}C NMR spectrum, and as a result the structure.

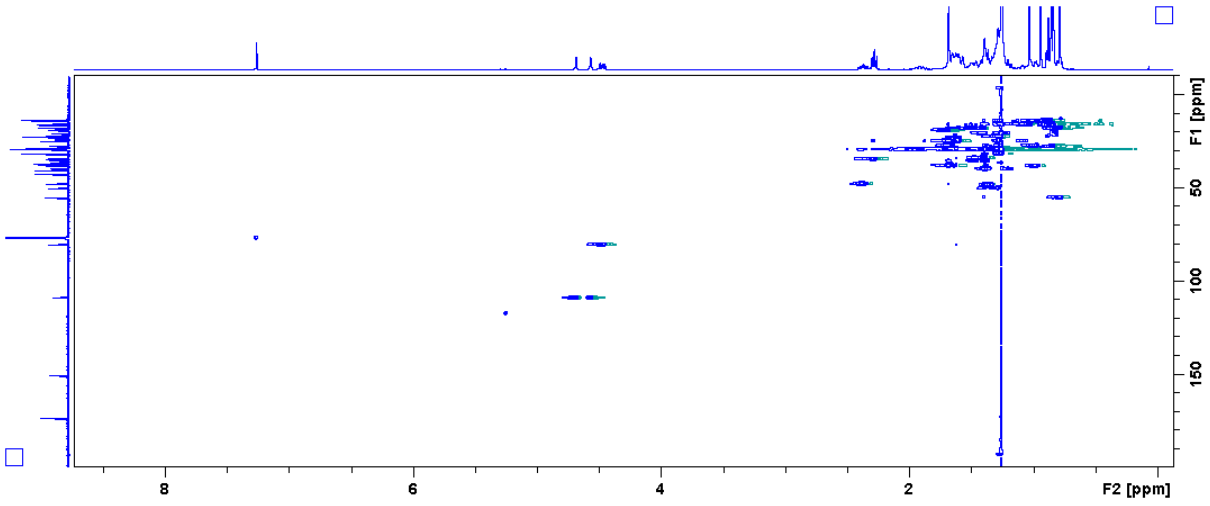

Figure 3.44. HSQC NMR spectrum of lupeol palmitate **(3.27)**.

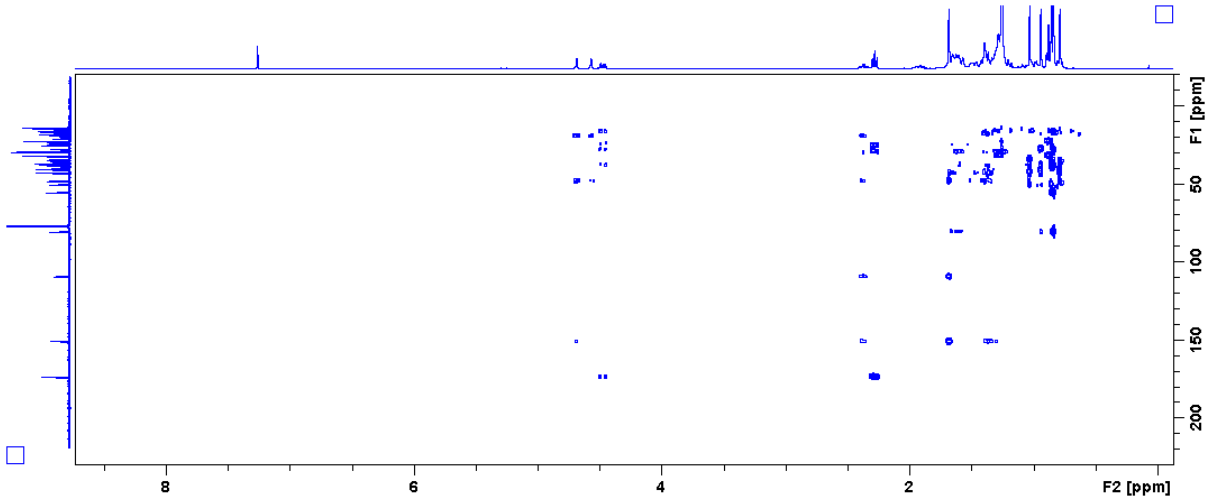

Figure 3.45. HMBC NMR spectrum of lupeol palmitate **(3.27)**.

Table 3.4. ^{1}H (400 MHz) and ^{13}C (100 MHz) NMR data for lupeol palmitate **(3.27)** in $CDCl_3$.

Position	δ_H (ppm), *J* (Hz)	δ_C (ppm)	HMBC
1		38.4	
2		23.8	
3	4.47 (1H, dd, 5.6, 10.7)	80.6	2, 4, 23, 24, 1´
4	-	37.8	
5		55.4	
6		18.2	
7		34.2	
8	-	40.9	
9		50.4	
10	-	37.1	
11		20.9	
12		25.1	
13		38.1	
14	-	42.8	
15		27.2	
16		35.6	
17	-	42.9	
18		48.3	
19	2.37 (1H, td, 11.0, 5.8)	48.0	18, 20, 21, 22, 29, 30
20	-	150.9	
21		29.85	
22		40.0	
23	0.86 (3H, s)	27.9	3, 4, 5, 24
24	0.83 (3H, s)	16.6	3, 4, 5, 23
25	0.88 (3H, s)	16.2	1, 5, 9, 10
26	1.03 (3H, s)	15.9	7, 8, 9, 14
27	0.94 (3H, s)	14.5	8, 13, 14, 15
28	0.79 (3H, s)	18.0	16, 17, 18, 22

29	4.57 (m), 4.68 (d, 2.2)	109.3	19, 20, 21, 30
30	1.68 (3H, s)	19.3	19, 20, 29
1´	-	173.7	
2´	2.28 (2H, t, 7.4)	34.9	1´, 3´, 4´
3´	1.62 (m)	25.2	
4´-13´	1.25 (24H, br, s)	29.2 - 29.7	
14´	1.25 (24H, br, s)	31.9	
15´	1.25 (24H, br, s)	22.7	
16´	0.89 (3H, br)	14.1	

With the exception of lupeol acetate (**3.24)**, the pentacyclic triterpenoids isolated in this study are reported for the first time from *B. discolor*. α-Amyrin acetate **(3.20)** have been reported from other plants. However, there are no reports of isolation from the *Brachylaena* genus. Recently, the compound was isolated from *Fraxinus rhynchophylla* Hance (Oleaceae). α-Amyrin acetate, among other activities, has been reported to have good anti-inflammatory properties,[156,160] and have exhibited antidiabetic activity *in vivo*, in STZ-induced diabetic rats.[161] As mentioned earlier in section **3.2.3**, β-amyrin acetate **(3.21)**, lupeol acetate **(3.24)**, α-amyrin palmitate **(3.25)**, and β-amyrin palmitate **(3.26)** were reported from *B. ramiflora* and all displayed poor cytotoxicity against A2780 human cancer cells. In the antidiabetic evaluation of compound **3.26**, it was shown that β-amyrin palmitate **(3.26)**, isolated from *Hemidesmus indicus* (L.) R. Br. (Periplocaceae), lowered diabetes in alloxan- and STZ-induced diabetic mice *in vivo*.[159]

Lupeol palmitate **(3.27)**, ψ-taraxasterol acetate **(3.22)**, and taraxasterol acetate **(3.23)** have never been isolated from a *Brachylaena* species. Lupeol palmitate **(3.27)**, in recent investigations, has been reported from the aerial parts of *Scurrula parasitica* L. (Loranthaceae).[162] ψ-Taraxasterol acetate **(3.22)** was reported from *Calotropis procera* (Ait.) R. Br. (Apocynaceae) by Ibrahim et al.[163] Taraxasterol acetate **(3.23)** was isolated from a hypoglycaemic ethanol extract of *Hibiscus trionum* L. (Malvaceae).[164] In the literature it has also been revealed that the de-*O*-acetyl analogues of these compounds can act as promising antidiabetic agents. Seong et al.[20] investigated lupeol **(3.32)**, and found the compound to have potent α-glucosidase inhibitory activity. Taraxasterol **(3.31)** from *Taraxacum mongolicum* Hand.-Mazz (Asteraceae) was assayed against α-glucosidase and the compound displayed excellent activity.[165]

3.3.7 Characterization of α-amyrin (3.28) and β-amyrin (3.29)

The compounds isolated from the non-polar fractions of the *B. discolor* leaf extract (**3.20-3.27**) were extremely non-polar. To increase the polarity, the acetate pentacyclic triterpenoids, α-amyrin acetate **(3.20)**, β-amyrin acetate **(3.21)**, ψ-taraxasterol acetate **(3.22)**, taraxasterol acetate **(3.23)**, and lupeol acetate **(3.24)** were hydrolysed to yield more polar triterpenoid compounds, that can be assayed for the inhibition of selected enzymes associated with diabetes.

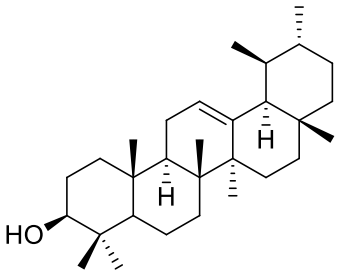

α-Amyrin **(3.28)**

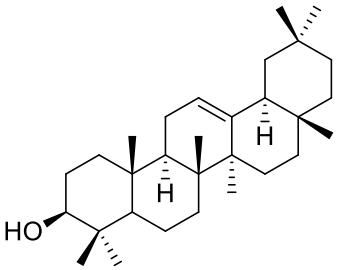

β-Amyrin **(3.29)**

The hydroxide-promoted hydrolysis of the amyrin acetate mixture, afforded a mixture of α-amyrin (B) and β-amyrin (A), as a white amorphous solid. GC-MS showed the presence of two compounds, the retention times **(Fig. 3.46)** were shorter as compared to those of the corresponding acetate compounds. The EI-MS spectra **(Fig. 3.47)** of the compounds revealed the molecular ions of *m/z* 426, which confirmed the removal of the acetate groups in both the parent compounds. The HR-API-(+)-MS spectrum **(Fig. 3.48)** has an ion fragment of *m/z* 409.3823, which supports the amyrin molecular formula of $C_{30}H_{50}O$. The fragment of *m/z* 409.3823 is in agreement with the loss of water (calculated for $C_{30}H_{49}$, 409.3834), during the fragmentation of the compounds in the MS. This fragmentation arises from a remote hydrogen rearrangement in the C_2-C_3 position in these hydroxy containing triterpenoids (see **Scheme 3.2**), and was also observed in other similar compounds, like triterpenoid aglycones.[166-167]

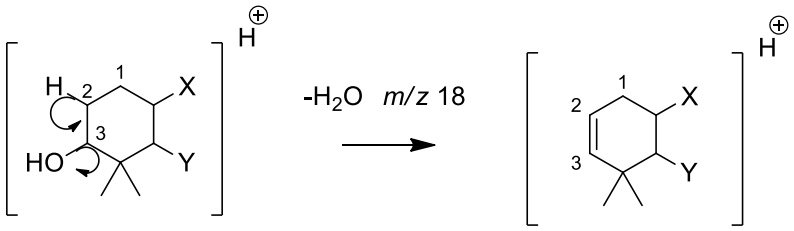

Scheme 3.2. Remote hydrogen rearrangement of triterpenoid alcohols in the mass spectrometer, resulting in the loss of water.

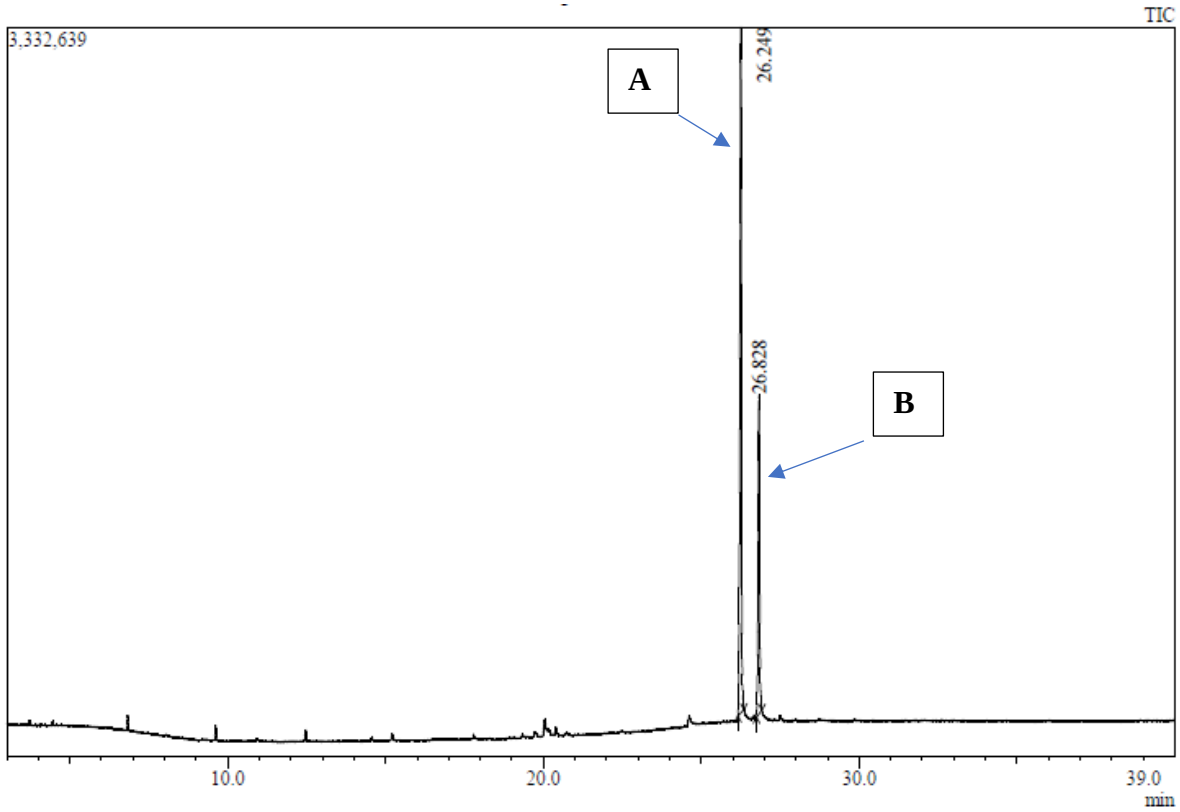

Figure 3.46. GC-MS chromatogram of α-amyrin **(3.28)** and β-amyrin **(3.29)** mixture.

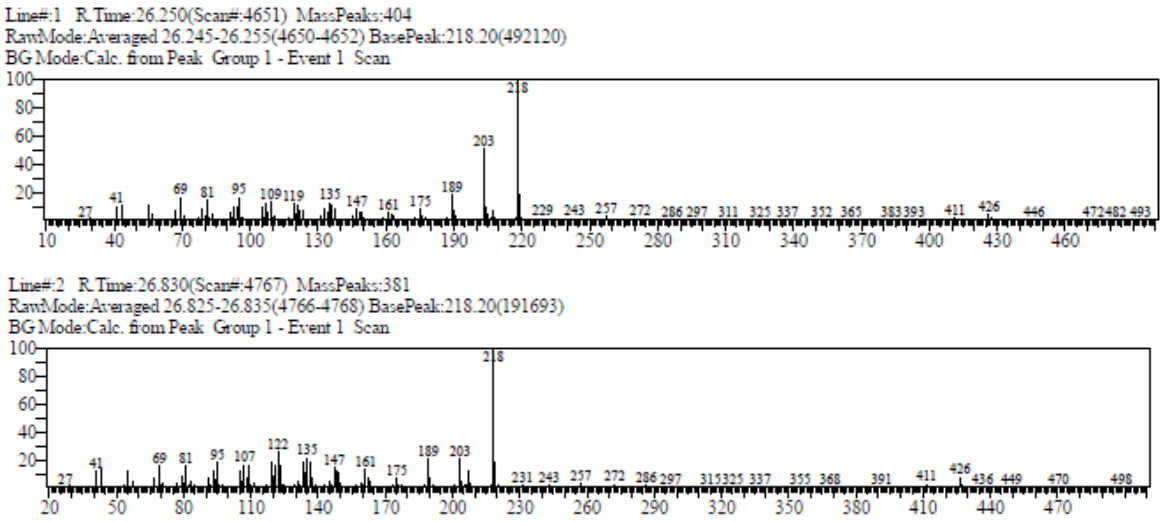

Figure 3.47. EI-MS spectra of β-amyrin **(3.29)** (above) and α-amyrin **(3.28)** (bottom).

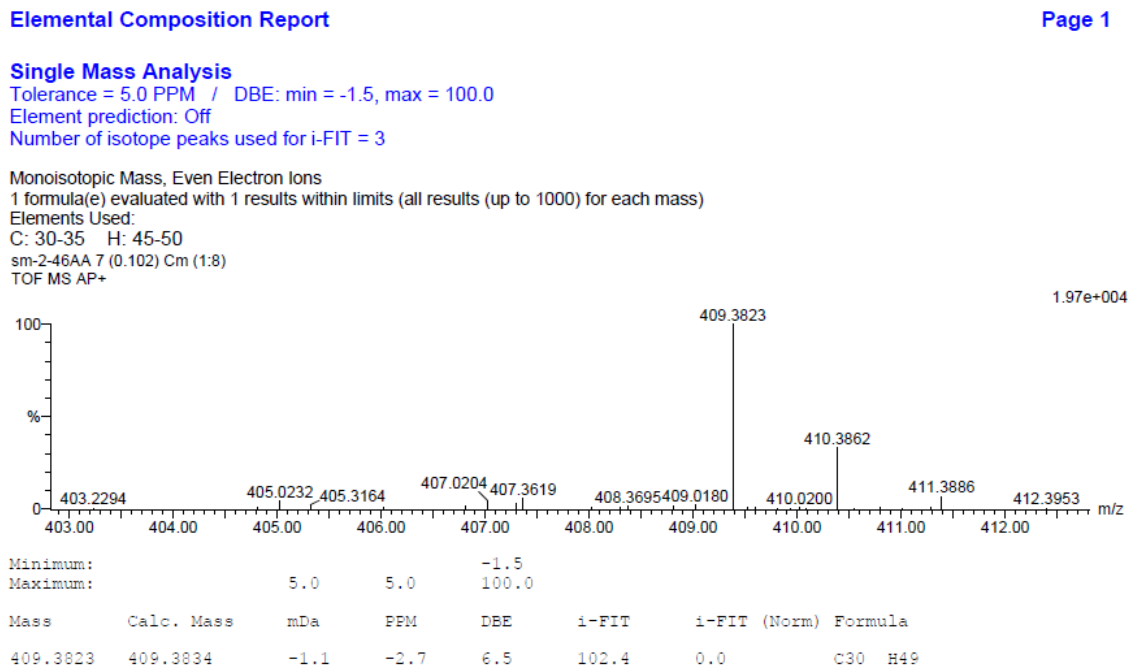

Figure 3.48. HR-API-(+)-MS spectrum of α-amyrin **(3.28)** and β-amyrin **(3.29)** mixture.

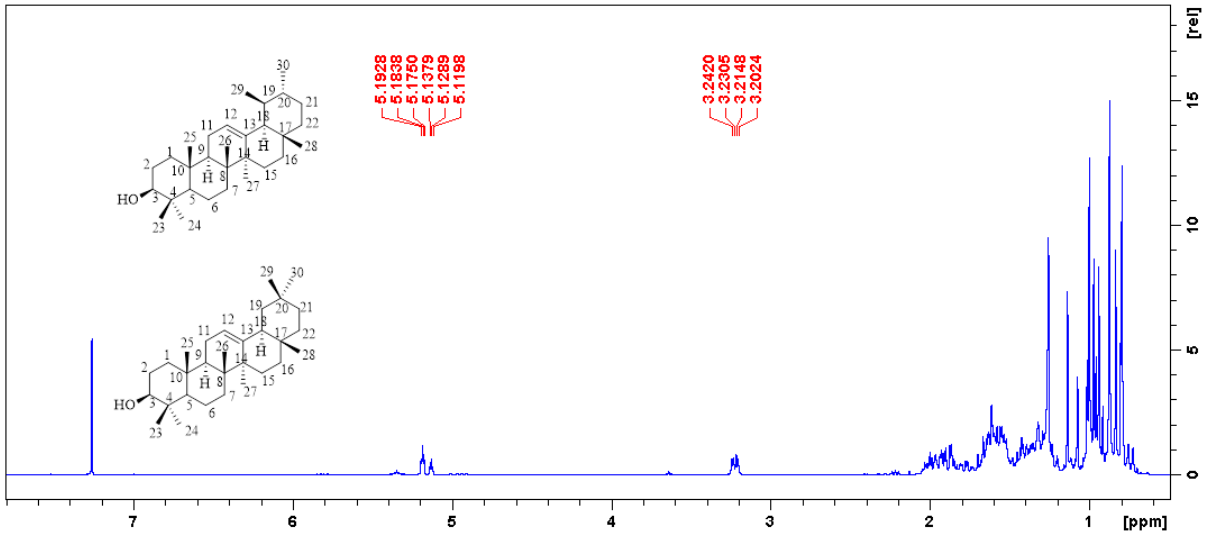

Figure 3.49. ^{1}H NMR spectrum of α-amyrin **(3.28)** and β-amyrin **(3.29)** mixture in $CDCl_3$ (400 MHz).

In the ^{1}H NMR spectrum **(Fig. 3.49)** of the α-amyrin **(3.28)** and β-amyrin **(3.29)** mixture the most distinctive change as compared to the parent compounds, is the chemical shift of the doublet of doublets at δ_H 3.22 (J = 4.8, 11.1 Hz) that was upfield as a result of the removal of an acetate moiety. In the 3-acetoxy analogue, the carbonyl causes deshielding of H-3 as a result of the anisotropic effect. The acetate removal was supported by the absence of the acetate methyl signal in the spectrum.

3.3.8 Characterization of ψ-taraxasterol (3.30)

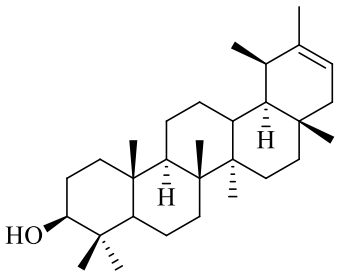

ψ -Taraxasterol **(3.30)**

Hydroxide-promoted hydrolysis of taraxasterol acetate **(3.22)** yielded compound **3.30** as a white amorphous solid. The triterpenoid alcohol had a retention time of 28.312 min in the GC-MS chromatogram **(Fig. 3.50)**, this retention time was less than that of its acetate analogue, compound **3.23**. The EI-MS spectrum of the compound **(Fig. 3.51)** showed an M^+ ion of *m/z* 426 which is the molecular mass of ψ-taraxasterol **(3.30)**. Furthermore, in the HR-

API-(+)-MS spectrum **(Fig. 3.51)** of the compound an ion peak of *m/z* 409.3827 was obtained , which resulted from a loss of water from the parent compound, with the molecular formula of $C_{30}H_{50}O$ (calculated for $C_{30}H_{49}$, 409.3834, $[M\text{-}H_2O+H]^+$).

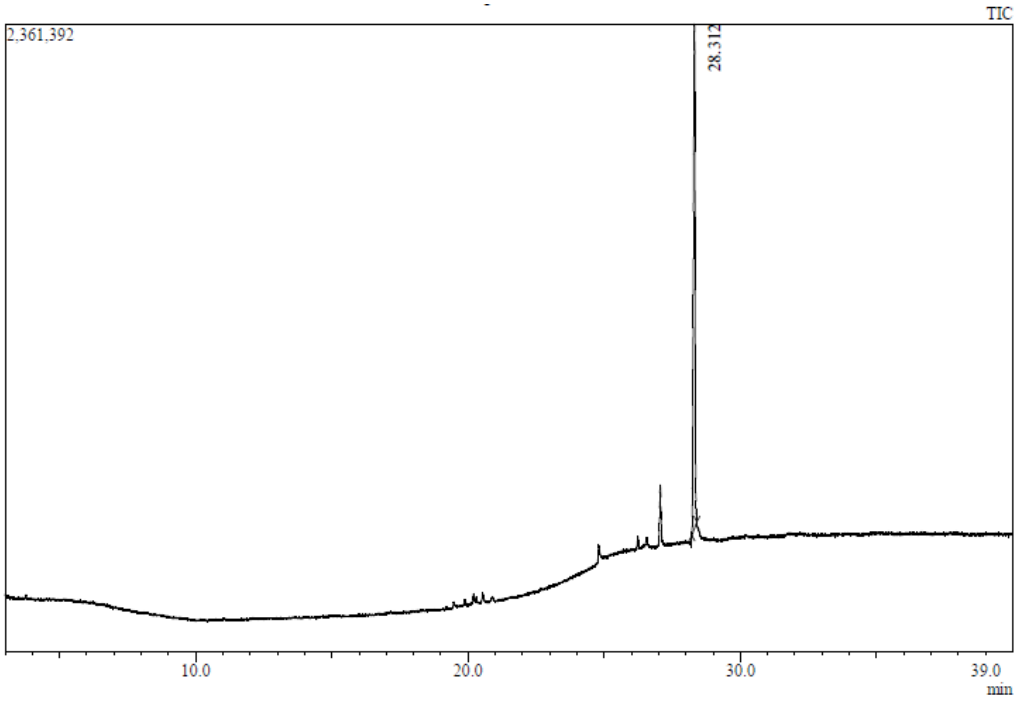

Figure 3.50. GC-MS chromatogram of ψ-taraxasterol **(3.30)**.

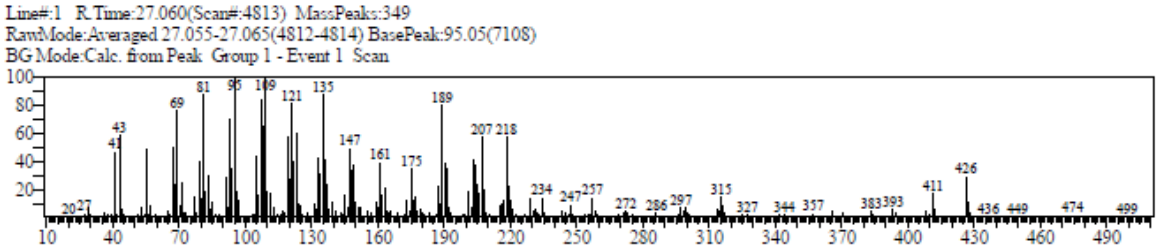

Figure 3.51. EI-MS spectrum of ψ-taraxasterol **(3.30)**.

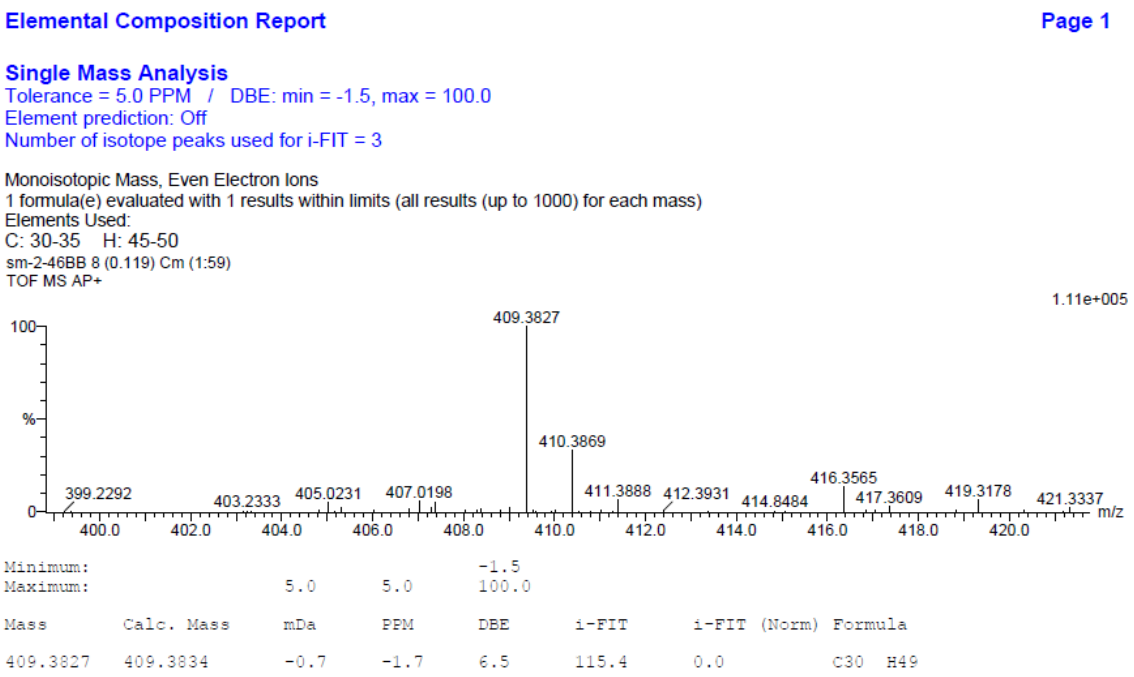

Figure 3.52. HR-API-(+)-MS spectrum of ψ-taraxasterol **(3.30)**.

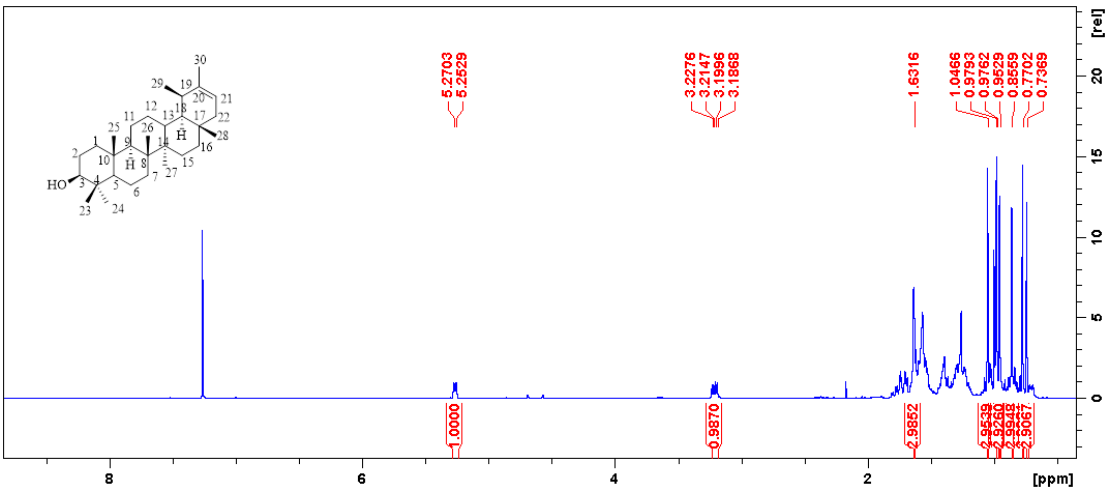

Figure 3.53. ^{1}H NMR of ψ-taraxasterol **(3.30)** in $CDCl_3$ (400 MHz).

The structure of ψ-taraxasterol (**3.30**), obtained by hydrolysis of the parent acetate, was corroborated by the ^{1}H NMR spectrum of the compound **(Fig. 3.53)**, since an acetate methyl signal was not present, and the C-3 proton was shifted upfield as a result (from δ_H 4.49 to δ_H 3.21). The ^{1}H NMR data was supported by the data reported in the literature for ψ-taraxasterol **(3.30)**, as shown in **Table 3.5**.

Table 3.5. ^{1}H NMR (400 MHz) data for ψ-taraxasterol **3.30** in $CDCl_3$.

Position	Experimental	Reported, [168]
	δ_H (ppm), *J* (Hz)	**δ_H (ppm), *J* (Hz)**
3	3.21 (1H, dd, 5.1, 11.2)	3.19 (dd)
21	5.26 (1H, d, 7.0)	5.25 (d)
23	0.98 (3H, s)	0.98 (s)
24	0.77 (3H, s)	0.78 (s)
25	0.86 (3H, s)	0.86 (s)
26	1.05 (3H, s)	1.04 (s)
27	0.95 (3H, s)	0.95 (s)
28	0.74 (3H, s)	0.73 (s)
29	0.98 (3H, d, 6.7)	0.99 (d)
30	1.63 (3H, s)	1.64 (s)

3.3.9 Characterization of taraxasterol (3.31)

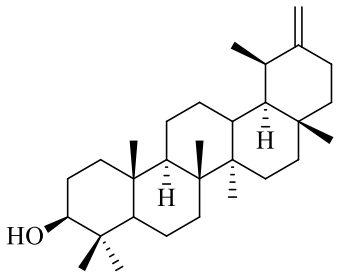

Taraxasterol **(3.31)**

Hydrolysis of taraxasterol acetate **(3.23)** afforded compound **3.31** as a white amorphous solid. In the GC-MS chromatogram **(Fig. 3.54)** the compound had a retention time of 28.452 min. The EI-MS spectrum **(Fig. 3.55)** showed a molecular ion of *m/z* 426, which is aligned with the molecular formula of taraxasterol. The HR-API-(+)-MS spectrum **(Fig. 3.56)** revealed an ion peak of *m/z* 409.3820 corresponding to the ion $[M\text{-}H_2O+H]^+$. The removal of water from $C_{30}H_{50}O$ is achieved, through the remote hydrogen rearrangement as discussed earlier in **Scheme 3.2**. The calculated *m/z* for $C_{30}H_{49}$ is 409.3834.

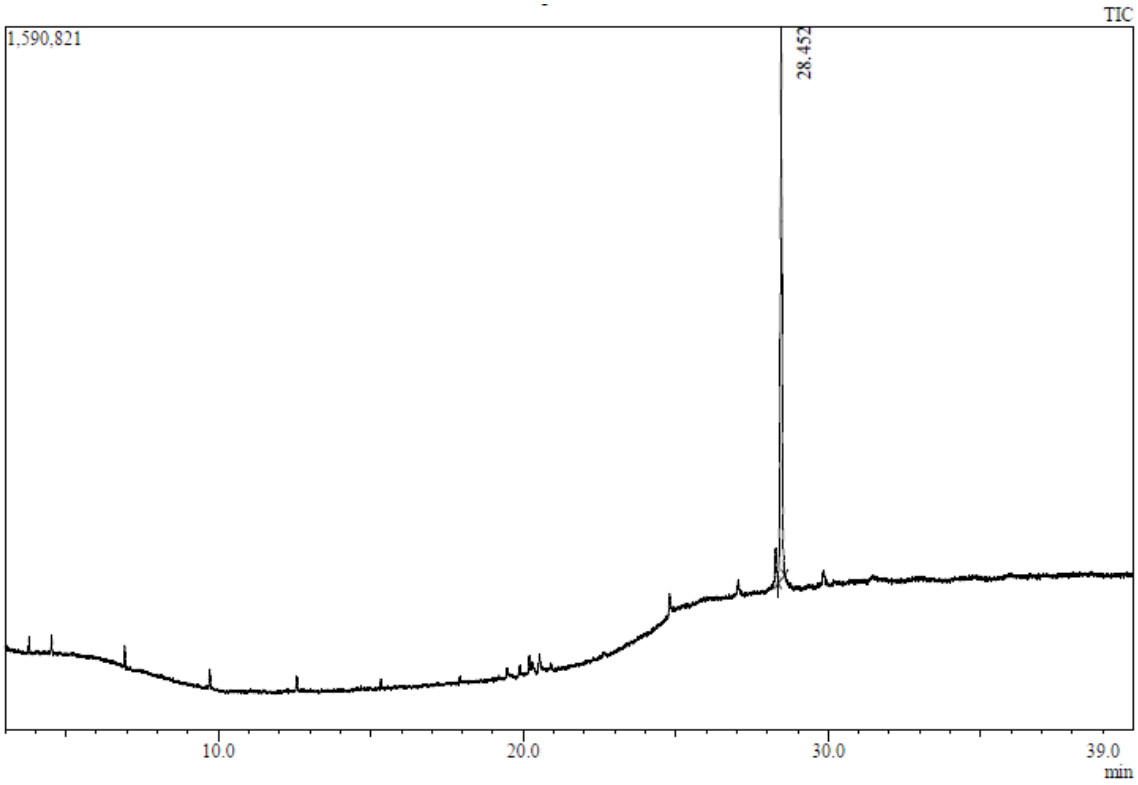

Figure 3.54. GC-MS chromatogram of taraxasterol **(3.31)**.

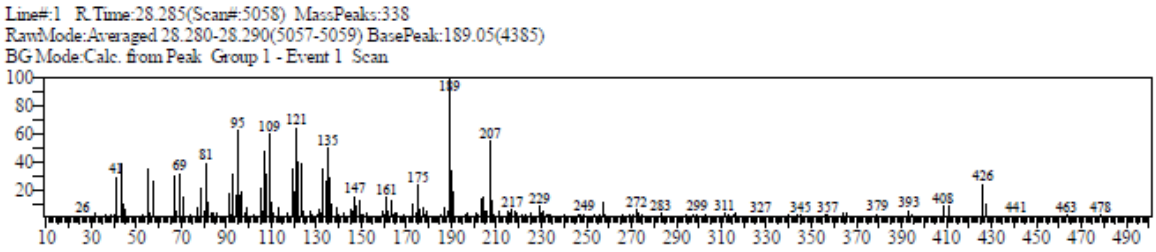

Figure 3.55. EI-MS spectrum of taraxasterol **(3.31)**.

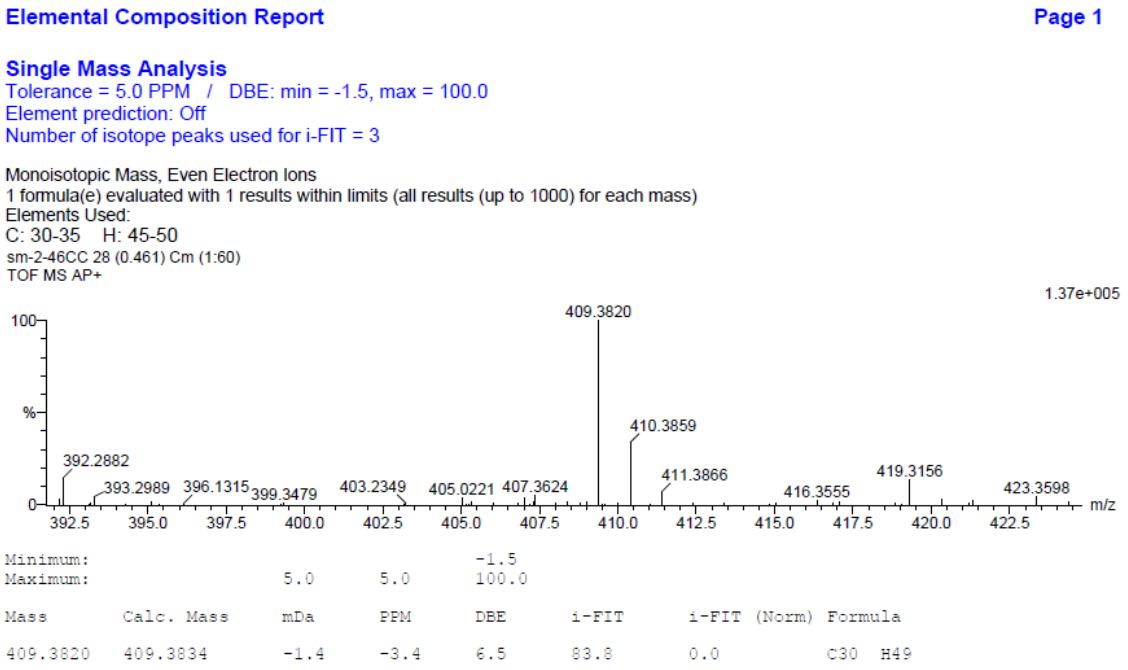

Figure 3.56. HR-API-(+)-MS spectrum of taraxasterol **(3.31)**.

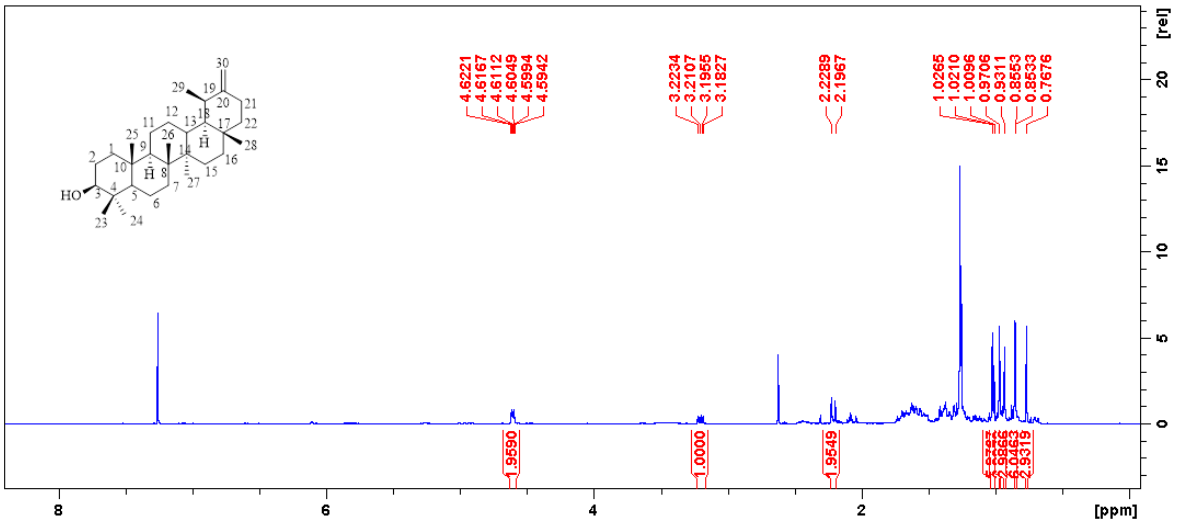

Figure 3.57. ^{1}H NMR of taraxasterol **(3.31)** in $CDCl_3$ (400 MHz).

The ^{1}H NMR spectrum of compound **3.31 (Fig. 3.57)** had differences as compared to that of taraxasterol acetate, with the absence of an acetate methyl signal, and the position of the doublet of doublets proton at C-3 was observed relatively upfield at δ_H 3.20. The ^{1}H NMR data was compared with literature reported data (**Table 3.6**).

Table 3.6. ^{1}H NMR (400 MHz) data for taraxasterol **(3.31)** in $CDCl_3$.

Position	**Experimental**	**Reported,** [168]
	δ_H (ppm), *J* (Hz)	**δ_H (ppm), *J* (Hz)**
3	3.20 (1H, dd, 5.1, 11.2)	3.20 (dd)
19		2.11 (m)
21	2.20–2.23 (m)	2.20 (m), 2.45 (m)
23	0.97 (3H, s)	0.97 (s)
24	0.77(3H, s)	0.76 (s)
25	0.85 (3H, s)	0.85 (s)
26	1.02 (3H, s)	1.02 (s)
27	0.93 (3H, s)	0.94 (s)
28	0.86 (3H, s)	0.86 (s)
29	1.02 (3H, d, 6.8)	1.02 (d)
30	4.61 (2H, m)	4.61 (m)

3.3.10 Characterization of lupeol (3.32)

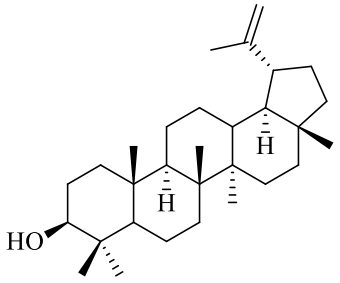

Lupeol **(3.32)**

The pentacyclic triterpenoid alcohol lupeol **(3.32)** was obtained as a white amorphous solid by the hydrolysis of lupeol acetate **(3.24)**. The compound had a retention time of 26.872 min in the GC-MS chromatogram **(Fig. 3.58)**. The $C_{30}H_{50}O$ molecular formula of the compound was accounted for by the EI-MS spectrum of the compound **(Fig. 3.59)** which showed a molecular ion of *m/z* 426, and from the HR-API-(+)-MS spectrum **(Fig. 3.60)** in which an $[M\text{-}H_2O+H]^+$ ion peak of *m/z* 409.3835 was observed (calculated for $C_{30}H_{49}$, 409.3834).

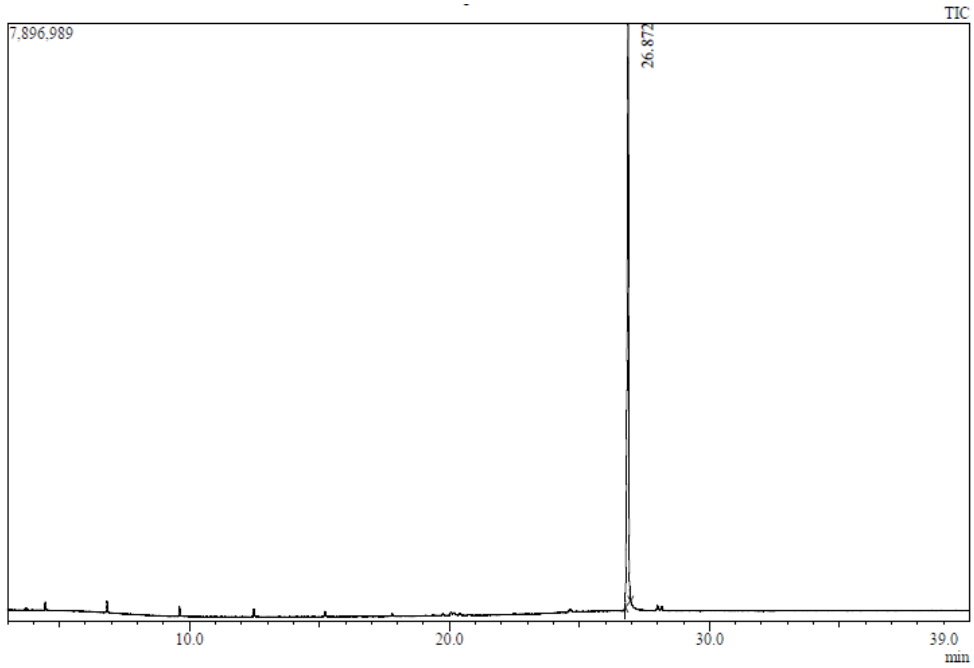

Figure 3.58. GC-MS chromatogram of lupeol **(3.32)**.

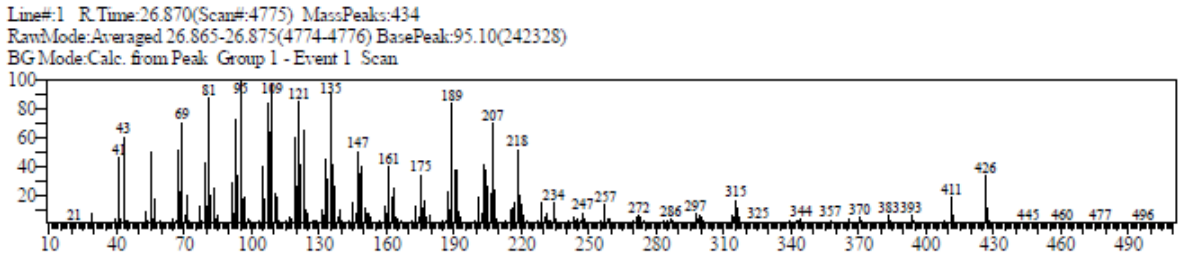

Figure 3.59. EI-MS spectrum of lupeol **(3.32)**.

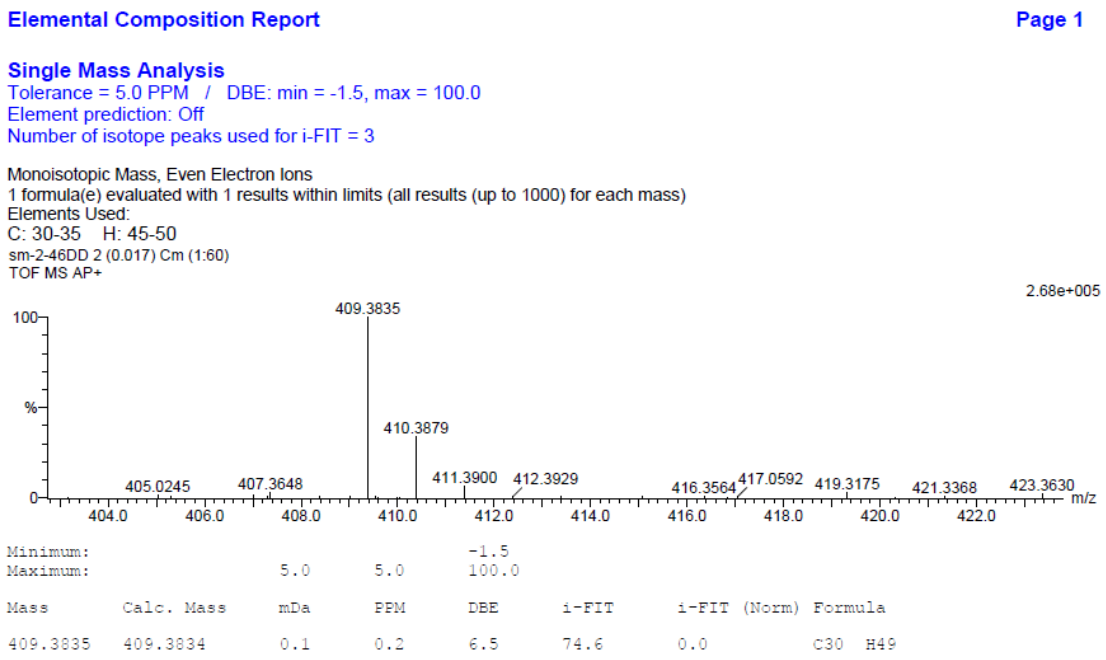

Figure 3.60. HR-API-(+)-MS spectrum of lupeol **(3.32)**.

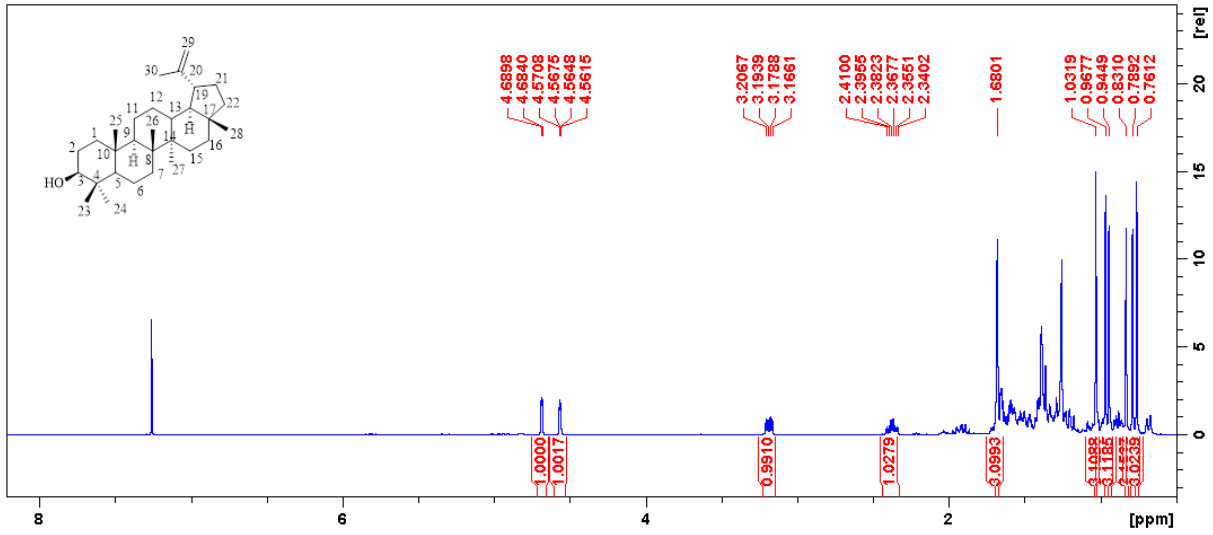

Figure 3.61. ^{1}H NMR spectrum of lupeol **(3.32)** in $CDCl_3$ (400 MHz).

The ^{1}H NMR spectra of the other triterpenoid alcohols were similar to those of the parent acetates, with the only significant differences, the removal of the acetate signal and the upfield shift of the C-3 proton. This was the case with lupeol as well, the acetate signal was absent, and the C-3 proton was shifted from δ_H 4.47 to δ_H 3.19 since it is now situated in a relatively less deshielded environment. The ^{1}H NMR data of lupeol was comparable with literature values as shown in **Table 3.7**.

Table 3.7. ^{1}H NMR (400 MHz) data for lupeol **(3.32)** in $CDCl_3$.

Position	Experimental	Reported, [168]
	δ_H (ppm), *J* (Hz)	**δ_H (ppm), *J* (Hz)**
3	3.19 (1H, dd, 5.1, 11.1)	3.18 (dd)
19	2.38 (1H, td, 11.1, 5.9)	2.39 (m)
23	0.97 (3H, s)	0.98 (s)
24	0.76 (3H, s)	0.77 (s)
25	0.83 (3H, s)	0.84 (s)
26	1.03 (3H, s)	1.04 (s)
27	0.94 (3H, s)	0.97 (s)
28	0.79 (3H, s)	0.79 (s)
29	4.57 (1H, m), 4.69 (1H, m)	4.56 (m), 4.69 (m)
30	1.68 (3H, s)	1.69 (s)

3.3.11 α-Glucosidase Inhibition Assay

In chapter **3.2.3**, it was reported that *B. discolor* is a medicinal plant used for treatment of diabetes. In vitro activity was observed with different plant leaf extracts, including DCM-MeOH, MeOH, and water extracts.[24-25,54] One of the objectives of this study was to investigate the inhibition of the crude extract and isolated compounds of α-glucosidase, one of the prominent targets for the management of diabetes. Inhibition of the carbohydrate metabolism enzyme α-glucosidase was performed using a method adopted from Xu et al.,[169] as described in detail in section **4.7**. The DCM-MeOH extract was evaluated in varying concentrations (20–160 μg/mL), and it exhibited considerable dose-dependent inhibition (see **Fig. 3.63**) with an estimated IC_{50} value of 95.95 μg/mL, when compared with a standard inhibitor, acarbose, with an IC_{50} of 1149.07 μg/mL. Unfortunately, the isolated compounds (pentacyclic triterpenoids) could not be assayed due to their poor solubility in the assay-tolerable solvent, DMSO. On account of that, the compounds were hydrolysed, but still the solubility of the more polar compounds remained a problem in the assay medium. However, some of these compounds have been assayed and reported elsewhere.[20,165]

Mellem et al.[25] has investigated the polar methanol and water extracts of *B. discolor* leaves but has obtained much lower IC_{50} values of 5180 and 7180 µg/mL, respectively, for the two extracts. For the inhibition of acarbose an IC_{50} value of 1200 µg/mL was reported,[25] which is comparable with the one we have obtained in this study (1149.07 µg/mL). In the literature, a variety of IC_{50} values are reported for acarbose, ranging from 4.75 µg/mL[22] to 1200 µg/mL (1.2 mg/mL).[25] However, looking at a number of papers, it was found that many research groups reported a high IC_{50} value for acarbose against α-glucosidase, e.g. Silva et al.[170] reported a value of 859.79 µM (554 µg/mL), and Zhang et al.[171] reported an IC_{50} of 2479 µM.

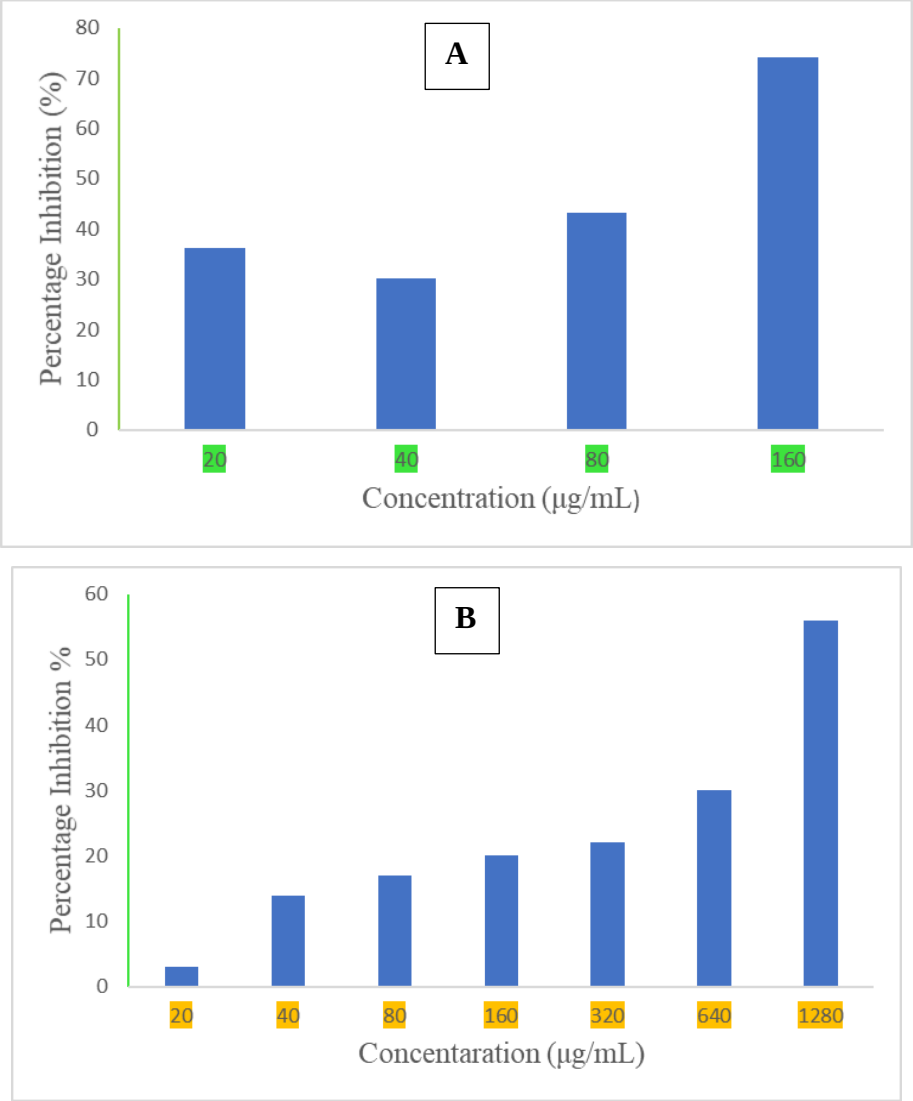

Figure 3.63. Inhibition of α-glucosidase by a leaf extract (A) and acarbose (B).

3.3.12 Molecular Docking Studies

In the prediction of the binding affinities of α-amyrin, β-amyrin, ψ-taraxasterol, taraxasterol and lupeol to the α-glucosidase active site, UCSF chimera-integrated AutoDock Vina software was used. The docking simulations revealed that the investigated triterpenoids were capable of binding with the enzyme active site pocket, as all the compounds clearly interacted with the amino acid residues in the active site. The amyrin compounds (**3.28** and **3.29**) were relatively the most promising since they had the best binding energies (see **Table 3.8.**) (the lower the binding energy the higher the binding capacity). Overall, α-amyrin was the most potent substrate, with a binding energy of -8.90 kcal/mol. The compound was interacting with amino acid residues, LYS 506, ALA 602, PHE 236, PHE 601, TRP 329 and PHE 476 as clearly seen from **Fig. 3.62**. The types of interactions involved were only alkyl and π-alkyl interactions, where the latter was only experienced between the unsaturated centre in the compound and PHE 476 residue. From the *in silico* study it was concluded that the compounds had the potential to inhibit the active site of the diabetes therapeutic target, α-glucosidase. However, from the computational docking, more practical investigations (biological assay) were in need to further corroborate the predicted results.

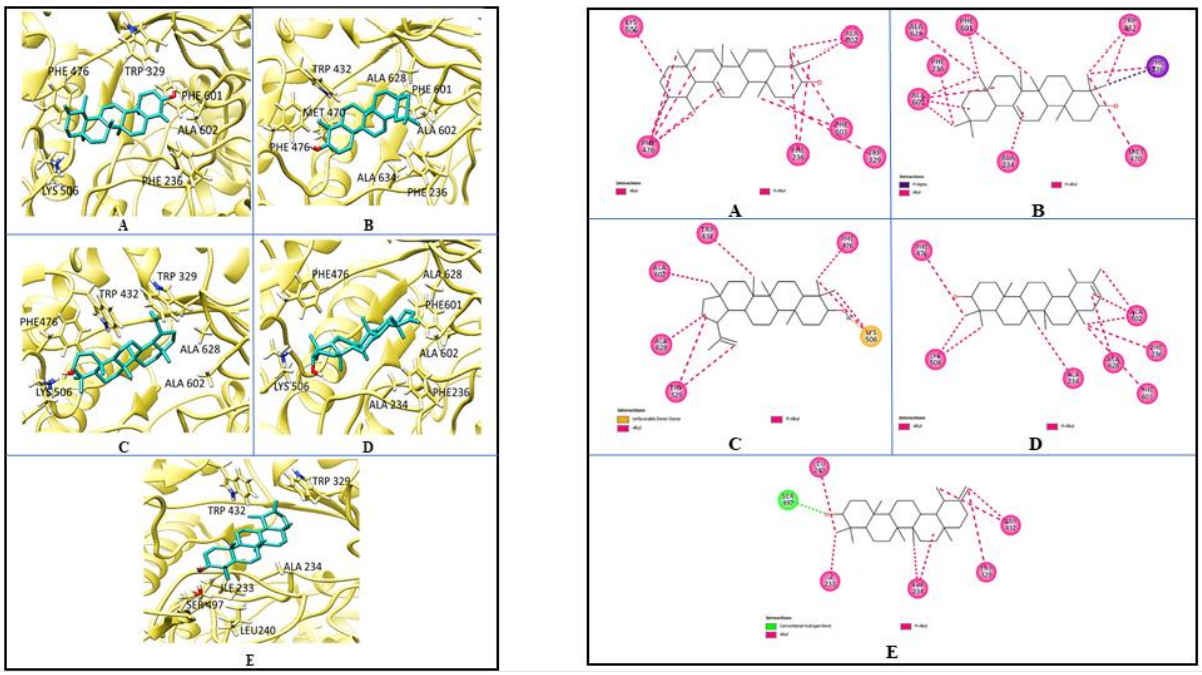

Figure 3.61. Molecular docking interactions of α-amyrin **(A)**, β-amyrin **(B)**, lupeol **(C)**, ψ-taraxasterol **(D)** and taraxasterol **(E)** with α-glucosidase binding site.

Table 3.8. Predicted binding capacities of compounds with α-glucosidase.

	Compound	**Binding Energy (kcal/mol)**	**Types of interactions**
A	α-Amyrin	-8.90	Alkyl, π-alkyl
B	β-Amyrin	-8.00	Alkyl, π-σ, π-alkyl
C	Lupeol	-7.90	Alkyl, unfavourable donor-donor, π-alkyl
D	ψ-Taraxasterol	-7.90	Alkyl, π-alkyl
E	Taraxasterol	-7.90	Alkyl, conventional hydrogen bond, π-alkyl

In sight of the triterpenoid binding capacities to α-glucosidase, the good inhibition ability of the DCM-MeOH extract and the reported triterpenoid activity claims (as with taraxasterol isolated from *Taraxacum mongolicum*)[165], there is justified motivation to further derivatize the compounds and study them for antidiabetic properties.

CHAPTER 4: EXPERIMENTAL

4.1 GENERAL EXPERIMENTAL PROCEDURES

GC-MS chromatograms were obtained on a Shimadzu gas chromatography-mass spectrometer (GCMS-QP2010 SE) equipped with a Zebron (ZB-5MSplus) capillary column (0.25 mm internal diameter, 30 m length and 0.25 μM film thickness). Optimum conditions of analysis employed are column temperature (150 °C), injection temperature (300 °C), injection mode (split), flow control mode (linear velocity), column flow (2.00 mL/min), and ion source temperature (200 °C). The oven temperature program started from 150 °C and was raised to 300 °C at 6 °C/min and the hold time was 15 min. The run time for this method was 40 min. High-resolution mass spectra of the compounds were obtained on a TOF (time-of-flight) Waters LCT Premier mass spectrometer using electrospray ionisation. A Cary 6630 FTIR instrument from Agilent Technologies was used to obtain infrared spectra.

A Bruker Avance III 400 (400 MHz for ^{1}H and 100 MHz for ^{13}C) spectrometer was used to perform NMR experiments (i.e. ^{1}H, ^{13}C, COSY, DEPT-135, HSQC and HMBC). All spectra were recorded in deuterated chloroform at 30 °C using a 5 mm TBIZ probe or a 5 mm BBOZ probe. Chemical shifts (δ) are given in parts per million (ppm) relative to tetramethylsilane (δ_H 0) and are corrected based on the residual protonated solvent peaks, for $CDCl_3$ (^{1}H, δ_H 7.26 and ^{13}C, δ_C 77.0).

Column chromatography was performed with silica gel 60 (40–63 μm, Merck). Thin-layer chromatography (TLC) plates (Kieselgel 60 F_{254}, 0.25 mm, Merck) were used to detect or profile components in the extracts and isolates. In the study, silica gel impregnated with silver nitrate was also used for both column and TLC analysis. By applying a method described by Li et al.,[172] a $AgNO_3$ aqueous solution of 10% (w/v) was mixed with silica gel (in a ratio solution: silica gel, 3:5) and then ground for 5 min. The ground silica gel was then placed in an oven (150 °C) for 1 h to remove the water. Thereafter, the resultant off-white silica was ready for use. $AgNO_3$-TLC plates were prepared using the same principle as described above, where TLC plates were sprayed with a 10% $AgNO_3$ solution and were oven-dried for 1 h (temperature, 110 °C). In the TLC analysis, after development, the plates

were sprayed with an anisaldehyde stain reagent and heated with a heat gun for visualisation of spots.

4.2 COLLECTION OF PLANT MATERIAL

Fresh *Brachylaena discolor* DC plant material was collected on 21 April 2018 at 133 Buldana Road, Bluff, Durban (KwaZulu-Natal). The plant was identified by Prof Himansu Baijnath, a plant taxonomist from the University of KwaZulu-Natal, School of Life Sciences, Westville Campus. A voucher specimen was prepared and deposited at the University of KwaZulu-Natal Bews Herbarium (NU) (accession number NU0077001).

4.3 EXTRACTION OF PLANT MATERIAL

Leaves of *B. discolor* were left to dry in a sunlight-free drying room for three weeks, and then a hammer mill was employed to grind the material into a fine powder. This powder was subsequently packed in brown paper packets for storage. The mass of the ground leaf powder was 3.488 kg. Leaf powder (961 g) of the plant was extracted by soaking the material in dichloromethane (4.5 L) for 24 h. The mixture was filtered under suction, and the filtrate was then concentrated to dryness on a rotary evaporator at 40-50 °C. The dried extract (31.971 g) was stored at 4 °C. The DCM extract (5.008 g) was fractionated using vacuum-liquid chromatography on a column packed with 83.308 g of silica eluting with solvents/solvent systems of increasing polarity to afford six subfractions as shown in **Table 4.1**.

Table 4.1. Fractions obtained by VLC of a DCM extract of *B. discolor* leaves.

Solvent	Volume (mL)	Fraction	Amount (mg)
Hex-DCM 8 : 2	300	Sm-2-18A	602
Hex-DCM 6 : 4	200	Sm-2-18B	792
Hex-DCM 4 : 6	200	Sm-2-18C	540
Hex-DCM 2 : 8	200	Sm-2-18D	141
Methanol	100	Sm-2-18E	51
Methanol	300	Sm-2-18F	2580

The fractions were analysed for triterpenoids by GC-MS. Fractions containing triterpenoids were further purified using argentation chromatography as described in section **4.4** below

4.4 ISOLATION OF TRITERPENOIDS USING ARGENTATION COLUMN CHROMATOGRAPHY

The compounds in the VLC fractions, Sm-2-18B, Sm-2-18C, Sm-2-18D and Sm-2-18E were purified using argentation column chromatography, which makes use of silver nitrate ($AgNO_3$)-impregnated silica, as described in section **4.1**. A summarised schematic of the performed isolations is shown in **Fig. 4.1**. The Hex-DCM solvent systems used for the purifications are shown in **Table 4.2**. In all the columns, fractions were collected in small volumes of 3-5 mL.

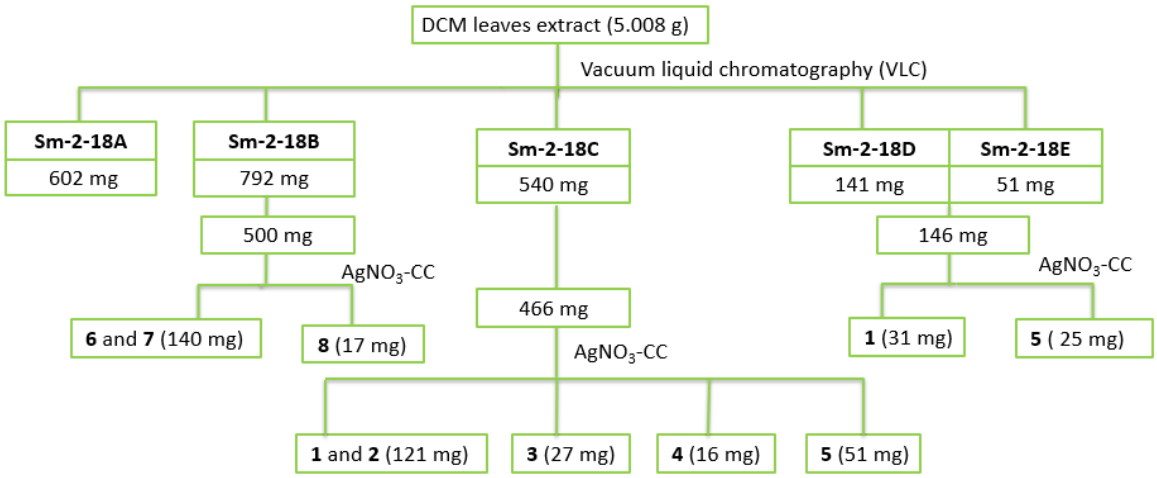

Figure 4.1. Flow chart of the purification of triterpenoids from *B. discolor* leaves DCM extract.

Table 4.2. Summary of the eluents used in the performed purifications.

Column	Solvent systems	Volume (mL)
Sm-2-18B (500 mg)	Hex-DCM 95 : 5	100
	Hex-DCM 190 : 10	100
	Hex-DCM 85 : 15	100
	Hex-DCM 170 : 30	1675
Sm-2-18D,E (146 mg)	Hex-DCM 8 : 2	100
	Hex-DCM 6 : 4	950
Sm-2-18C (466 mg)	Hex-DCM 9 : 1	150
	Hex-DCM 6 : 4	400

4.5 HYDROLYSIS OF THE TRITERPENOID ACETATES

The five triterpenoid acetates **(3.20**-**3.24)** were hydrolysed in a basic medium. The respective compounds were firstly dissolved in small amounts of DCM, then refluxed in a 5% KOH methanolic solution at 60 °C for 6 h. The ratio between compound and 5% KOH solution was maintained at 5 mg/mL. Upon completion of the reaction, acetone was added to precipitate the potassium acetate salt, and the solid residues were filtered off. The acetone was evaporated, and distilled water was added to the sample. The excess base in the product mixture was neutralised with acetic acid, and the product was extracted with chloroform. The α/β-amyrin acetate mixture **(3.20**, **3.21)**: 15 mg was hydrolysed and this yielding 10.7 mg mixture of α-amyrin (**3.28)** and β-amyrin (**3.29)**. 16.6 mg of ψ-taraxasterol acetate **(3.32)** gave 8.3 mg of ψ-taraxasterol **(3.30)**, 9.1 mg of taraxasterol acetate **(3.23)** afforded 8.8 mg of taraxasterol **(3.31)**, and 19.9 mg of lupeol was obtained from the hydrolysis of 25 mg of lupeol acetate **(3.24)**. A breakdown of the hydrolysis performed is clearly shown in **Fig. 4.4**.

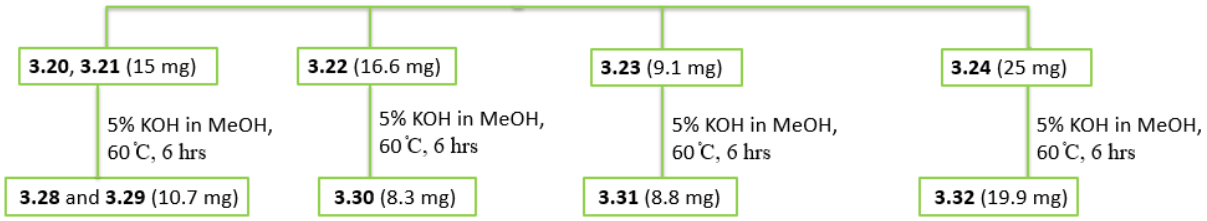

Figure 4.2. Flow chart of the hydrolysis of the triterpenoid acetate compounds.

4.6 PHYSICAL, CHEMICAL AND SPECTRAL DATA OF ALL COMPOUNDS

α-Amyrin acetate (3.20) and β-amyrin acetate (3.21)

Molecular formula: $C_{32}H_{53}O_2$, physical description: white amorphous solid, yield: 121 mg. ^{1}H NMR: **(Fig. 3.7)**, ^{13}C NMR: **(Fig. 3.8)**, DEPT-135: Plate 1A, COSY: Plate 1A, HSQC: **(Fig. 3.9)**, HMBC: **(Fig. 3.10)**, GC-MS: **(Fig. 3.3)**. EI-MS: **(Fig. 3.4)** *m/z* 468 (M^+), *m/z* 189, 203, 218 (100) (for both **3.20** and **3.21**, but different intensities in some fragments). HR-MS:

(Fig. 3.5) *m/z* 469.4061 $[M+1]^+$, $C_{32}H_{53}O_2$ (Calculated for 469.4046). FT-IR: **(Fig. 3.6)** 2916.643 cm^{-1} (m, C-H), 1731.198 cm^{-1} (s, C=O), 1246.646 cm^{-1} (s, C-O).

ψ-Taraxasterol acetate (3.22)

Molecular formula: $C_{32}H_{53}O_2$, physical description: colorless amorphous solid, yield: 27 mg. ^1H NMR: (**Fig. 3.14**, **Table 3.1**) (400 MHz, $CDCl_3$) δ_H: 5.26 (1H, d, *J* = 6.8 Hz), 4.49 (1H, dd, *J* = 6.7, 10.5 Hz), 2.04 (s), 1.63 (s), 1.04 (s), 0.99 (d, *J* = 6.4 Hz), 0.95 (s), 0.87 (s), 0.85 (s), 0.84 (s), 0.73 (s). ^{13}C NMR: (**Fig. 3.15**, **Table 3.1**) ^{13}C NMR (400 MHz, $CDCl_3$) δ_C: 170.9, 139.8, 118.9, 80.9, 55.4, 50.4, 48.7, 42.3, 42.2, 41.1, 39.2, 38.5, 37.8, 37.0, 36.7, 36.3, 34.4, 34.2, 27.9, 27.6, 27.0, 23.7, 22.5, 21.6, 21.6, 21.3, 18.2, 17.7, 16.5, 16.3, 16.0, 14.7.DEPT-135: **(Fig.3.15)**, COSY: Plate 2A, HSQC: **(Fig.3.16)**, HMBC: **(Fig.3.17)**, GC-MS: **(Fig.3.11)**, EI-MS: **(Fig. 3.12)** *m/z* 468 (M^+), *m/z* 95, 109, 121, 189 (100), 249, 408. HR-MS: **(Fig.3.13)** *m/z* 469.4057 $[M+1]^+$, $C_{32}H_{53}O_2$ (Calculated for 469.4046).

Taraxasterol acetate (3.23)

Molecular formula: $C_{32}H_{53}O_2$, physical description: colorless crystals, yield: 16 mg. ^1H NMR: (**Fig. 3.22**, **Table 3.2**) (400 MHz, $CDCl_3$) δ_H: 4.61 (2H, m), 4.48 (1H, dd, *J* = 6.6, 10.3 Hz), 2.44 (1H, m), 2.20 (1H, m), 2.10 (1H, m), 1.02 (d, *J* = 6.7 Hz), 1.02 (s), 0.93 (s), 0.88 (s), 0.85 (s), 0.85 (s), 0.84 (s), 0.73 (s).^{13}C NMR: (**Fig. 3.23**, **Table 3.2**) ^{13}C NMR (400 MHz, $CDCl_3$) δ_C: 170.9, 154.6, 107.1, 80.9, 55.5, 50.4, 48.7, 42.1, 40.9, 39.4, 39.2, 38.9, 38.5, 38.3, 37.8, 37.1, 34.5, 34.0, 27.9, 26.7, 26.2, 25.6, 25.5, 23.7, 21.5, 21.3, 19.5, 18.2, 16.5, 16.3, 15.9, 14.7.DEPT-135: **(Fig. 3.23)**, COSY: Plate 3A, HSQC: **(Fig. 3.24)**, HMBC: **(Fig. 3.25)**, GC-MS: **(Fig. 3.19)**, EI-MS: **(Fig. 3.20)** *m/z* 468 (M^+), *m/z* 95, 109,121, 135, 189 (100), 249, 399. HR-MS: **(Fig. 3.21)** *m/z* 426.4056 $[M+1]^+$, $C_{32}H_{53}O_2$ (Calculated for 469.4046).

Lupeol acetate (3.24)

Molecular formula: $C_{32}H_{53}O_2$, physical description: off-white amorphous solid, yield: 51 mg. ^{1}H NMR: (**Fig. 3.30**, **Table 3.3**) (400 MHz, $CDCl_3$) δ_H: 4.69 (1H, d, *J* = 2.2 Hz), 4.57 (1H, m), 4.47 (1H, dd, *J* = 5.6, 10.8 Hz), 2.37 (1H, td, *J* = 5.8, 10.9, 11.0 Hz), 2.04 (s), 1.68 (s), 1.02 (s), 0.94 (s), 0.86 (s), 0.85 (s), 0.84 (s), 0.79 (s). ^{13}C NMR: (**Fig. 3.31**, **Table 3.3**) ^{13}C NMR (400 MHz, $CDCl_3$) δ_C: 170.9, 150.9, 109.3, 80.9, 55.4, 50.4, 48.3, 48.0, 42.9, 42.8, 40.9, 40.0, 38.4, 38.1, 37.8, 37.1, 35.6, 34.2, 29.8, 27.9, 27.4, 25.1, 23.7, 21.3, 20.9, 19.3, 18.2, 18.0, 16.5, 16.2, 15.9, 14.5.DEPT-135: **(Fig. 3.31)**, COSY: Plate 4A, HSQC: **(Fig. 3.32)**, HMBC: **(Fig. 3.33)**, GC-MS: **(Fig. 3.36)**. EI-MS: **(Fig. 3.27)** *m/z* 468 (M^+), *m/z* 95, 109, 121, 135, 147, 189 (100), 204, 218, 357. HR-MS: **(Fig. 3.28)** *m/z* 469.4055 $[M+1]^+$, $C_{32}H_{53}O_2$ (Calculated for 469.4046). FT-IR: **(Fig. 3.29)** 2940.086 cm^{-1} (m, C-H), 1732.05 cm^{-1} (s, C=O), 1244.101 cm^{-1} (s, C-O).

α-Amyrin palmitate (3.25) and β-amyrin palmitate (3.26)

Molecular formula: $C_{46}H_{80}O_2$, physical description: Colorless viscous substance, yield: 140 mg. ^{1}H NMR: **(Fig. 3.36)**, ^{13}C NMR: **(Fig. 3.37)** , DEPT-135: Plate 5A, COSY: Plate 5A, HSQC: **(Fig. 3.38)**, HMBC: **(Fig. 3.39)**, HR-MS: **(Fig. 3.34)** *m/z* 663.6064 $[M-1]^+$, $C_{46}H_{79}O_2$ (Calculated for 663.6080). FT-IR: **(Fig. 3.35)** 2916.109 and 2850.413 cm^{-1} (s, C-H), 1728.208 cm^{-1} (s, C=O).

Lupeol palmitate (3.27)

Molecular formula: $C_{46}H_{80}O_2$, physical description: white amorphous solid, yield: 17 mg. ^{1}H NMR: (**Fig. 3.42**, **Table 3.4**) (400 MHz, $CDCl_3$) δ_H : 4.68 (d, *J* = 2.2 Hz), 4.57 (m), 4.47 (1H, dd, *J* = 5.6, 10.7 Hz), 2.37 (1H, td, J = 5.8, 11.0, 10.9 Hz), 2.28 (2H, t, *J* = 7.4 Hz), 1.68 (s), 1.62 (m), 1.25 (24H, br, s), 1.03 (s), 0.94 (s), 0.89 (br), 0.88 (s), 0.86 (s), 0.83 (s). ^{13}C NMR: (**Fig. 3.43**, **Table 3.4**) (400 MHz, $CDCl_3$) δ_C: 173.7, 150.9, 109.3, 80.6, 55.4, 50.4, 48.3, 48.0, 42.9, 42.8, 40.9, 40.0, 38.4, 38.1, 37.8, 37.1, 35.6, 34.9, 34.2, 31.9, 29.85, 27.9, 29.2-29.7, 27.2, 25.2, 25.1, 23.8, 22.7, 20.9, 19.3, 18.2, 18.0, 16.6, 16.2, 15.9, 14.5, 14.1. DEPT-135: **(Fig. 3.43)**. COSY: Plate 6A. HSQC: **(Fig. 3.44)**. HMBC: **(Fig. 3.45)**. HR-MS: **(Fig.3.40)** *m/z* 663.6076 $[M-1]^+$, $C_{46}H_{79}O_2$ (Calculated for 663.6080). FT-IR: **(Fig. 3.41)** 2914.376 and 2849.471 cm^{-1} (s, C-H), 1726.171 cm^{-1} (s, C=O).

α-Amyrin (3.28) and β-amyrin (3.29)

Molecular formula: $C_{30}H_{50}O$, physical description: White amorphous solid, yield: 10.7 mg, GC-MS: **(Fig. 3.46)**. EI-MS: **(Fig. 3.47)** MS data: 426(M^+), *m/z* 189, 203, 218 (100) (for both **3.28** and **3.29**). HR-MS: **(Fig. 3.48)** *m/z* 409.3823 $[M-H_2O+H]^+$, (Calculated for 409.3834). ^1H NMR: **(Fig. 3.49)**.

ψ-Taraxasterol (3.30)

Molecular formula: $C_{30}H_{50}O$, physical description: white amorphous solid, yield: 8.3 mg, GC-MS: **(Fig. 3.50)**. EI-MS: **(Fig. 3.51)** *m/z* 426 (M^+), *m/z* 69, 81, 95(100), 109, 121, 135, 189, 207, 218, 411.HR-MS: **(Fig. 3.52)** *m/z* 409.3827 $[M-H_2O+H]^+$, (Calculated for 409.3834). ^1H NMR: (**Fig. 3.53**, **Table 3.5**) (400 MHz, $CDCl_3$) δ_H : 5.26 (1H, d, *J* = 7.0 Hz), 3.21 (1H, dd, *J* = 5.1, 11.2 Hz), 1.63 (s), 1.05 (s), 0.99 (d, *J* = 6.7 Hz), 0.98 (s), 0.95 (s), 0.86 (s), 0.77 (s), 0.74 (s).

Taraxasterol (3.31)

Molecular formula: $C_{30}H_{50}O$, Physical description: white amorphous solid, yield: 8.8 mg, GC-MS: **(Fig. 3.54)**, MS Spectra: **(Fig. 3.55)** *m/z* 426 (M^+), *m/z* 69,81, 95, 109, 121, 135, 189(100), 207, 408. HR-MS: **(Fig. 3.56)** *m/z* 409.3820 $[M-H_2O+H]^+$, (Calculated for 409.3834). ^1H NMR: (**Fig. 3.57**, **Table 3.6**) (400 MHz, $CDCl_3$) δ_H : 4.61 (m), 3.20 (1H, dd, *J* = 5.1, 11.2 Hz), 2.20-2.23 (m), 1.02 (d, *J* = 6.8 Hz), 1.02 (s), 0.97 (s), 0.93 (s), 0.86 (s), 0.85 (s), 0.77 (s).

Lupeol (3.32)

Molecular formula: $C_{30}H_{50}O$, physical description: white amorphous solid, yield: 19.9 mg, GC-MS: **(Fig. 3.58)** EI-MS: **(Fig. 3.59)** *m/z* 426 (M^+), *m/z* 69, 81, 95(100), 109, 121, 135, 189, 218. HR-MS: **(Fig. 3.60)** *m/z* 409.3835 $[M-H_2O+H]^+$, (Calculated for 409.3834). ^1H NMR: (**Fig. 3.61**, **Table 3.7**) (400 MHz, $CDCl_3$) δ_H : 4.56 (1H, m), 4.57 (1H, m), 3.19 (1H, dd, *J* = 5.1, 11.1 Hz), 2.38 (1H, td, *J* = 5.9, 11.1, 11.0 Hz), 1.68 (s), 1.03 (s), 0.97 (s), 0.94 (s), 0.83 (s), 0.79 (s), 0.76 (s).

4.7 α-GLUCOSIDASE INHIBITION ASSAY

Inhibition of the enzyme α-glucosidase was determined by a procedure described by Xu et al.[169] 3 µL α-Glucosidase solution (2 units/mL) in potassium phosphate buffer (0.1 M, pH 6.8) was mixed with 2 µL test sample (dissolved in DMSO), then incubated at 37 °C for 5 min. The reaction was started by the addition of 15 µL of 10 mM *p*-nitrophenyl-*α*-D-glucoside solution (PNPG) and 80 µL of 0.1 M potassium phosphate buffer, followed by incubation at 37 °C for 30 min (note: DMSO final concentration was 0.2%). The reaction was terminated by addition of 200 µL of Na_2CO_3. Absorbance was measured at 405 nm for the quantification of *p*-nitrophenol (product formed from the enzyme-substrate interaction). For a negative control, 2 µL of 0.2% DMSO was used in place of the test sample, and acarbose was used as a positive control. On account of the coloured test samples, the samples in different concentrations were assayed in a similar procedure but in place of the enzyme solution, 3 µL of buffer was used. The following equation, adopted from Sagbo et al.,[148] was used in the calculation of percentage inhibition:

$$\% \text{ Inhibition} = \left(1 - \left(\frac{\text{Absorbance of test sample}}{\text{Absorbance of negative control}}\right)\right) \times 100$$

It must be noted that all the experiments were performed in triplicate, and for the estimation of IC_{50} values, regression analysis was used.

4.8 COMPUTATIONAL METHODS

4.8.1 Initial structure preparation

The crystal structure of α-glucosidase in complex with an inhibitor (PDB entry 3W37) was used as an initial structure. All crystal water molecules and bound inhibitor were deleted from the PDB file. The missing residues were added by Modeler.[173] In order to get the most stable conformations of the inhibitors, 3D structures of all compounds were fully optimized at the B3LYP/6-311++G(d,p) level of theory with the Gaussian16 program package.[174-175] All compounds were characterized as minima by the absence of imaginary frequencies. Then, optimized structures were used for molecular docking using UCSF Chimera.[176]

4.8.2 Molecular docking

All compounds optimized at the B3LYP/ 6-311++G(d,p) level of theory were used for computational docking, UCSF Chimera was used to approximate free binding energy. The site of molecular docking was selected based on grid box centered on the active site with definitions of 23.17 × 24.02 × 23.56. It is important to mention that the similar coordinates were employed for all compounds. In the docking process, the inhibitors were set as flexible while α-glucosidase was positioned as rigid. Polar hydrogen atoms and Kollman charges were assigned to HCV RdRp while Gasteiger partial charges and non-polar hydrogen atoms were assigned to the inhibitors. Molecular docking between the inhibitors and protein was then carried out with the aid of AutoDock Vina.[177] The best poses with the highest negative energy scoring were identified and corresponding complexes were saved with UCSF Chimera.

CHAPTER 5: CONCLUSIONS AND FUTURE WORK

The global prevalence of type 2 diabetes mellitus is on the increase and this metabolic disease is becoming an epidemic of astronomical proportions. Diabetes mellitus has no cure and needs to be managed by lifestyle changes and drugs to avoid the serious complications associated with it. In South Africa, several plants are used in traditional medicine for the management of diabetes. The phytochemistry and active components of most of these plants are still not well understood due to limited studies. More investigations are necessary on these plants to validate the activity of the plants and to protect the users of traditional medicine. Such investigations might also yield new antidiabetic drugs.

In this study, a medicinal plant, *Brachylaena discolor* DC that is used in South Africa for the treatment of diabetes, was investigated. In the literature, several studies on the antidiabetic properties of natural triterpenoids and their synthetic derivatives have been reported. As a result, in the current investigation of *B. discolor*, the emphasis was on the triterpenoids present in the plant. The dichloromethane leaf extract of *B. discolor* was purified using argentation chromatography and eight triterpenoid esters were afforded, α-amyrin acetate **(3.20)**, β-amyrin acetate **(3.21)**, ψ-taraxasterol acetate **(3.22)**, taraxasterol acetate **(3.23)**, lupeol acetate **(3.24)**, α-amyrin palmitate **(3.25)**, β-amyrin palmitate **(3.26)**, and lupeol palmitate **(3.28)**. Both the acetyl and palmity esters of α-amyrin and β-amyrin were isolated as inseparable mixture of the two triterpenes. The other compounds were isolated as pure compounds and all the structures were determined by spectroscopic and spectrometric methods. Except for compound **3.24**, all the compounds are reported for the first time from this *Brachylaena* species. Hydrolysis of the esters yielded five free triterpenoids, (i.e. α-amyrin **(3.28)**, β-amyrin **(3.29)**, ψ-taraxasterol **(3.30)**, taraxasterol **(3.31)**, and lupeol **(3.32)**). The *in vitro* and *in vivo* antidiabetic activity of the isolated compounds have been reported previously, e.g. β-amyrin palmitate **(3.26)** was active in treating diabetic mice.[159]

The activity of the DCM-MeOH extract was investigated, and it was observed that the extract was a more active inhibitor of α-glucosidase, an enzyme in the intestines that breaks down carbohydrates to glucose, than acarbose, a drug used for the treatment of diabetes. An attempt to assay the single compounds against this enzyme was not successful due to the lack of solubility of the compounds in the assay medium.

In silico studies by molecular docking of compounds **3.28**–**3.32** revealed that all these triterpenes could interact effectively with the α-glucosidase active-site pocket. Among the compounds, α-amyrin **(3.20)** had the highest binding potential. In future studies, the solubility limitations of the isolated triterpenoids need to be addressed, either by using surfactants as part of the assay mixture or by derivatization of the compounds to increase the polarity. The compounds should then be assayed against other molecular therapeutic targets for diabetes, i.e. enzyme inhibition of α-amylase, α-glucosidase and PTP1B. Further *in silico* experiments need to be performed to identify the triterpenoid derivatives with the highest potential. In conclusion, it has been shown that the plant extract has activity and that the triterpenoids present in the extract may play a role in the activity of the plant.

REFERENCES

1. Moreira, A. C.; Müller, A. C. A.; Pereira Jr, N.; Antunes, A. M. D. S., Pharmaceutical patents on plant derived materials in Brazil: Policy, law and statistics. *World Patent Information* **2006,** *28* (1), 34–42.
2. Newman, D. J.; Cragg, G. M., Natural products as sources of new drugs from 1981 to 2014. *Journal of Natural Products* **2016,** *79* (3), 629–661.
3. Newman, D. J.; Cragg, G. M.; Kingston, D. G., Natural Products as Pharmaceuticals and Sources for Lead Structures. In *The Practise of Medicinal Chemistry*, "Second Edition" ed.; Wermuth, C. G., Ed. Academic Press: 2003; pp 91–109.
4. Newman, D. J.; Cragg, G. M., Natural products as sources of new drugs over the last 25 years. *Journal of Natural Products* **2007,** *70* (3), 461–477.
5. Newman, D. J.; Cragg, G. M., Natural products as sources of new drugs over the 30 years from 1981 to 2010. *Journal of Natural Products* **2012,** *75* (3), 311–335.
6. Newman, D. J.; Cragg, G. M.; Snader, K. M., Natural products as sources of new drugs over the period 1981− 2002. *Journal of Natural Products* **2003,** *66* (7), 1022–1037.
7. Newman, D. J., From natural products to drugs. *Physical Sciences Reviews* **2018**.
8. Zhou, B.; Hu, Z.-J.; Zhang, H.-J.; Li, J.-Q.; Ding, W.-J.; Ma, Z.-J., Bioactive staurosporine derivatives from the *Streptomyces* sp. NB-A13. *Bioorganic Chemistry* **2019,** *82*, 33–40.
9. RYDAPT® (midostaurin) capsules, for oral use. https://www.accessdata.fda.gov/drugsatfda_docs/label/2017/207997s000lbl.pdf (accessed 02 October 2019).
10. Levis, M., Midostaurin approved for FLT3-mutated AML. *Blood* **2017,** *129* (26), 3403–3406.
11. Campbell, R. K.; White Jr, J. R.; Saulie, B. A., Metformin: a new oral biguanide. *Clinical therapeutics* **1996,** *18* (3), 360–371.
12. Bailey, C. J., Metformin: historical overview. *Diabetologia* **2017,** *60* (9), 1566–1576.
13. Dhillon, S., Semaglutide: first global approval. *Drugs* **2018,** *78* (2), 275–284.
14. Bodeker, G.; Graz, B., Traditional medicine. In *Hunter's Tropical Medicine and Emerging Infectious Diseases*, Elsevier: 2020; pp 194–199.
15. Rankovic, Z.; Morphy, R., *Lead Generation Approaches in Drug Discovery*. John Wiley & Sons: 2010.
16. Weiner, R. S., *Pain management: A practical guide for clinicians*. CRC press: 2001.
17. Deutschländer, M. S. Isolation and identification of a novel anti-diabetic compound from *Euclea undulata* Thunb. PhD Thesis, University of Pretoria, 2010.
18. Robinson, M. M.; Zhang, X., The world medicines situation 2011, traditional medicines: Global situation, issues and challenges. *World Health Organization, Geneva* **2011**, 1–12.
19. Ali, H.; Houghton, P.; Soumyanath, A., α-Amylase inhibitory activity of some Malaysian plants used to treat diabetes; with particular reference to *Phyllanthus amarus*. *Journal of Ethnopharmacology* **2006,** *107* (3), 449–455.
20. Seong, S. H.; Roy, A.; Jung, H. A.; Jung, H. J.; Choi, J. S., Protein tyrosine phosphatase 1B and α-glucosidase inhibitory activities of *Pueraria lobata* root and its constituents. *Journal of Ethnopharmacology* **2016,** *194*, 706–716.
21. Deutschländer, M.; Lall, N.; Van De Venter, M., Plant species used in the treatment of diabetes by South African traditional healers: An inventory. *Pharmaceutical Biology* **2009,** *47* (4), 348–365.

22. Deutschländer, M.; Lall, N.; Van de Venter, M.; Hussein, A. A., Hypoglycemic evaluation of a new triterpene and other compounds isolated from *Euclea undulata* Thunb. var. *myrtina* (Ebenaceae) root bark. *Journal of Ethnopharmacology* **2011,** *133* (3), 1091–1095.
23. Nkobole, N.; Houghton, P. J.; Hussein, A.; Lall, N., Antidiabetic activity of *Terminalia sericea* constituents. *Natural Product Communications* **2011,** *6* (11), 1585–1588.
24. Mellem, J.; Baijnath, H.; Odhav, B., Effect of the methanolic extract of *Brachylaena discolor* in a streptozotocin-induced diabetic rat model. *African Journal of Pharmacy and Pharmacology* **2013,** *7* (12), 636–642.
25. Mellem, J.; Baijnath, H.; Odhav, B., Antidiabetic potential of *Brachylaena discolor*. *African Journal of Traditional, Complementary and Alternative Medicines* **2015,** *12* (1), 38–44.
26. American-Diabetes-Association, Diagnosis and classification of diabetes mellitus. *Diabetes care* **2014,** *37* (Supplement 1), S81–S90.
27. WHO, Classification of Diabetes Mellitus. **2019**.
28. WHO, Definition and diagnosis of diabetes mellitus and intermediate hyperglycaemia: report of a WHO/IDF consultation. **2006**.
29. Alberti, K. G. M. M.; Zimmet, P. f., Definition, diagnosis and classification of diabetes mellitus and its complications. Part 1: diagnosis and classification of diabetes mellitus. Provisional report of a WHO consultation. *Diabetic medicine* **1998,** *15* (7), 539–553.
30. WHO, *Global Report on Diabetes*. World Health Organization: 2016.
31. International-Diabetes-Federation, IDF Diabetes Atlas Eighth Edition 2017. **2017**.
32. Gutteridge, I. F., Diabetes mellitus: a brief history, epidemiology, definition and classification. *Clinical and Experimental Optometry* **1999,** *82* (2-3), 102–106.
33. Petersmann, A.; Nauck, M.; Müller-Wieland, D.; Kerner, W.; Müller, U. A.; Landgraf, R.; Freckmann, G.; Heinemann, L., Definition, classification and diagnosis of diabetes mellitus. *Experimental and Clinical Endocrinology & Diabetes* **2018,** *126* (07), 406–410.
34. Ríos, J. L.; Francini, F.; Schinella, G. R., Natural products for the treatment of type 2 diabetes mellitus. *Planta Medica* **2015,** *81* (12/13), 975–994.
35. Kerner, W.; Brückel, J., Definition, classification and diagnosis of diabetes mellitus. *Experimental and Clinical Endocrinology & Diabetes* **2014,** *122* (07), 384–386.
36. Chaudhury, A.; Duvoor, C.; Dendi, R.; Sena, V.; Kraleti, S.; Chada, A.; Ravilla, R.; Marco, A.; Shekhawat, N. S.; Montales, M. T., Clinical review of antidiabetic drugs: Implications for type 2 diabetes mellitus management. *Frontiers in Endocrinology* **2017,** *8*, 6.
37. Kerru, N.; Singh-Pillay, A.; Awolade, P.; Singh, P., Current anti-diabetic agents and their molecular targets: a review. *European Journal of Medicinal Chemistry* **2018,** *152*, 436–488.
38. Tundis, R.; Loizzo, M.; Menichini, F., Natural products as α-amylase and α-glucosidase inhibitors and their hypoglycaemic potential in the treatment of diabetes: an update. *Mini Reviews in Medicinal Chemistry* **2010,** *10* (4), 315–331.
39. Truscheit, E.; Frommer, W.; Junge, B.; Müller, L.; Schmidt, D. D.; Wingender, W., Chemistry and biochemistry of microbial α-glucosidase inhibitors. *Angewandte Chemie International Edition in English* **1981,** *20* (9), 744–761.
40. Jones, R. M., *New Therapeutic Strategies for Type 2 Diabetes: Small Molecule Approaches*. Royal Society of Chemistry: 2012.

41. Yee, H. S.; Fong, N. T., A review of the safety and efficacy of acarbose in diabetes mellitus. *Pharmacotherapy: The Journal of Human Pharmacology and Drug Therapy* **1996,** *16* (5), 792–805.
42. Jin, T.; Yu, H.; Huang, X.-F., Selective binding modes and allosteric inhibitory effects of lupane triterpenes on protein tyrosine phosphatase 1B. *Scientific Reports* **2016,** *6*, 20766.
43. Johnson, T. O.; Ermolieff, J.; Jirousek, M. R., Protein tyrosine phosphatase 1B inhibitors for diabetes. *Nature Reviews Drug Discovery* **2002,** *1* (9), 696.
44. Stanford, S. M.; Bottini, N., Targeting tyrosine phosphatases: time to end the stigma. *Trends in Pharmacological Sciences* **2017,** *38* (6), 524–540.
45. Zhang, R.-Y.; Yu, Z.-H.; Zeng, L.; Zhang, S.; Bai, Y.; Miao, J.; Chen, L.; Xie, J.; Zhang, Z.-Y., SHP2 phosphatase as a novel therapeutic target for melanoma treatment. *Oncotarget* **2016,** *7* (45), 73817.
46. Ukkola, O.; Santaniemi, M., Protein tyrosine phosphatase 1B: a new target for the treatment of obesity and associated co-morbidities. *Journal of Internal Medicine* **2002,** *251* (6), 467–475.
47. Mooney, M.; Fogarty, S.; Stevenson, C.; Gallagher, A.; Palit, P.; Hawley, S.; Hardie, D.; Coxon, G.; Waigh, R.; Tate, R., Mechanisms underlying the metabolic actions of galegine that contribute to weight loss in mice. *British Journal of Pharmacology* **2008,** *153* (8), 1669–1677.
48. Van Wyk, B.-E.; Van Staden, J., A review of ethnobotanical research in southern Africa. *South African Journal of Botany* **2002,** *68* (1), 1–13.
49. Erasto, P.; Adebola, P.; Grierson, D.; Afolayan, A., An ethnobotanical study of plants used for the treatment of diabetes in the Eastern Cape Province, South Africa. *African Journal of Biotechnology* **2005,** *4* (12).
50. Matsiliza, B.; Barker, N., A preliminary survey of plants used in traditional medicine in the Grahamstown area. *South African Journal of Botany* **2001,** *67* (2), 177–182.
51. Oyedemi, S.; Bradley, G.; Afolayan, A., Ethnobotanical survey of medicinal plants used for the management of diabetes mellitus in the Nkonkobe municipality of South Africa. *Journal of Medicinal Plants Research* **2009,** *3* (12), 1040–1044.
52. Davids, D.; Gibson, D.; Johnson, Q., Ethnobotanical survey of medicinal plants used to manage high blood pressure and type 2 diabetes mellitus in Bitterfontein, Western Cape Province, South Africa. *Journal of Ethnopharmacology* **2016,** *194*, 755–766.
53. Semenya, S.; Potgieter, M.; Erasmus, L., Ethnobotanical survey of medicinal plants used by Bapedi healers to treat diabetes mellitus in the Limpopo Province, South Africa. *Journal of Ethnopharmacology* **2012,** *141* (1), 440–445.
54. van de Venter, M.; Roux, S.; Bungu, L. C.; Louw, J.; Crouch, N. R.; Grace, O. M.; Maharaj, V.; Pillay, P.; Sewnarian, P.; Bhagwandin, N., Antidiabetic screening and scoring of 11 plants traditionally used in South Africa. *Journal of Ethnopharmacology* **2008,** *119* (1), 81–86.
55. Coates, P. K., *Trees of Southern Africa*. Struik: Cape Town, 1984.
56. Iwu, M. M., *Handbook of African Medicinal Plants*. CRC Press: Boca Raton, FL, 1993.
57. Van Wyk, B.-E.; Van Oudtshoorn, B.; Gericke, N., *Medicinal Plants of South Africa*. Briza Publications: Pretoria, 2005.
58. Boaduo, N. K. K.; Katerere, D.; Eloff, J. N.; Naidoo, V., Evaluation of six plant species used traditionally in the treatment and control of diabetes mellitus in South Africa using *in vitro* methods. *Pharmaceutical Biology* **2014,** *52* (6), 756–761.
59. Van Wyk, B.-E.; Gericke, N., *People's Plants*. Briza Publications: Pretoria, 2000.

60. Thring, T.; Weitz, F., Medicinal plant use in the Bredasdorp/Elim region of the Southern Overberg in the Western Cape Province of South Africa. *Journal of Ethnopharmacology* **2006,** *103* (2), 261–275.
61. Van Wyk, B.-E.; De Wet, H.; Van Heerden, F., An ethnobotanical survey of medicinal plants in the southeastern Karoo, South Africa. *South African Journal of Botany* **2008,** *74* (4), 696–704.
62. van Huyssteen, M.; Milne, P. J.; Campbell, E. E.; van de Venter, M., Antidiabetic and cytotoxicity screening of five medicinal plants used by traditional African health practitioners in the Nelson Mandela Metropole, South Africa. *African Journal of Traditional, Complementary and Alternative Medicines* **2011,** *8* (2).
63. Van Wyk, B.-E., A review of Khoi-San and Cape Dutch medical ethnobotany. *Journal of Ethnopharmacology* **2008,** *119* (3), 331–341.
64. Van Wyk, B.-E., A broad review of commercially important southern African medicinal plants. *Journal of ethnopharmacology* **2008,** *119* (3), 342–355.
65. Van Wyk, B.-E., The potential of South African plants in the development of new medicinal products. *South African Journal of Botany* **2011,** *77* (4), 812–829.
66. Gao, Y.; Zhang, M.; Wu, T.; Xu, M.; Cai, H.; Zhang, Z., Effects of D-pinitol on insulin resistance through the PI3K/Akt signaling pathway in type 2 diabetes mellitus rats. *Journal of Agricultural and Food Chemistry* **2015,** *63* (26), 6019–6026.
67. Afolayan, A. J.; Sunmonu, T. O., In vivo studies on antidiabetic plants used in South African herbal medicine. *Journal of Clinical Biochemistry and Nutrition* **2010,** *47* (2), 98–106.
68. Mnonopi, N.; Levendal, R.-A.; Mzilikazi, N.; Frost, C., Marrubiin, a constituent of *Leonotis leonurus*, alleviates diabetic symptoms. *Phytomedicine* **2012,** *19* (6), 488–493.
69. Ojewole, J., Hypoglycemic and hypotensive effects of *Psidium guajava* Linn.(Myrtaceae) leaf aqueous extract. *Methods and Findings in Experimental and Clinical Pharmacology* **2005,** *27* (10), 689–696.
70. Tholl, D.; Lee, S., Terpene specialized metabolism in *Arabidopsis thaliana*. *The Arabidopsis Book/American Society of Plant Biologists* **2011,** *9*.
71. Dev, S., *Handbook of Terpenoids*. CRC Press: 1986.
72. Alqahtani, A.; Hamid, K.; Kam, A.; Wong, K.; Abdelhak, Z.; Razmovski-Naumovski, V.; Chan, K.; Li, K. M.; Groundwater, P. W.; Li, G. Q., The pentacyclic triterpenoids in herbal medicines and their pharmacological activities in diabetes and diabetic complications. *Current Medicinal Chemistry* **2013,** *20* (7), 908–931.
73. Mohammed, A.; Ibrahim, H.; Islam, M. S., Plant-Derived Antidiabetic Compounds Obtained From African Medicinal Plants: A Short Review. In *Studies in Natural Products Chemistry*, Elsevier: 2017; Vol. 54, pp 291–314.
74. American-Diabetes-Association, Postprandial blood glucose. *Clinical Diabetes* **2001,** *19* (3), 127–130.
75. Hou, W.; Li, Y.; Zhang, Q.; Wei, X.; Peng, A.; Chen, L.; Wei, Y., Triterpene acids isolated from *Lagerstroemia speciosa* leaves as α-glucosidase inhibitors. *Phytotherapy Research: An International Journal Devoted to Pharmacological and Toxicological Evaluation of Natural Product Derivatives* **2009,** *23* (5), 614–618.
76. Lai, Y.-C.; Chen, C.-K.; Tsai, S.-F.; Lee, S.-S., Triterpenes as α-glucosidase inhibitors from *Fagus hayatae*. *Phytochemistry* **2012,** *74*, 206–211.
77. Uddin, G.; Rauf, A.; Al-Othman, A. M.; Collina, S.; Arfan, M.; Ali, G.; Khan, I., Pistagremic acid, a glucosidase inhibitor from *Pistacia integerrima*. *Fitoterapia* **2012,** *83* (8), 1648–1652.

78. Kuang, H.-X.; Li, H.-W.; Wang, Q.-H.; Yang, B.-Y.; Wang, Z.-B.; Xia, Y.-G., Triterpenoids from the roots of *Sanguisorba tenuifolia* var. alba. *Molecules* **2011,** *16* (6), 4642–4651.
79. Wang, Z.-W.; Wang, J.-S.; Luo, J.; Kong, L.-Y., α-Glucosidase inhibitory triterpenoids from the stem barks of *Uncaria laevigata*. *Fitoterapia* **2013,** *90*, 30–37.
80. Gutierrez, R. M. P., Evaluation of the hypoglycemic and hypolipidemic effects of triterpenoids from *Prosthechea michuacana* in streptozotocin-induced type 2 diabetic mice. *Pharmacologia, 4: 170* **2013,** *179*.
81. Ma, J.; Whittaker, P.; Keller, A. C.; Mazzola, E. P.; Pawar, R. S.; White, K. D.; Callahan, J. H.; Kennelly, E. J.; Krynitsky, A. J.; Rader, J. I., Cucurbitane-type triterpenoids from *Momordica charantia*. *Planta Medica* **2010,** *76* (15), 1758–1761.
82. Xiong, J.; Wan, J.; Ding, J.; Wang, P.-P.; Ma, G.-L.; Li, J.; Hu, J.-F., Camellianols A–G, barrigenol-like triterpenoids with PTP1B inhibitory effects from the endangered ornamental plant *Camellia crapnelliana*. *Journal of Natural Products* **2017,** *80* (11), 2874–2882.
83. de Cássia Lemos Lima, R.; T Kongstad, K.; Kato, L.; José das Silva, M.; Franzyk, H.; Staerk, D., High-resolution PTP1B inhibition profiling combined with HPLC-HRMS-SPE-NMR for identification of PTP1B inhibitors from *Miconia albicans*. *Molecules* **2018,** *23* (7), 1755.
84. Kwon, J. H.; Chang, M. J.; Seo, H. W.; Lee, J. H.; Min, B. S.; Na, M.; Kim, J. C.; Woo, M. H.; Choi, J. S.; Lee, H. K., Triterpenoids and a sterol from the stem-bark of *Styrax japonica* and their protein tyrosine phosphatase 1B inhibitory activities. *Phytotherapy Research* **2008,** *22* (10), 1303–1306.
85. Na, M.; Kim, B. Y.; Osada, H.; Ahn, J. S., Inhibition of protein tyrosine phosphatase 1B by lupeol and lupenone isolated from *Sorbus commixta*. *Journal of Enzyme Inhibition and Medicinal Chemistry* **2009,** *24* (4), 1056–1059.
86. Sasaki, T.; Li, W.; Morimura, H.; Li, S.; Li, Q.; Asada, Y.; Koike, K., Chemical constituents from *Sambucus adnata* and their protein–tyrosine phosphatase 1B inhibitory activities. *Chemical and Pharmaceutical Bulletin* **2011,** *59* (11), 1396–1399.
87. Thuong, P. T.; Lee, C. H.; Dao, T. T.; Nguyen, P. H.; Kim, W. G.; Lee, S. J.; Oh, W. K., Triterpenoids from the leaves of *Diospyros kaki* (persimmon) and their inhibitory effects on protein tyrosine phosphatase 1B. *Journal of Natural Products* **2008,** *71* (10), 1775–1778.
88. Ramírez-Espinosa, J. J.; Rios, M. Y.; López-Martínez, S.; López-Vallejo, F.; Medina-Franco, J. L.; Paoli, P.; Camici, G.; Navarrete-Vázquez, G.; Ortiz-Andrade, R.; Estrada-Soto, S., Antidiabetic activity of some pentacyclic acid triterpenoids, role of PTP–1B: *In vitro, in silico*, and *in vivo* approaches. *European Journal of Medicinal Chemistry* **2011,** *46* (6), 2243–2251.
89. Seo, C.; HanYim, J.; Kum Lee, H.; Oh, H., PTP1B inhibitory secondary metabolites from the Antarctic lichen *Lecidella carpathica*. *Mycology* **2011,** *2* (1), 18–23.
90. Choi, Y. H.; Zhou, W.; Oh, J.; Choe, S.; Kim, D. W.; Lee, S. H.; Na, M., Rhododendric acid A, a new ursane-type PTP1B inhibitor from the endangered plant *Rhododendron brachycarpum* G. Don. *Bioorganic & Medicinal Chemistry Letters* **2012,** *22* (19), 6116–6119.
91. Na, M.; Cui, L.; Min, B. S.; Bae, K.; Yoo, J. K.; Kim, B. Y.; Oh, W. K.; Ahn, J. S., Protein tyrosine phosphatase 1B inhibitory activity of triterpenes isolated from *Astilbe koreana*. *Bioorganic & medicinal chemistry letters* **2006,** *16* (12), 3273–3276.
92. Na, M. K.; Yang, S.; He, L.; Oh, H.; Kim, B. S.; Oh, W. K.; Kim, B. Y.; Ahn, J. S., Inhibition of protein tyrosine phosphatase 1B by ursane-type triterpenes isolated from *Symplocos paniculata*. *Planta Medica* **2006,** *72* (03), 261–263.

93. Na, M.; Thuong, P. T.; Hwang, I. H.; Bae, K.; Kim, B. Y.; Osada, H.; Ahn, J. S., Protein tyrosine phosphatase 1B inhibitory activity of 24-norursane triterpenes isolated from *Weigela subsessilis*. *Phytotherapy Research* **2010,** *24* (11), 1716–1719.
94. Zhang, X.-S.; Bi, X.-L.; Cao, J.-Q.; Xia, X.-C.; Diao, Y.-P.; Zhao, Y.-Q., Protein tyrosine phosphatase 1B inhibitory effect by dammarane-type triterpenes from hydrolyzate of total *Gynostemma pentaphyllum* saponins. *Bioorganic & Medicinal Chemistry Letters* **2013,** *23* (1), 297–300.
95. Lee, M. S.; Thuong, P. T., Stimulation of glucose uptake by triterpenoids from *Weigela subsessilis*. *Phytotherapy Research* **2010,** *24* (1), 49–53.
96. Perez G, R.; Perez G, C.; Perez G, S.; Zavala S, M., Effect of triterpenoids of *Bouvardia terniflora* on blood sugar levels of normal and alloxan diabetic mice. *Phytomedicine* **1998,** *5* (6), 475–478.
97. Ardiles, A. E.; González-Rodríguez, Á.; Núñez, M. J.; Perestelo, N. R.; Pardo, V.; Jiménez, I. A.; Valverde, Á. M.; Bazzocchi, I. L., Studies of naturally occurring friedelane triterpenoids as insulin sensitizers in the treatment type 2 diabetes mellitus. *Phytochemistry* **2012,** *84*, 116–124.
98. Peng, K.; Pan, Y.; Li, J.; Khan, Z.; Fan, M.; Yin, H.; Tong, C.; Zhao, Y.; Liang, G.; Zheng, C., 11β-Hydroxysteroid dehydrogenase type 1 (11β-HSD1) mediates insulin resistance through JNK activation in adipocytes. *Scientific Reports* **2016,** *6*, 37160.
99. Guo, J.; Zhou, L.-Y.; He, H.-P.; Leng, Y.; Yang, Z.; Hao, X.-J., Inhibition of 11β-HSD1 by tetracyclic triterpenoids from *Euphorbia kansui*. *Molecules* **2012,** *17* (10), 11826–11838.
100. Jiang, B.; Ji, M.; Liu, W.; Chen, L.; Cai, Z.; Zhao, Y.; Bi, X., Antidiabetic activities of a cucurbitane-type triterpenoid compound from *Momordica charantia* in alloxan-induced diabetic mice. *Molecular Medicine Reports* **2016,** *14* (5), 4865–4872.
101. Han, J. H.; Tuan, N. Q.; Park, M. H.; Quan, K. T.; Oh, J.; Heo, K. S.; Na, M.; Myung, C. S., Cucurbitane triterpenoids from the fruits of *Momordica Charantia* improve insulin sensitivity and glucose homeostasis in streptozotocin-induced diabetic mice. *Molecular Nutrition & Food Research* **2018,** *62* (7), 1700769.
102. Tuan, N. Q.; Lee, D.-H.; Oh, J.; Kim, C. S.; Heo, K.-S.; Myung, C.-S.; Na, M., Inhibition of proliferation of vascular smooth muscle cells by cucurbitanes from *Momordica charantia*. *Journal of Natural Products* **2017,** *80* (7), 2018–2025.
103. Khanra, R.; Bhattacharjee, N.; Dua, T. K.; Nandy, A.; Saha, A.; Kalita, J.; Manna, P.; Dewanjee, S., Taraxerol, a pentacyclic triterpenoid, from *Abroma augusta* leaf attenuates diabetic nephropathy in type 2 diabetic rats. *Biomedicine & Pharmacotherapy* **2017,** *94*, 726–741.
104. Waksmundzka-Hajnos, M.; Sherma, J.; Kowalska, T., *Thin Layer Chromatography in Phytochemistry*. CRC Press: 2008.
105. Gammacurta, M.; Waffo-Teguo, P.; Winstel, D.; Cretin, B. N.; Sindt, L.; Dubourdieu, D.; Marchal, A., Triterpenoids from *Quercus petraea*: Identification in wines and spirits and sensory assessment. *Journal of Natural Products* **2019,** *82* (2), 265–275.
106. Marston, A., Role of advances in chromatographic techniques in phytochemistry. *Phytochemistry* **2007,** *68* (22-24), 2786–2798.
107. Jarvis, A. P.; Morgan, E. D.; Edwards, C., Rapid separation of triterpenoids from Neem seed extracts. *Phytochemical Analysis* **1999,** *10* (1), 39–43.
108. James, J.; Dubery, I., Identification and quantification of triterpenoid centelloids in *Centella asiatica* (L.) Urban by densitometric TLC. *JPC-Journal of Planar Chromatography-Modern TLC* **2011,** *24* (1), 82–87.
109. Vázquez, L. H.; Palazon, J.; Navarro-Ocaña, A., The pentacyclic triterpenes α,β-amyrins: A review of sources and biological activities

In *Phytochemicals-A Global Perspective of their Role in Nutrition and Health*, IntechOpen: 2012.
110. Naumoska, K.; Vovk, I., Analysis of triterpenoids and phytosterols in vegetables by thin-layer chromatography coupled to tandem mass spectrometry. *Journal of Chromatography A* **2015,** *1381*, 229–238.
111. Kaur, P.; Gupta, R.; Dey, A.; Pandey, D. K., Simultaneous quantification of oleanolic acid, ursolic acid, betulinic acid and lupeol in different populations of five *Swertia* species by using HPTLC-densitometry: Comparison of different extraction methods and solvent selection. *Industrial Crops and Products* **2019,** *130*, 537–546.
112. Lin, C.; Liu, F.; Zhang, R.; Liu, M.; Zhu, C.; Zhao, J.; Li, S., High-performance thin-layer chromatographic fingerprints of triterpenoids for distinguishing between *Isodon lophanthoides* and *Isodon lophanthoides* var. *gerardianus*. *Journal of AOAC International* **2019**.
113. Banu, K. S.; Cathrine, L., General techniques involved in phytochemical analysis. *International Journal of Advanced Research in Chemical Science* **2015,** *2* (4), 25–32.
114. Takeoka, G.; Dao, L.; Teranishi, R.; Wong, R.; Flessa, S.; Harden, L.; Edwards, R., Identification of three triterpenoids in almond hulls. *Journal of Agricultural and Food Chemistry* **2000,** *48* (8), 3437–3439.
115. Napoli, E.; Gentile, D.; Ruberto, G., GC–MS analysis of terpenes from *Sicilian Pistacia vera* L. oleoresin. A source of biologically active compounds. *Biomedical Chromatography* **2019,** *33* (2), e4381.
116. Burdziej, A.; Pączkowski, C.; Destrac-Irvine, A.; Richard, T.; Cluzet, S.; Szakiel, A., Triterpenoid profiles of the leaves of wild and domesticated grapevines. *Phytochemistry Letters* **2019**.
117. Courtney, R.; Sirdaarta, J.; White, A.; Cock, I., Inhibition of Caco-2 and HeLa proliferation by *Terminalia carpentariae* CT White and *Terminalia grandiflora* Benth. extracts: Identification of triterpenoid components. *Pharmacognosy Journal* **2017,** *9* (4).
118. Çetin, B.; Şahin, H.; Sarı, A., Triterpenoids from *Scorzonera veratrifolia* Fenzl. *Istanbul Journal of Pharmacy* **2018,** *48* (2), 23–27.
119. Rogowska, A.; Styczyński, M.; Pączkowski, C.; Szakiel, A.; de Carvalho, M. Â. A. P., GC-MS analysis of steroids and triterpenoids occurring in leaves and tubers of *Tamus edulis* Lowe. *Phytochemistry Letters* **2019,** *30*, 231–234.
120. Li, B.; Abliz, Z.; Tang, M.; Fu, G.; Yu, S., Rapid structural characterization of triterpenoid saponins in crude extract from *Symplocos chinensis* using liquid chromatography combined with electrospray ionization tandem mass spectrometry. *Journal of Chromatography A* **2006,** *1101* (1-2), 53–62.
121. Zhang, F. L.; Wei, Y. J.; Zhu, J.; Gong, Z. N., Simultaneous quantitation of three major triterpenoid glycosides in *Centella asiatica* extracts by high performance liquid chromatography with evaporative light scattering detection. *Biomedical Chromatography* **2008,** *22* (2), 119–124.
122. Yang, G.; Fen, W.; Xiao, W.; Sun, H., Study on determination of pentacyclic triterpenoids in *Chaenomeles* by HPLC-ELSD. *Journal of Chromatographic Science* **2009,** *47* (8), 718–722.
123. Ichikawa, M.; Ohta, S.; Komoto, N.; Ushijima, M.; Kodera, Y.; Hayama, M.; Shirota, O.; Sekita, S.; Kuroyanagi, M., Rapid identification of triterpenoid saponins in the roots of *Codonopsis lanceolata* by liquid chromatography–mass spectrometry. *Journal of Natural Medicines* **2008,** *62* (4), 423.
124. Li, J.; Li, P.; Li, H. J.; Song, Y.; Bi, Z. M.; Li, Y. J., Simultaneous qualification and quantification of eight triterpenoids in *Radix Achyranthis* Bidentatae by high-performance

liquid chromatography with evaporative light scattering detection and mass spectrometric detection. *Journal of Separation Science* **2007,** *30* (6), 843–850.
125. Martelanc, M.; Vovk, I.; Simonovska, B., Separation and identification of some common isomeric plant triterpenoids by thin-layer chromatography and high-performance liquid chromatography. *Journal of Chromatography A* **2009,** *1216* (38), 6662–6670.
126. David, F.; Medvedovici, A.; Sandra, P., *Oils, Fats and Waxes: Supercritical Fluid Chromatography*. Academic Press, Cambridge, MA: 2000.
127. Frimpong, E.; Nlooto, M., Clinical relevance and application of traditional complementary and alternative medicine for the management of diabetes and hypertension on the African continent, 2000-2017: A narrative review. *Indian Journal of Traditional Knowledge* **2018**, 635–644.
128. Sabiu, S.; Madende, M.; Ayokun-nun Ajao, A.; Adepemi Ogundeji, O.; Lekena, N.; Adekunle Alayande, K., The scope of phytotherapy in southern African antidiabetic healthcare. *Transactions of the Royal Society of South Africa* **2019,** *74* (1), 1–18.
129. Odeyemi, S.; Bradley, G., Medicinal plants used for the traditional management of diabetes in the Eastern Cape, South Africa: Pharmacology and toxicology. *Molecules* **2018,** *23* (11), 2759.
130. Bayer, R. J.; Funk, V. A.; Stuessy, T. F.; Susanna, A., *Systematics, Evolution, and Biogeography of Compositae*. International Association for Plant Taxonomy: 2009.
131. Wu, Q.-X.; Shi, Y.-P.; Jia, Z.-J., Eudesmane sesquiterpenoids from the Asteraceae family. *Natural Product Reports* **2006,** *23* (5), 699–734.
132. Zdero, C.; Bohlmann, F., Systematics and evolution within theCompositae, seen with the eyes of a chemist. *Plant Systematics and Evolution* **1990,** *171* (1-4), 1–14.
133. Lajter, I. Biologically active secondary metabolites from Asteraceae and Polygonaceae species. University of Szeged, 2016.
134. Beentje, H., The genus *Brachylaena* (Compositae: Mutisieae). *Kew Bulletin* **2000**, 1–41.
135. Cilliers, S., Synopsis of the genus *Brachylaena* (Asteraceae) in southern Africa. *Bothalia* **1993,** *23* (2), 175–184.
136. SANBI *Brachylaena*. http://posa.sanbi.org/sanbi/Explore (accessed 28 November 2019).
137. Bohlmann, F.; Zdero, C., Sesquiterpene lactones from *Brachylaena* species. *Phytochemistry* **1982,** *21* (3), 647–651.
138. Brooks, C.; Campbell, M., Brachylaenalones A and B: tricyclic sesquiterpenoid keto-aldehydes from heartwood of *Brachylaena hutchinsii* Hutch.(Compositae). *Journal of the Chemical Society D: Chemical Communications* **1969,** (12), 630–631.
139. Klein, E.; Schmidt, W., Structure of brachyl oxide. *Journal of Agricultural and Food Chemistry* **1971,** *19* (6), 1115–1117.
140. Vieira, P. C.; Himejima, M.; Kubo, I., Sesquiterpenoids from *Brachylaena hutchinsii*. *Journal of Natural Products* **1991,** *54* (2), 416–420.
141. Zdero, C.; Bohlmann, F., Sesquiterpene lactones from the genus *Brachylaena*. *Phytochemistry* **1987,** *26* (9), 2597–2601.
142. Zdero, C.; Bohlmann, F.; Wasshausen, D., Guaianolides from *Brachylaena* species. *Phytochemistry* **1991,** *30* (11), 3810–3811.
143. Adam, S. A. E. Isolation and Identification of Antidiabetic Compounds from *Brachylaena discolor* DC. University of KwaZulu-Natal, Pietermaritzburg, 2017.
144. Chaturvedula, V. P.; Schilling, J. K.; Miller, J. S.; Andriantsiferana, R.; Rasamison, V. E.; Kingston, D. G., Two new triterpene esters from the twigs of *Brachylaena ramiflora* from the Madagascar rainforest. *Journal of Natural Products* **2002,** *65* (8), 1222–1224.

145. Donno, D.; Randriamampionona, D.; Andriamaniraka, H.; Torti, V.; Mellano, M. G.; Giacoma, C.; Beccaro, G. L., Biodiversity and traditional medicinal plants from Madagascar: Phytochemical evaluation of *Brachylaena ramiflora* (DC.) Humbert decoctions and infusions. *Journal of Applied Botany and Food Quality* **2017,** *90*, 205–213.
146. Naidoo, G., Ecophysiological responses of six coastal dune species along the eastern seaboard of South Africa. *African Journal of Ecology* **2018,** *56* (3), 507–517.
147. Herman, P., Asteraceae: A note on the *Brachylaena discolor* complex. *Bothalia* **1998,** *28* (1), 42–45.
148. Sagbo, I. J.; van de Venter, M.; Koekemoer, T.; Bradley, G., *In vitro* antidiabetic activity and mechanism of action of *Brachylaena elliptica* (Thunb.) DC. *Evidence-Based Complementary and Alternative Medicine* **2018,** *2018*.
149. Nciki, S.; Vuuren, S.; van Eyk, A.; de Wet, H., Plants used to treat skin diseases in northern Maputaland, South Africa: antimicrobial activity and in vitro permeability studies. *Pharmaceutical Biology* **2016,** *54* (11), 2420–2436.
150. Monjane, J. A.; Capusiri, D.; Giménez, A.; Sterner, O., Leishmanicidal activity of onopordopicrin isolated from the leaves of *Brachylaena discolor*. *Tropical Journal of Natural Product Research* **2018,** *4*, 11–13.
151. Morris, L., Separations of lipids by silver ion chromatography. *Journal of Lipid Research* **1966,** *7* (6), 717–732.
152. Shiojima, K.; Masuda, K.; Lin, T.; Suzuki, H.; Ageta, H.; Inoue, M.; Ishida, T., Composite constituents: Three gammacer-16-ene derivatives, novel triterpenoids isolated from roots of *Picris hieracioides* subsp. *japonica*. *Tetrahedron Letters* **1989,** *30* (37), 4977–4980.
153. Fingolo, C. E.; Santos Tde, S.; Filho, M. D.; Kaplan, M. A., Triterpene esters: natural products from *Dorstenia arifolia* (Moraceae). *Molecules* **2013,** *18* (4), 4247–56.
154. Shiojima, K.; Arai, Y.; Masuda, K.; Takase, Y.; Ageta, T.; Ageta, H., Mass spectra of pentacyclic triterpenoids. *Chemical and Pharmaceutical Bulletin* **1992,** *40* (7), 1683–1690.
155. Bruice, P. Y., Substitution reactions of alkyl halides. *Organic Chemistry, 5th ed. Pearson International Inc., Upper Saddle river, NJ* **2007**, 344–388.
156. Okoye, N. N.; Ajaghaku, D. L.; Okeke, H. N.; Ilodigwe, E. E.; Nworu, C. S.; Okoye, F. B., beta-Amyrin and alpha-amyrin acetate isolated from the stem bark of *Alstonia boonei* display profound anti-inflammatory activity. *Pharmaceutical Biology* **2014,** *52* (11), 1478–86.
157. da Silva, U. P.; Furlani, G. M.; Demuner, A. J.; da Silva, O. L. M.; Varejão, E. V. V., Allelopathic activity and chemical constituents of extracts from roots of *Euphorbia heterophylla* L. *Natural Product Research* **2018**, 1–4.
158. Shimadzu LCMS-2020 Liquid chromatograph mass spectrometer, dual ion source. https://www.shimadzu.com/an/lcms/lcms2020/duis.html (accessed 28 November 2019).
159. Nair, S. A.; Sabulal, B.; Radhika, J.; Arunkumar, R.; Subramoniam, A., Promising anti-diabetes mellitus activity in rats of beta-amyrin palmitate isolated from *Hemidesmus indicus* roots. *European journal of pharmacology* **2014,** *734*, 77–82.
160. Seo, D.-G.; Kim, S.; Lee, D. K.; Kim, N. Y.; Lee, J.-S.; Hwang, K. W.; Park, S.-Y., Inhibitory effect of α-amyrin acetate isolated from *Fraxinus rhynchophylla* on Th17 polarization. *Phytomedicine* **2019,** *63*, 153056.
161. Singh, A.; Yadav, D.; Maurya, R.; Srivastava, A., Antihyperglycaemic activity of α-amyrin acetate in rats and db/db mice. *Natural Product Research* **2009,** *23* (9), 876–882.
162. Muhammad, K. J. a.; Jamil, S.; Basar, N., Phytochemical study and biological activities of *Scurrula parasitica* L (Loranthaceae) leaves. *Marmara Pharmaceutical Journal* **2019,** *23* (3).

163. Ibrahim, S. R.; Mohamed, G. A.; Shaala, L. A.; Banuls, L. M. Y.; Van Goietsenoven, G.; Kiss, R.; Youssef, D. T., New ursane-type triterpenes from the root bark of Calotropis procera. *Phytochemistry letters* **2012,** *5* (3), 490–495.
164. Ateya, A.-M.; El Sayed, Z. I.; Fekry, M., Chemical Constituents, Cytotoxicity, Anti-oxidant, Hypoglycemic and antihypertensive activities of egyptian hibiscus trionum. *Australian Journal of Basic and Applied Sciences* **2012,** *6* (3), 756–766.
165. Xiao-Ping, Y.; Chun-Qing, S.; Ping, Y.; Ren-Gang, M., α-Glucosidase and α-amylase inhibitory activity of common constituents from traditional Chinese medicine used for diabetes mellitus. *Chinese Journal of Natural Medicines* **2010,** *8* (5), 349–352.
166. Demarque, D. P.; Crotti, A. E.; Vessecchi, R.; Lopes, J. L.; Lopes, N. P., Fragmentation reactions using electrospray ionization mass spectrometry: an important tool for the structural elucidation and characterization of synthetic and natural products. *Natural Product Reports* **2016,** *33* (3), 432–455.
167. Xia, Y.-G.; Li, G.-Y.; Liang, J.; Ortori, C. A.; Yang, B.-Y.; Kuang, H.-X.; Barrett, D. A., A strategy for characterization of triterpene saponins in Caulophyllum robustum hairy roots by liquid chromatography with electrospray ionization quadrupole time-of-flight mass spectrometry. *Journal of Pharmaceutical and Biomedical Analysis* **2014,** *100*, 109–122.
168. Reynolds, W. F.; McLean, S.; Poplawski, J.; Enriquez, R. G.; Escobar, L. I.; Leon, I., Total assignment of ^{13}C and ^{1}H spectra of three isomeric triterpenol derivatives by 2D NMR: an investigation of the potential utility of ^{1}H chemical shifts in structural investigations of complex natural products. *Tetrahedron* **1986,** *42* (13), 3419–3428.
169. Xu, J.; Cao, J.; Yue, J.; Zhang, X.; Zhao, Y., New triterpenoids from acorns of *Quercus liaotungensis* and their inhibitory activity against α-glucosidase, α-amylase and protein-tyrosine phosphatase 1B. *Journal of Functional Foods* **2018,** *41*, 232–239.
170. Silva, E.; Lobo, J.; Vinther, J.; Borges, R.; Staerk, D., High-resolution α-glucosidase inhibition profiling combined with HPLC-HRMS-SPE-NMR for identification of antidiabetic compounds in Eremanthus crotonoides (Asteraceae). *Molecules* **2016,** *21* (6), 782.
171. Zhang, B.-w.; Xing, Y.; Wen, C.; Yu, X.-x.; Sun, W.-l.; Xiu, Z.-l.; Dong, Y.-s., Pentacyclic triterpenes as α-glucosidase and α-amylase inhibitors: structure-activity relationships and the synergism with acarbose. *Bioorganic & Medicinal Chemistry Letters* **2017,** *27* (22), 5065–5070.
172. Li, T.-S.; Li, J.-T.; Li, H.-Z., Modified and convenient preparation of silica impregnated with silver nitrate and its application to the separation of steroids and triterpenes. *Journal of Chromatography A* **1995,** *715* (2), 372–375.
173. Šali, A.; Blundell, T. L., Comparative protein modelling by satisfaction of spatial restraints. *Journal of Molecular Biology* **1993,** *234* (3), 779–815.
174. Becke, A. D., Density-functional thermochemistry. III. The role of exact exchange. *The Journal of Chemical Physics* **1993,** *98* (7), 5648–5652.
175. Frisch, M.; Trucks, G.; Schlegel, H.; Scuseria, G.; Robb, M.; Cheeseman, J.; Scalmani, G.; Barone, V.; Petersson, G.; Nakatsuji, H., Gaussian 16, Revision A. 03, Gaussian. *Inc., Wallingford CT* **2016**.
176. Pettersen, E. F.; Goddard, T. D.; Huang, C. C.; Couch, G. S.; Greenblatt, D. M.; Meng, E. C.; Ferrin, T. E., UCSF Chimera - A visualization system for exploratory research and analysis. *Journal of Computational Chemistry* **2004,** *25* (13), 1605–1612.
177. Trott, O.; Olson, A. J., AutoDock Vina: improving the speed and accuracy of docking with a new scoring function, efficient optimization, and multithreading. *Journal of Computational Chemistry* **2010,** *31* (2), 455–461.

APPENDIX

Plate 1 A. DEPT-135 and COSY spectra of α-amyrin acetate and β-amyrin acetate mixture in $CDCl_3$.

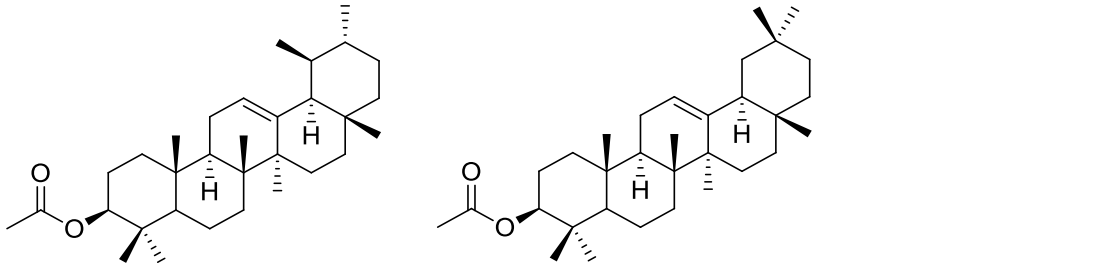

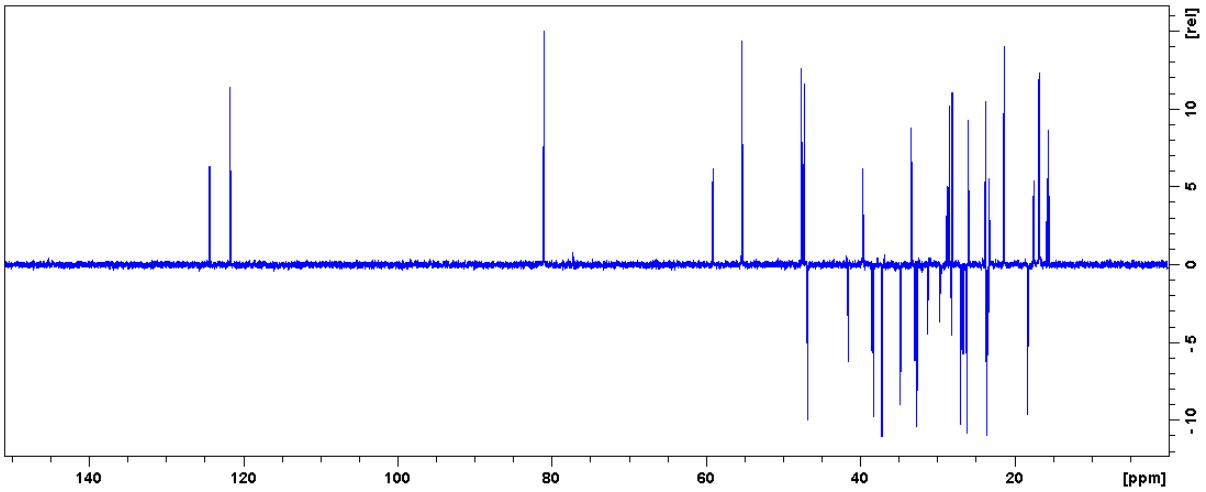

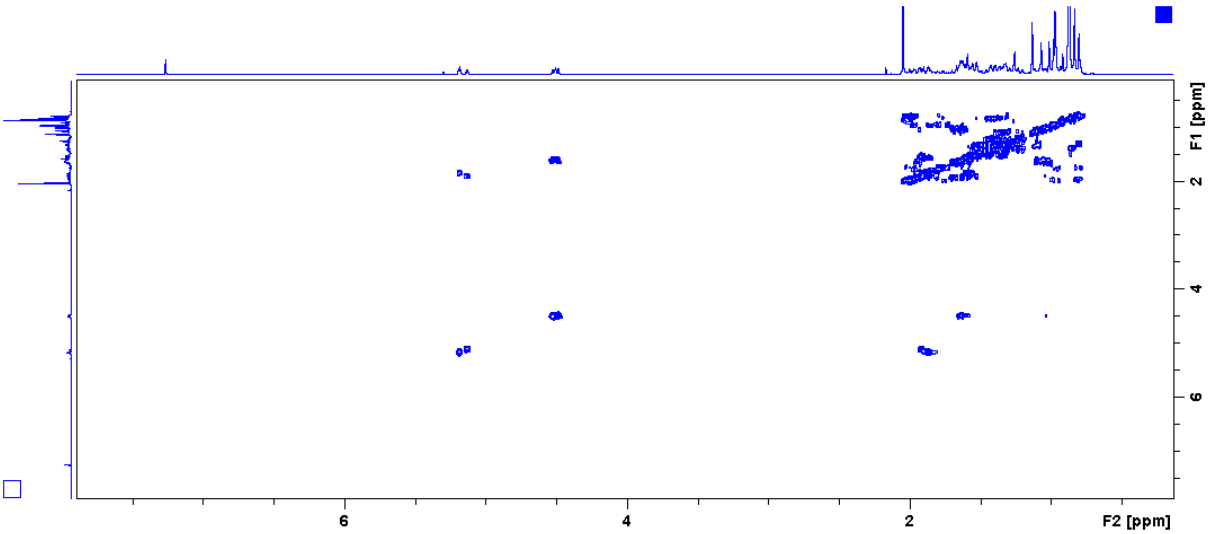

Plate 2 A. COSY spectrum of ψ-taraxasterol acetate in $CDCl_3$.

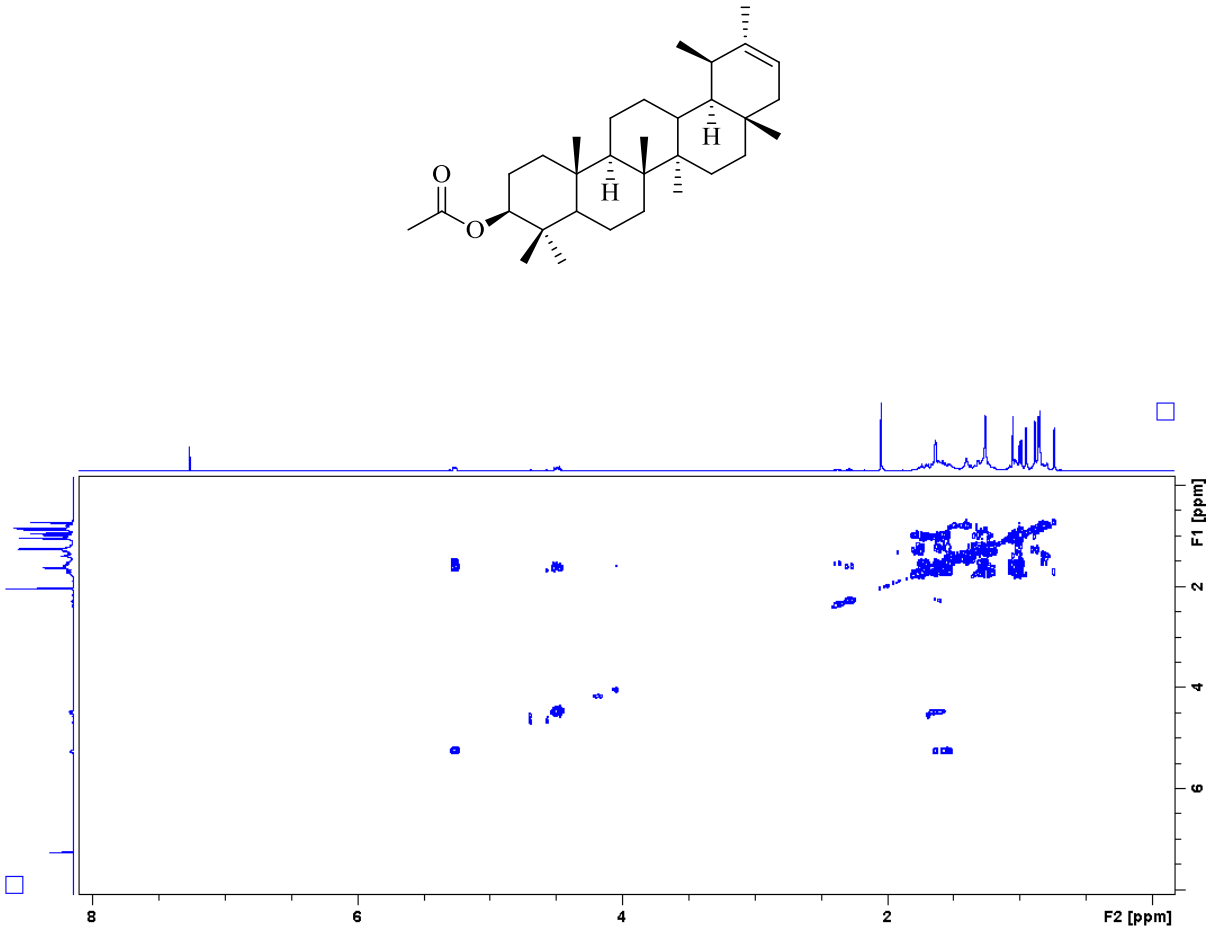

Plate 3 A. COSY spectrum of taraxasterol acetate in $CDCl_3$.

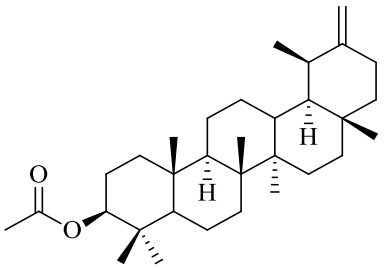

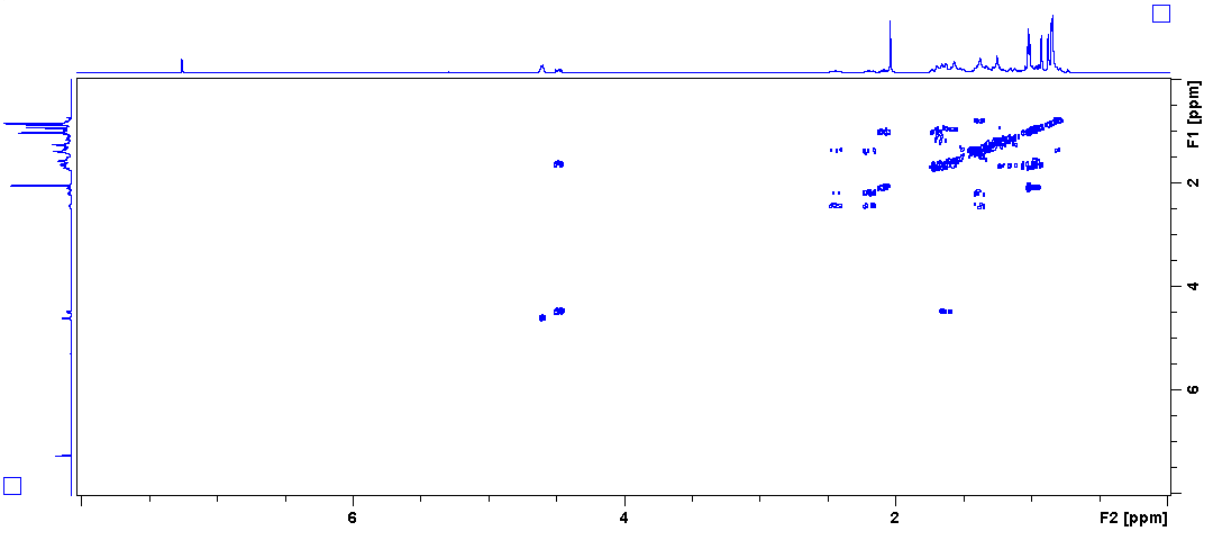

Plate 4 A. COSY spectrum of lupeol acetate in $CDCl_3$.

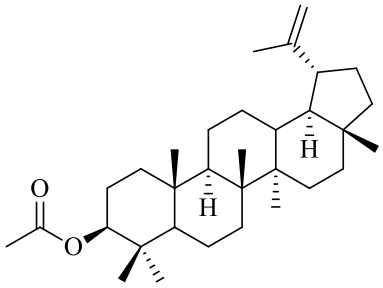

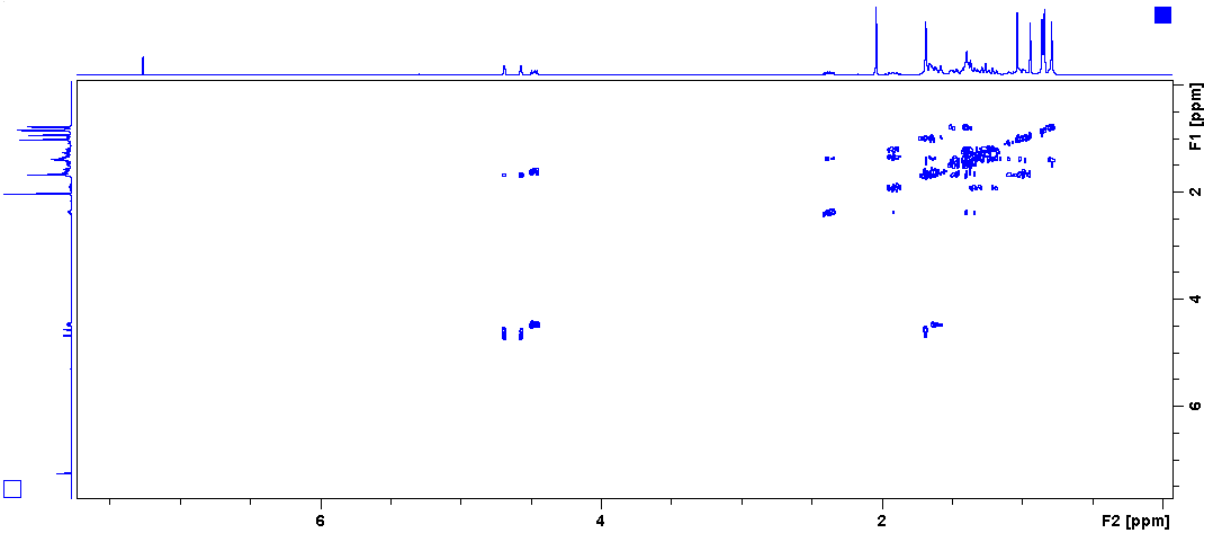

Plate 5 A. DEPT-135 and COSY spectra of α-amyrin palmitate and β-amyrin palmitate mixture in $CDCl_3$.

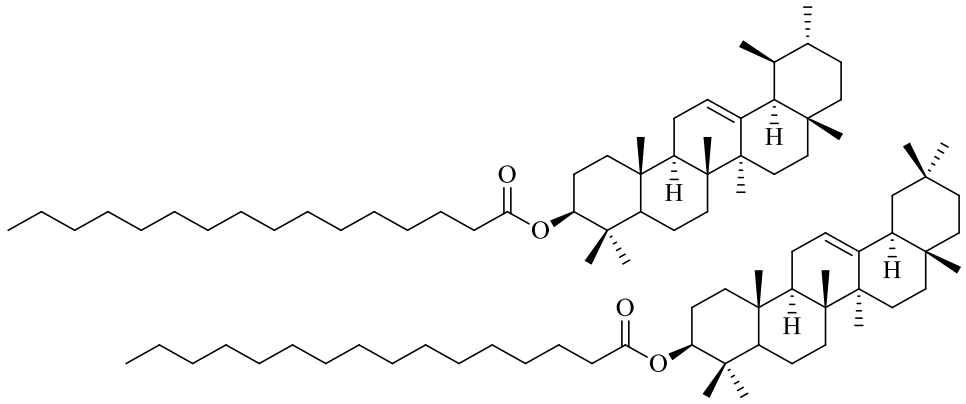

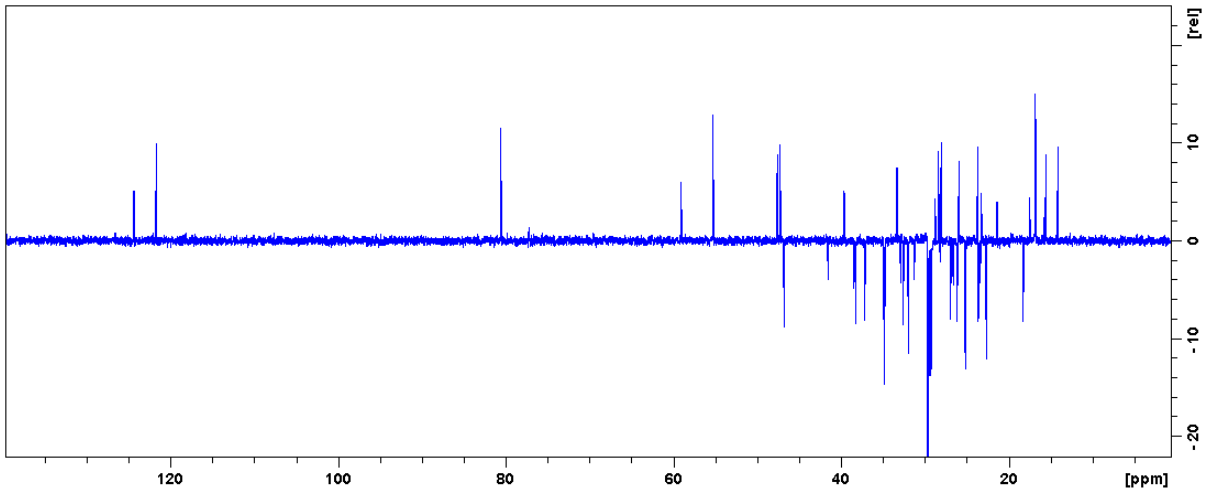

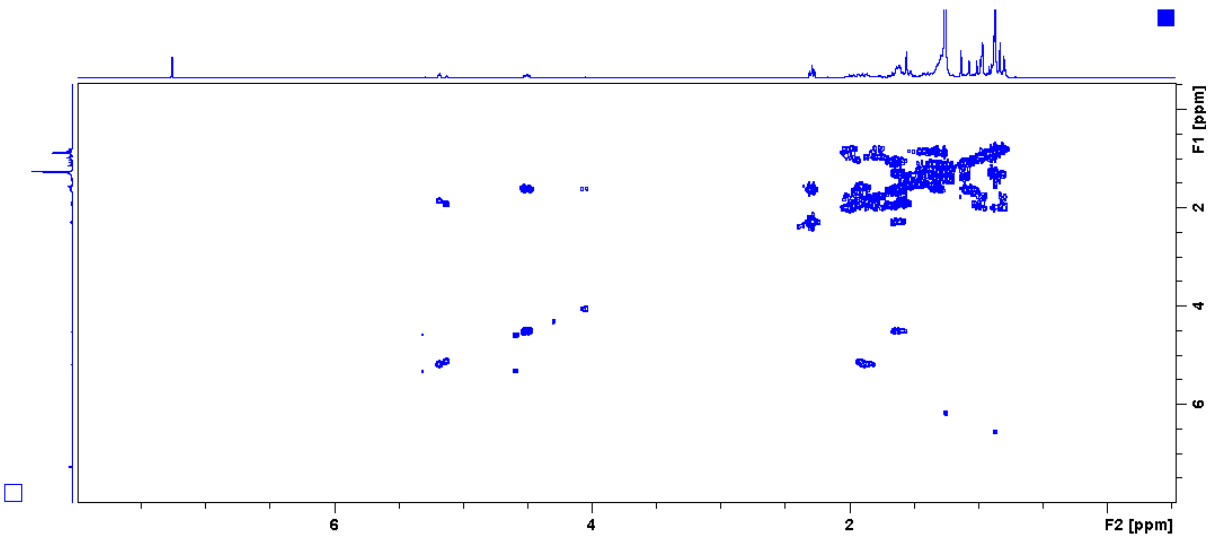

Plate 6 A. COSY spectrum of lupeol palmitate in $CDCl_3$.

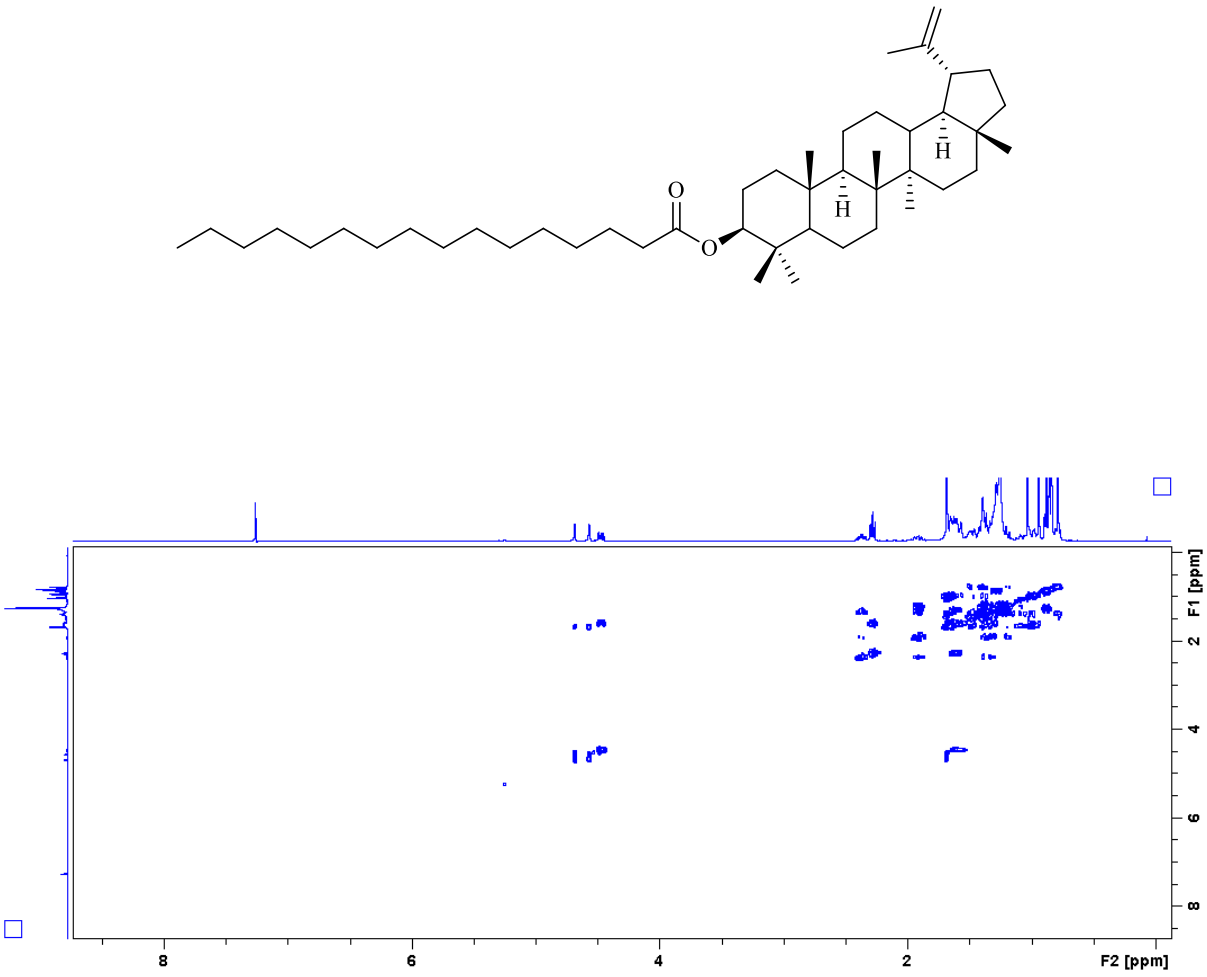

Plate 11 A. IC_{50} calculation Linear fit for DCM-MeOH (1:1) extract.

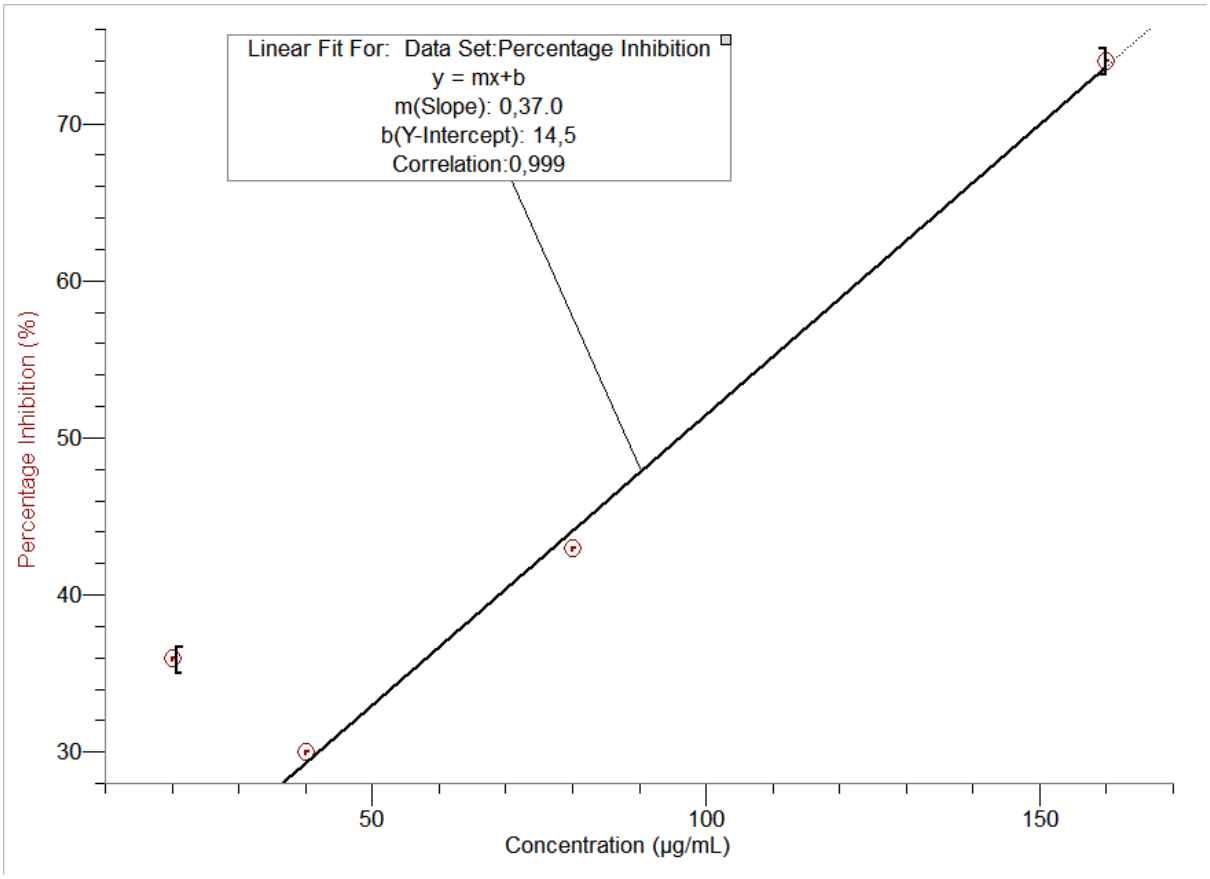

Plate 11 B. IC_{50} calculation Linear fit for acarbose.